

HE
18.5
.A37
no.
DOT-
TSC-
UMTA-
80-27
.III

PORT NO. UMTA-MA-06-0100-80-6

IMPROVED DESIGN OF TUNNEL SUPPORTS:
VOLUME 3 - FINITE ELEMENT ANALYSIS OF THE
PEACHTREE CENTER STATION IN ATLANTA

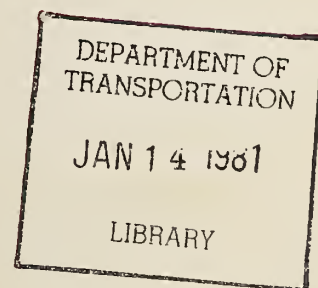
Amr. S. Azzouz
Charles W. Schwartz
Herbert H. Einstein

MASSACHUSETTS INSTITUTE OF TECHNOLOGY
Department of Civil Engineering
Cambridge MA 02139



JUNE 1980
FINAL REPORT

DOCUMENT IS AVAILABLE TO THE PUBLIC
THROUGH THE NATIONAL TECHNICAL
INFORMATION SERVICE, SPRINGFIELD,
VIRGINIA 22161



Prepared for
U.S. DEPARTMENT OF TRANSPORTATION
URBAN MASS TRANSPORTATION ADMINISTRATION
Office of Technology Development and Deployment
Office of Rail and Construction Technology
Washington DC 20590

NOTICE

This document is disseminated under the sponsorship of the Department of Transportation in the interest of information exchange. The United States Government assumes no liability for its contents or use thereof.

NOTICE

The United States Government does not endorse products or manufacturers. Trade or manufacturers' names appear herein solely because they are considered essential to the object of this report.

HE
18.5
A37
no.
DOT-TSC-UMTA-

80-27, III

1. Report No. UMTA-MA-06-0100-80-6		2. Government Accession No.		3. Recipient's Catalog No.	
4. Title and Subtitle IMPROVED DESIGN OF TUNNEL SUPPORTS: VOLUME 3 - FINITE ELEMENT ANALYSIS OF THE PEACHTREE CENTER STATION IN ATLANTA				5. Report Date June 1980	
				6. Performing Organization Code	
7. Author(s) A.S. Azzouz, C.W. Schwartz, H.H. Einstein				8. Performing Organization Report No. DOT-TSC-UMTA-80-27.III	
9. Performing Organization Name and Address Massachusetts Institute of Technology* Department of Civil Engineering Cambridge, MA 02139				10. Work Unit No. (TRAIS) UM048/R0720	
				11. Contract or Grant No. DOT-TSC-1489	
				13. Type of Report and Period Covered Final Report (Vol. 3) January 1978-August 1979	
12. U.S. Department of Transportation Urban Mass Transportation Administration Office of Technology Development & Deployment Office of Rail & Construction Technology Washington, DC 20590				14. Sponsoring Agency Code	
15. Supplementary Notes *Under contract to:		U.S. Department of Transportation Research and Special Programs Administration Transportation Systems Center Cambridge, MA 02142			
16. Abstract <p>Volume 3 contains the application of the three dimensional (3-D) finite element program, Automatic Dynamic Incremental Nonlinear Analysis (ADINA), to a specific location, the Peachtree Center Station in Atlanta. The purpose of the study was to demonstrate the practical use of such a methodology. The effectiveness of the 3-D analysis for design is constrained but not excluded by the time and total cost requirements of the analysis.</p> <p>Predictions of ground movements and stresses caused by the enlargement of the pilot tunnel to form the test chamber, and by the excavation of the main station cavern are displayed. Plots of calculated stresses and deformation are shown in a form suitable for practical comparisons with instrument readings.</p> <p>Volume 3 is the third of five volumes published on the Improved Design of Tunnel Supports. The Executive Summary of the five-volume report was published in December, 1979 (Report No. UMTA-MA-06-0100-79-15).</p> <p>The remaining final reports published in this five-volume series are:</p> <ul style="list-style-type: none"> Volume 1 - Simplified Analysis for Ground-Structure Interaction in Tunneling Volume 2 - Aspects of Yielding in Ground-Structure Interaction Volume 4 - Tunneling Practices in Austria and Germany Volume 5 - Empirical Methods in Rock Tunneling - Review and Recommendations. 					
17. Key Words Tunneling, Support Design, Ground-Structure Interaction			18. Distribution Statement DOCUMENT IS AVAILABLE TO THE PUBLIC THROUGH THE NATIONAL TECHNICAL INFORMATION SERVICE, SPRINGFIELD, VIRGINIA 22161		
19. Security Classif. (of this report) UNCLASSIFIED		20. Security Classif. (of this page) UNCLASSIFIED		21. No. of Pages 115	22. Price

1. Report No. UMTA-MA-06-0100-80-6		2. Government Accession No. PB 80-225170		3. Recipient's Catalog No.	
4. Title and Subtitle IMPROVED DESIGN OF TUNNEL SUPPORTS: Volume 3 - Finite Element Analysis of the Peachtree Center Station in Atlanta				5. Report Date June 1980	
				6. Performing Organization Code	
7. Author(s) A. S. Azzouz, C. W. Schwartz, and H. H. Einstein				8. Performing Organization Report No. DOT-TSC-UMTA-80-27.III	
9. Performing Organization Name and Address Massachusetts Institute of Technology* Department of Civil Engineering Cambridge, Massachusetts 02139				10. Work Unit No. (TRAILS) MA-06-0100(UM048/R0720)	
				11. Contract or Grant No. DOT-TSC-1489	
12. Sponsoring Agency Name and Address U.S. Department of Transportation Urban Mass Transportation Administration 400 Seventh Street, S.W. Washington, DC 20590				13. Type of Report and Period Covered Final Report Volume 3 of 5 January 1978-August 1979	
				14. Sponsoring Agency Code UTD-30	
15. Supplementary Notes *under contract to: U.S. Department of Transportation, Research and Special Programs Administration, Transportation Systems Center, Cambridge, MA 02142. Related reports are: Executive Summary (PB 80-134547); Volume 1 (UMTA-MA-06-0100-80-4); Volume 2 (UMTA-MA-06-0100-80-5); Volume 4 (UMTA-MA-06-0100-80-7); and Volume 5 (UMTA-MA-06-0100-80-8).					
16. Abstract This five-volume report includes the results of an extensive research effort by the Massachusetts Institute of Technology to improve the design methodologies available to tunnel designers. The purpose of this report is to provide the tunneling profession with improved practical tools in the technical or design area, which provide more accurate representations of the ground-structure interaction in tunneling. The design methods range from simple analytical and empirical methods to sophisticated finite element techniques as well as an evaluation of tunneling practices in Austria and Germany. Volume 3 contains the application of the three-dimensional (3-D) finite element program, Automatic Dynamic Incremental Nonlinear Analysis (ADINA), which was designed to replace the traditional 2-D plane strain analysis, to a specific location. The location is the Peachtree Center Station in Atlanta, Georgia. The purpose of the study was to demonstrate the practical use of such a methodology. Predictions of ground movements and stresses caused by the enlargement of the pilot tunnel to form the test chamber, and by the excavation of the main station cavern are displayed. Plots of calculated stresses and deformation are shown in a form suitable for practical comparisons with instrument readings. This application of the three-dimensional finite element model is intended to illustrate some of the advantages and limitations of such methods when used for design or to compare predicted movements with measured movements. The effectiveness of the 3-D analysis for design is constrained but not excluded by the time and total cost requirements of the analysis. The potential design savings will probably outweigh the analysis costs in cases where complex ground-structure interaction cannot be realistically modeled by other methods.					
17. Key Words Atlanta, Georgia; ADINA; Finite Element Analysis; Ground-Structure Interaction; Peachtree Center Station; Support Design; Tunnel Support; Tunneling; Tunnels and Tunneling; Underground Construction; Atlanta Research Chamber				18. Distribution Statement Available to the public through the National Technical Information Service, Springfield, Virginia 22161	
19. Security Classif. (of this report) Unclassified		20. Security Classif. (of this page) Unclassified		21. No. of Pages 111	22. Price A06

PREFACE

This report is the third of five publications (the Executive Summary of this five-volume report was published in December, 1979) which include the results of an extensive research effort by the Massachusetts Institute of Technology (MIT) to improve the design methodologies available to tunnel designers. The contract, DOT-TSC-1489, was funded by the U.S. Department of Transportation (DOT) and was sponsored by the Urban Mass Transportation Administration's (UMTA) Office of Rail and Construction Technology. The contract was monitored by the Transportation Systems Center (TSC) Construction and Engineering Branch.

Volume 3 contains a specific application of the three dimensional (3-D) finite element program, Automatic Dynamic Incremental Nonlinear Analysis (ADINA), which was designed to replace the traditional 2-D plane strain analysis. Significant amounts of time and money must be dedicated to such an effort, but considering the cost to be only 25 percent of the total project, the economics are not a major limitation. The potential design savings will probably outweigh the analysis costs in cases where complex ground-structure interaction cannot be realistically modeled by other methods.

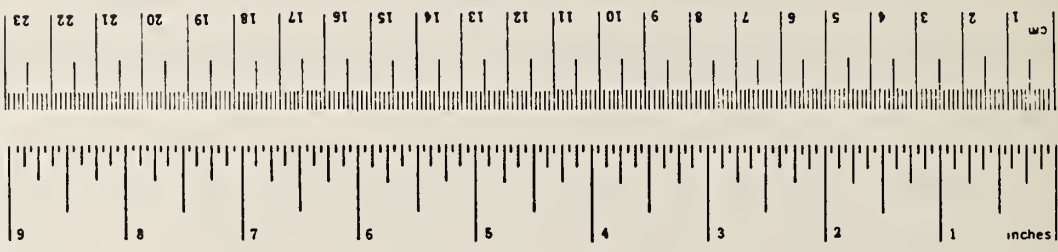
METRIC CONVERSION FACTORS

Approximate Conversions to Metric Measures

Symbol	When You Know	Multiply by	To Find	Symbol
LENGTH				
in	inches	2.5	centimeters	cm
ft	feet	30	centimeters	cm
yd	yards	0.9	meters	m
mi	miles	1.6	kilometers	km
AREA				
in ²	square inches	6.5	square centimeters	cm ²
ft ²	square feet	0.09	square meters	m ²
yd ²	square yards	0.8	square meters	m ²
mi ²	square miles	2.6	square kilometers	km ²
acres	acres	0.4	hectares	ha
MASS (weight)				
oz	ounces	28	grams	g
lb	pounds	0.45	kilograms	kg
	short tons	0.9	tonnes	t
	(2000 lb)			
VOLUME				
tap	teaspoons	5	milliliters	ml
Tbsp	tablespoons	15	milliliters	ml
fl oz	fluid ounces	30	milliliters	ml
c	cups	0.24	liters	l
pt	pints	0.47	liters	l
qt	quarts	0.95	liters	l
gal	gallons	3.8	liters	l
ft ³	cubic feet	0.03	cubic meters	m ³
yd ³	cubic yards	0.76	cubic meters	m ³
TEMPERATURE (exact)				
°F	Fahrenheit temperature	5/9 (after subtracting 32)	Celsius temperature	°C

Approximate Conversions from Metric Measures

Symbol	When You Know	Multiply by	To Find	Symbol
LENGTH				
mm	millimeters	0.04	inches	in
cm	centimeters	0.4	inches	in
m	meters	3.3	feet	ft
m	meters	1.1	yards	yd
km	kilometers	0.6	miles	mi
AREA				
cm ²	square centimeters	0.16	square inches	in ²
m ²	square meters	1.2	square yards	yd ²
km ²	square kilometers	0.4	square miles	mi ²
ha	hectares (10,000 m ²)	2.5	acres	acres
MASS (weight)				
g	grams	0.035	ounces	oz
kg	kilograms	2.2	pounds	lb
t	tonnes (1000 kg)	1.1	short tons	short tons
VOLUME				
ml	milliliters	0.03	fluid ounces	fl oz
l	liters	2.1	pints	pt
l	liters	1.06	quarts	qt
l	liters	0.26	gallons	gal
m ³	cubic meters	35	cubic feet	ft ³
m ³	cubic meters	1.3	cubic yards	yd ³
TEMPERATURE (exact)				
°C	Celsius temperature	9/5 (then add 32)	Fahrenheit temperature	°F



* 1 in = 2.54 exactly. For other exact conversions and more detailed tables, see NBS Misc. Publ. 286, Units of Weights and Measures, Price \$2.25, SD Catalog No. C13-10-286.

TABLE OF CONTENTS

<u>Section</u>		<u>Page</u>
1.	INTRODUCTION.....	1
2.	FINITE ELEMENT MODEL.....	5
2.1	Need for a Three-Dimensional Analysis.....	5
2.2	Geometry and Geotechnical Conditions.....	6
2.3	Finite Element Representation....	9
2.4	Analyses Performed.....	11
3.	RESULTS.....	13
3.1	Principal Stress Vectors.....	14
3.2	Displacement Vectors.....	16
3.3	Summary of Inclinator, Extensometer, and General Cavern Movements.....	19
3.4	Summary of Results from the 3-D Analysis.....	31
4.	COST AND SIZE OF THE ANALYSIS.....	33
5.	SUMMARY AND CONCLUSIONS.....	35
6.	FIGURES REFERENCED IN SECTIONS 2 AND 3.	39
7.	TABLES REFERENCED IN SECTIONS 3 AND 4..	95
8.	REFERENCES.....	99
APPENDIX A	- DESCRIPTION OF COMPUTER PROGRAM - ADINA.....	101
APPENDIX B	- REPORT OF NEW TECHNOLOGY.....	103

LIST OF ILLUSTRATIONS

<u>Figure</u>		<u>Page</u>
2.1	PROJECT LOCATION PLAN (FROM LAW ENGINEERING TESTING COMPANY, 1976).....	40
2.2	OBLIQUE VIEW OF THE PEACHTREE CENTER STATION AREA (AFTER KULHAWY, 1977).....	41
2.3	CROSS-SECTIONAL ELEVATION ALONG THE Y-Z PLANE OF SYMMETRY.....	42
2.4	FINITE ELEMENT MESH FOR A TYPICAL CROSS-SECTION.....	43
3.1a	PRINCIPAL STRESSES ALONG PLANE OF SYMMETRY -- STEP 2.....	44
3.1b	PRINCIPAL STRESSES AT STATION 20+35 -- STEP 2.....	45
3.1c	PRINCIPAL STRESSES AT STATION 20+50 -- STEP 2.....	46
3.1d	PRINCIPAL STRESSES AT STATION 20+65 -- STEP 2.....	47
3.1e	PRINCIPAL STRESSES AT STATION 21+30 -- STEP 2.....	48
3.1f	PRINCIPAL STRESSES AT STATION 23+00 -- STEP 2.....	49
3.2a	PRINCIPAL STRESSES ALONG PLANE OF SYMMETRY -- STEP 4.....	50
3.2b	PRINCIPAL STRESSES AT STATION 20+35 -- STEP 4.....	51
3.2c	PRINCIPAL STRESSES AT STATION 20+50 -- STEP 4.....	52
3.2d	PRINCIPAL STRESSES AT STATION 20+65 -- STEP 4.....	53
3.2e	PRINCIPAL STRESSES AT STATION 21+30 -- STEP 4.....	54
3.2f	PRINCIPAL STRESSES AT STATION 23+00 -- STEP 4.....	55

LIST OF ILLUSTRATIONS (CONTINUED)

<u>Figure</u>		<u>Page</u>
3.3a	INCREMENTAL DISPLACEMENTS ALONG PLANE OF SYMMETRY -- STEP 1.....	56
3.3b	INCREMENTAL DISPLACEMENTS OF THE FRONT END OF THE RESEARCH CHAMBER ALONG PLANE OF SYMMETRY -- STEP 1.....	57
3.3c	INCREMENTAL DISPLACEMENTS AT STATION 20+35 -- STEP 1.....	58
3.3d	INCREMENTAL DISPLACEMENTS AT STATION 20+50 -- STEP 1.....	59
3.3e	INCREMENTAL DISPLACEMENTS AT STATION 20+65 -- STEP 1.....	60
3.3f	INCREMENTAL DISPLACEMENT AT STATION 21+30 -- STEP 1.....	61
3.3g	INCREMENTAL DISPLACEMENT AT STATION 23+00 -- STEP 1.....	62
3.4a	DISPLACEMENTS ALONG PLANE OF SYMMETRY -- STEP 2.....	63
3.4b	DISPLACEMENTS AT THE FRONT END OF THE RESEARCH CHAMBER ALONG PLANE OF SYMMETRY -- STEP 2.....	64
3.4c	DISPLACEMENTS AT STATION 20+35 -- STEP 2..	65
3.4d	DISPLACEMENTS AT STATION 20+50 -- STEP 2..	66
3.4e	DISPLACEMENTS AT STATION 20+65 -- STEP 2..	67
3.4f	DISPLACEMENTS AT STATION 21+30 -- STEP 2..	68
3.4g	DISPLACEMENTS AT STATION 23+00 -- STEP 2..	69
3.5a	DISPLACEMENTS AT THE FRONT END OF THE RESEARCH CHAMBER ALONG PLANE OF SYMMETRY -- STEP 4.....	70
3.5b	DISPLACEMENTS AT STATION 20+35 -- STEP 4..	71
3.5c	DISPLACEMENTS AT STATION 20+50 -- STEP 4..	72
3.5d	DISPLACEMENTS AT STATION 20+65 -- STEP 4..	73

LIST OF ILLUSTRATIONS (CONTINUED)

<u>Figure</u>		<u>Page</u>
3.5e	DISPLACEMENTS AT STATION 21+30 -- STEP 4..	74
3.5f	DISPLACEMENTS AT STATION 23+00 -- STEP 4..	75
3.6a	DISPLACEMENTS ALONG PLANE OF SYMMETRY -- INC 24.....	76
3.6b	DISPLACEMENTS AT STATION 20+35 -- INC 24..	77
3.6c	DISPLACEMENTS AT STATION 20+50 -- INC 24..	78
3.6d	DISPLACEMENTS AT STATION 20+65 -- INC 24..	79
3.6e	DISPLACEMENTS AT STATION 21+30 -- INC 24..	80
3.6f	DISPLACEMENTS AT STATION 23+00 -- INC 24..	81
3.7a	INSTRUMENT LOCATIONS.....	82
3.7b	INSTRUMENT LOCATIONS (LOOKING NORTH).....	83
3.8	RELATIVE LATERAL DISPLACEMENTS ALONG INCLINOMETERS.....	84
3.9	RELATIVE DISPLACEMENTS ALONG EXTENSOMETERS AT CROWN CENTERLINE OF RESEARCH CHAMBER...	85
3.10	RELATIVE DISPLACEMENTS ALONG EXTENSOMETERS AT INVERT CENTERLINE OF RESEARCH CHAMBER..	86
3.11	RELATIVE DISPLACEMENTS ALONG INCLINED EXTENSOMETERS AT INVERT OF RESEARCH CHAMBER.....	87
3.12	RELATIVE DISPLACEMENTS ALONG EXTENSOMETERS AROUND MAIN STATION CAVERN -- STATION 23+00	88
3.13a	DEFORMED GEOMETRY OF OPENINGS.....	89
3.13b	DEFORMED GEOMETRY OF OPENINGS.....	90
3.14	"ZONE OF INFLUENCE" AROUND OPENINGS.....	91
3.15	COMPARISON OF 3-D AND PLANE STRAIN ANALYSIS RESULTS.....	92
3.16	COMPARISON OF MEASURED ROCK DISPLACEMENTS WITH PREDICTIONS FROM THE 3-D FINITE ELEMENT ANALYSIS.....	93

LIST OF TABLES

<u>Table</u>	<u>Page</u>
3.1 MOVEMENTS OF INSTRUMENT REFERENCE ANCHORS.....	50
4.1 SUMMARY OF THE SIZE OF THE FINITE ELEMENT ANALYSIS OF THE PEACHTREE CENTER STATION IN ATLANTA.....	51
4.2 SOLUTION TIME LOG IN SECONDS FOR ONE STEP OF THE FINITE ELEMENT ANALYSIS OF THE PEACHTREE CENTER STATION IN ATLANTA.....	52

1. INTRODUCTION

During the previous research on improved tunnel support design (period July 1, 1976 to June 30, 1977, Contract No. DOT OS-60136 under sponsorship of the Program for University Research), it was recognized that the application of a sophisticated method of analysis to tunneling should be investigated. In particular, it should be investigated which capabilities of such an analysis are, on the one hand, needed in practice and, on the other hand, required for the development of a simplified method of analysis (the latter mainly through parametric studies). Such capabilities would notably concern modeling of three-dimensional effects of ground-structure behavior, time effects, and elasto-plastic behavior with various constitutive relations. The finite element code ADINA is a very powerful analytical tool, whose suitability with regard to practical and research application was, to some extent, studied in the previous research mentioned above. In that research, it was already applied in basic development steps leading to a simplified method of analysis.

During the proposal preparation phase for the present research, the researchers involved in the Test Section at the Peachtree Center Station in Atlanta, notably Mr. W. Shepherd, saw the need to analyze the behavior of the Test Section as accurately as possible. Contacts between the Atlanta group and the MIT group were established through Mr. G. Butler,

Office of Rail Technology, UMTA. As a consequence, it was decided to include a "practical application" of ADINA in addition to its use for developing the simplified analysis in the proposed research. The practical application should mainly focus on the very complicated three dimensional geometry of and around the Test Section, and, if necessary, include non-linear ground behavior.

The details of the finite element analysis were **defined** during fall 1977 and in January 1978. Prof. H. Einstein discussed the analysis during his stay in Atlanta for the 3rd Annual Conference on DOT Research and Development in Tunneling Technology. The discussion was mainly conducted with Mr. Don Rose and Dr. Ian Weir-Jones; this was followed by letters and phone calls, a detailed review of the design and geotechnical information and a trip by Mr. Charles W. Schwartz, Research Assistant, to finalize the problem statement:

three-dimensional capabilities of ADINA will be used to predict the movements caused by the enlargement of the pilot tunnel to the Test Chamber and caused by the excavation of the main station cavern. The predicted movements will be compared to extensometer and inclinometer readings. Since the ground behavior is expected to be close to linearly elastic with small absolute deformations, the effect of the station cavern excavation may be overriding. Also, due to the expected elastic

behavior, it was decided to restrict the study to isotropic linear elastic analysis. Finally, the model will be prepared to investigate the effect of the running tunnel excavation (which runs under and roughly parallel to the test chamber); however, this step will not be executed at the present time since it will not provide much more information than a previously performed plane strain analysis (Kulhawy, 1977). If need arises, this last step, as well as more complex material behavior, can be analyzed at any time.

The study has been completed and results reported in this part represent deformations and stresses due to the Test Chamber enlargement and due to station cavern excavation. The results have been plotted in a form that makes a comparison with instrument readings easily possible. Unfortunately, the actual comparison could not be accomplished since the instruments and measurements were adversely affected by construction procedures. However, the study has given us some valuable insight into the complexity of setting up and using three dimensional finite element analyses. This information, as well as that on the associated cost, is important in deciding on the practical usefulness and applicability of sophisticated analytical methods.

The following sections provide the reader with the above

mentioned information and results by first discussing the selection of geometry, material properties and the finite element model (Section 2) and by presenting and discussing the results (Section 3). In Section 4, the cost and the size of the problem are reviewed and Section 5 reports the conclusions drawn from this study. Section 6 contains all figures referenced in Volume 3 and Section 7 contains all tables referenced in this volume.

2. FINITE ELEMENT MODEL

The purpose of this study is to examine, by three-dimensional finite element methods, the ground behavior at Peachtree Center Station area in Atlanta (Figures 2.1 and 2.2) due to:

1. excavation of the pilot tunnel in an initially stressed rock mass;
2. enlargement of the pilot tunnel to form a test cavern (research chamber);
3. excavation of the main station cavern;
4. excavation of the two running tunnels under and parallel to the test cavern (optional)

and to:

5. predict extensometer and inclinometer movements in the test cavern and compare them with actual measurements.

2.1 NEED FOR A THREE-DIMENSIONAL ANALYSIS

A three-dimensional (3-D) analysis was chosen over the conventional plane strain (2-D) analysis for the following reasons:

1. The geometry of the problem is three dimensional, as is clearly illustrated in Figure 2.2. In particular, we were interested in analyzing the effects that the excavation of the main station cavern had on the research chamber, which is a

truly 3-D problem.

2. Three-dimensional solutions will allow us to analyze movements in the longitudinal direction (along the z axis, Figure 2.2). These movements are expected to be substantial since the initial longitudinal stresses are very high.

3. Studies performed at MIT. (Einstein et al., 1977; and Schwartz and Einstein, 1978) showed that the plane strain solutions, which are incapable of taking into consideration the ground movements occurring ahead of a tunnel face, will give an inaccurate picture of the ground behavior.

4. Since the inclinometers at the Peachtree Center Station are approximately located on the y-z plane of symmetry (Figure 2.2), a plane strain analysis would predict zero inclinometer movements in all directions (in the x-y plane due to symmetry and in the y-z plane due to the definition of a plane strain analysis). However, the 3-D analysis will predict nonzero y-z displacements and hence will provide data that can be compared with actual inclinometers.

2.2 GEOMETRY AND GEOTECHNICAL CONDITIONS

This section presents the details of the actual geometry of the Peachtree Center Station and the ground conditions existing in its vicinity, as well as the simplified geometry and ground conditions used for the finite element analysis. As can be seen from Figure 2.2, the actual geometry is very complex. Hence, it was decided to only model the major

openings, namely the pilot tunnel, research chamber, running tunnels and station cavern. Any additional openings and entrances were neglected. Furthermore, the Ellis Street entrance intersecting the Peachtree Center Station cavern (Figure 2.2) was assumed to be flat roofed. Figure 2.3 shows a cross-sectional elevation of the simplified geometry. The modeled zone is located between stations 19+50 and 23+00 and extends from the ground surface, El. 1077, to El. 812, approximately 165 ft. below the centerline of the station cavern.

A detailed subsurface investigation program for the Peachtree Center Station project has been conducted by Law Engineering Testing Company (LETCO) and the results are presented in two sets of reports:

"Report of Subsurface Investigation--Final Design (Construction Unit DN-11/Tunneling Alternatives;" and "Report of Geology and Instrumentation--Peachtree Center Station Pilot Tunnel (Construction Unit CN-124)."

Based on the results of this subsurface investigation program, it was found that the geologic profile in the zone of interest consists of a layer of residual soils (firm and very firm micaceous silty sands) of a depth ranging from 10 to 30 ft. Beneath the residual soil is a 5 to 15 ft. layer of weathered rock underlain by the parent rock. The predominant rock types are biotite gneiss and biotite amphibole gneiss with an intact rock

strength ranging from 6 to 29 ksi (unconfined compressive strength) and with an E_{50} (tangent modulus of elasticity at 50% strength) varying between 1400 to 11,000 ksi. The intact rock shows primarily elastic behavior with no time dependent strain. The rock mass is of excellent quality having RQD values greater than 90 percent. There are four sets of discontinuities, but in our area of interest they are all tight and/or widely spaced.

The in situ stresses were obtained from the results of flat jack and overcore tests performed in the pilot tunnel. The results of these tests showed that the in situ state of stress may be described by a maximum principal stress of approximately 1000 psi in the north-south direction (i.e., parallel to the station axis) and minor and intermediate principal stresses of 100 to 200 psi in the east-west and vertical directions.

Careful examination of the geologic profiles (LETCO, 1976) showed the rock mass to be reasonably homogeneous and without any apparent major open discontinuities. Also, although there are several rock subtypes, they all have similar properties (at least no systematic differences that we could determine). Therefore, the analysis performed herein assumed the entire mass to be homogeneous. This also includes the overlying soil layer since it is located at a sufficiently large distance from the openings to have an insignificant influence on the results. The average elastic material properties for the ground mass of interest were approximated by the intact rock

properties, which were taken from unconfined compression test results of 20 core specimens from boreholes in the vicinity of the research chamber. These average values of the elastic constants for the rock mass are $E = 4.6 \times 10^6$ psi and $\nu = 0.17$. Some judgement was required in the selection of the values of the in situ stresses to use in the finite element analysis, particularly in the longitudinal direction. The values chosen were $\sigma_z = 580$ psi, $\sigma_y = 116$ psi and $\sigma_x = 116$ psi. The value of $\sigma_y = 116$ psi represents the value of the overburden stress at approximately El. 975, which is roughly the elevation of the station's center line. The variation of stress with depth was neglected.

Thus, for purposes of the analysis, we employed simplifying assumptions regarding geometry and material properties, although it would have been possible to model the exact geometry and also most of the actual material behavior. The simplifications were made to save preparation time and computer costs.

2.3 FINITE ELEMENT REPRESENTATION

The finite element mesh was designed to represent the simplified geometry shown in Figure 2.3, which is symmetrical about the y-z plane (because of this symmetry, only one half of the problem was analyzed). In order to model the geometrical variations in the longitudinal direction (y-z plane), 16 transversal cross sections dividing the mesh into 8 segments were used. Figure 2.4 shows one of these cross sections. The final mesh consisted of 1093 3-D isoparametric elements. The

number of nodes per element varied between 8 to 20, yielding a total of 2915 nodal points. Referring to Figures 2.3 and 2.4, the displacement and stress boundary conditions are as follows:

$$U_x = 0 \text{ for the } x = 0' \text{ plane (plane of symmetry)}$$

$$U_y = 0 \text{ for the } y = 812' \text{ plane}$$

$$U_z = 0 \text{ for the } z = 1950' \text{ plane}$$

$$\sigma_x = 116 \text{ psi on the } x = 165' \text{ plane}$$

$$\sigma_y = 116 \text{ psi on the } y = 1077' \text{ plane (ground surface)}$$

$$\sigma_z = 580 \text{ psi on the } z = 2300' \text{ plane}$$

The problem setup and the finite element mesh were designed such that different material properties and models, and/or excavation operations, can be easily taken into consideration in any future analyses.

A preprocessor computer program, supplemented with plotting routines, was developed for constructing the finite element mesh and generating the input data needed for the analysis. Such a program is considered essential in the case of large-size problems such as the one treated herein. Starting from a certain transversal cross-section, and following a set of given instructions, the program automatically generates the rest of the mesh and prepares the input information in a format consistent with the computer program ADINA. To check the accuracy of the generated mesh and to get an idea of the overall cost of the analysis, each one of the eight segments described above was analyzed individually as a linear elastic plane strain problem using three-dimensional elements (the displacements along the tunnel axis were

prevented) and subjected to a uniform state of stress. The calculated state of stress was compared to the expected results based on elasticity theory, and errors in the generated mesh were then corrected.

2.4 ANALYSES PERFORMED

The finite element analyses reported herein were performed to examine the ground behavior due to the excavation of the pilot tunnel, research chamber and station cavern. The anticipated sequence of excavation operations were simulated in three steps. The first step involved the excavation of the pilot tunnel. Enlargement of the southern end of the pilot tunnel to form the research chamber and excavation of the main station cavern were simulated in steps two and four, respectively. Step 3, the excavation of the main cavern top heading, was performed simultaneously with Step 4, excavation of the lower heading.* As mentioned in Section 1, the excavation of the running tunnels* was not simulated in this analysis. As it turned out, the actual excavation sequence was different in that the running tunnel excavation came first. Nevertheless, it is possible to run the analysis again to simulate the different sequence and also to separate steps 3 and 4 by simply changing some initial instructions.

Static isotropic linear elastic analyses were conducted using the computer program ADINA (Automatic Dynamic Incremental

* These steps, as well as others, can be done at a later time if so desired.

Nonlinear Analysis) developed by Bathe, 1976. A description of the program capabilities is given in Appendix A. Each one of the above-mentioned excavation steps was analyzed separately.

A postprocessor computer program was developed to process output files from the finite element program into a more usable form. This program also contains graphic routines to plot displacements and stress vectors at various planes in the finite element mesh, as well as inclinometer and extensometer displacement data.

3. RESULTS

The results of the three-dimensional finite element analysis are grouped into the following three categories:

- 1) Stress conditions within the rock mass (Section 3.1).
- 2) Overall displacement patterns within the rock mass (Section 3.2).
- 3) A summary of the predicted inclinometer and extensometer displacements and a discussion of the general movements of the underground caverns (Section 3.3).

Comparisons of the results from the three-dimensional analysis with those from a previous plane strain analysis (Kulhawy, 1977), as well as with data obtained during construction of the pilot tunnel, will also be included under category 3 above.

The steps in the excavation of the pilot tunnel, research chamber, and main station cavern are designated as:

STEP 0 - Initial conditions before excavation of the pilot tunnel.

STEP 1 - Excavation of the pilot tunnel.

STEP 2 - Enlargement of the southern end of the pilot tunnel to form the research chamber.

STEP 4*- Excavation of the main station cavern.

As will be shown later in this chapter, the stress and displacement fields existing in the rock mass at Step 0 are either

*As mentioned in Section 2, Step 3, excavation of the top heading of the main station cavern, was incorporated into Step 4.

known or can be easily calculated; thus, the finite element analysis starts directly with Step 1.

Although most of the figures illustrating the data are self-explanatory the following discussions will highlight the principal findings from the analysis.

3.1 PRINCIPAL STRESS VECTORS

The total stress states existing in the rock mass around the caverns are illustrated in the form of principal stress vectors in Figure 3.1 for excavation Step 2 and Figure 3.2 for Step 4. In these figures, the stress vectors are represented as crosses centered on nodes in the finite element mesh; the orientation of each cross represents the orientation of the corresponding in-plane principal stresses, and the lengths of the arms of each cross are proportional to the magnitudes of the major and minor in-plane principal stresses. Tensile stresses are designated by small arrowheads at the ends of the crossarm(s), and a scale indicating the magnitude of the stresses is given at the bottom of each figure. The stress vectors are plotted for a longitudinal cross-section along the assumed vertical plane of symmetry through the mesh and for transversal cross-sections at Sta. 20+35, 20+50, and 20+65 (instrumented sections of the research chamber), Sta. 21+30 (south wall of the main station cavern), and at Sta. 23+00 (instrumented section of the main station cavern); the locations of these cross-sections within the overall station geometry can be determined by using Figure 2.3.

Very little about the stress distributions is remarkable; at all locations, the magnitude of the calculated stresses is low (maximum = 100 ksf or 700 psi), much lower than the average unconfined compressive strength (6000-29000 psi) of the intact rock. Along the vertical plane of symmetry, the longitudinal stresses are approximately 5 times the vertical stresses (i.e., near their original in situ value), with a decrease to zero near the south faces of the research chamber and main station caverns (Figures 3.1a and 3.2a); the radial stresses decrease to zero near the openings and there is a localized rotation of principal stresses near the corners of the openings. In the transversal cross-sections through the research chamber (Sta. 20+35, 20+50, 20+65, Figures 3.1b-3.1d and 3.2b-3.2d), the major and minor principal stresses are approximately tangential and radial; the maximum tangential stress concentration (relative to the original major principal stress) equals about 2, which is in agreement with closed-form elasticity solutions.

At excavation Step 4, a small zone of biaxial tensile stresses forms at the south wall of the main station cavern, (Sta. 21+30); this zone is surrounded by a zone of small tension-compression or compression-compression stresses. The high longitudinal stresses are responsible for these tension zones. Small radial tensile stresses also form in the flat parts of the crown, side-wall, and invert of the main station cavern, Figure 3.2f, (sta. 23+00).

3.2 DISPLACEMENT VECTORS

As an aid for understanding the behavior of the rock mass around the station and for interpreting the extensometer and inclinometer data, the total patterns of rock mass displacements are illustrated in Figures 3.3 through 3.6. In these figures, the displacement vectors are plotted at the nodes of the finite element mesh; the small circles represent the original position of the nodes and the short line segments emanating from the circles represent the displacement vectors. At each node, the angular orientation of the line segment is the (in-plane) orientation of the displacement vector, and the length of the line segment is proportional to the magnitude of the (in-plane) displacements. The displacements are plotted at a greatly magnified scale in the figures; the scale used to compute the displacement magnitudes is given in a key at the bottom of each figure (this scale changes between figures).

The displacement vectors are plotted along the assumed vertical plane of symmetry through the station and at transverse cross-sections at stations 20.35, 20.50, 20.65, 21.30 and 23.00. The cases illustrated in the figures are as follows:

<u>Case</u>	<u>Figure</u>	<u>Datum</u>
Step 1	3.3	Step 0
Step 2	3.4	Step 1
Step 4	3.5	Step 1
Inc 24	3.6	Step 2

Case "Inc 24" is the incremental movement between Steps 2 and 4 and therefore uses Step 2 as datum. Case "Step 1" represents

the movements induced in the rock mass by the excavation of the pilot tunnel and is really supplementary information to the present investigation; it has been included for the sake of completeness. Since Step 0, the datum for Step 1, represents the rock mass before any excavation has occurred, no numerical analysis is required; the initial stress and displacement fields at Step 0 can be simply expressed as:

$$\begin{aligned}\sigma_Y &= \sigma_v \\ \sigma_X &= K_X \sigma_v \\ \sigma_Z &= K_Z \sigma_v \\ U_X &= \frac{1}{E} [\sigma_X - \nu(\sigma_Y + \sigma_Z)] (X - X_0) \\ U_Y &= \frac{1}{E} (\sigma_Y - \nu(\sigma_X + \sigma_Z)) (Y - Y_0) \\ U_Z &= \frac{1}{E} [\sigma_Z - \nu(\sigma_X + \sigma_Y)] (Z - Z_0)\end{aligned}$$

where

$$\begin{aligned}\sigma_v &= \text{in situ vertical stress} \\ &= 116 \text{ psi}\end{aligned}$$

$$\begin{aligned}K_X &= \text{lateral stress ratio} \\ &= 1\end{aligned}$$

$$\begin{aligned}K_Z &= \text{longitudinal stress ratio} \\ &= 5\end{aligned}$$

$$\sigma_X, \sigma_Y, \sigma_Z = \text{in situ stress components}$$

$$U_X, U_Y, U_Z = \text{ground displacement components}$$

$$X, Y, Z = \text{coordinates}$$

$$\begin{aligned}X_0, Y_0, Z_0 &= \text{coordinates of fixed boundaries of mesh} \\ &= 0.0, 812.0, \text{ and } 1950.0, \text{ respectively (Fig. 2.4)}\end{aligned}$$

$$\begin{aligned}E, \nu &= \text{elastic constants for ground} \\ &= 4.6 \times 10^6 \text{ psi, } 0.17\end{aligned}$$

At all locations and at all excavation steps, the magnitude of the displacements is very small: Maximum movements, occurring at the end of Step 4, of approximately 0.06 inches longitudinally (Figure 3.5a) and 0.025 inches radially (Figure 3.5f) occur around the main station cavern, while the largest displacements around the research chamber are limited to 0.018 inches (Figure 3.5a), and 0.0048 inches (Figure 3.5b), respectively (The longitudinal displacements are larger than the radial movements because of the high initial longitudinal stresses - $K_z=5$). These movements are, of course, inversely related to the elastic modulus used in the analysis; if the actual rock mass modulus is lower than that assumed in the analysis, $E=4.6 \times 10^6$ psi, (e.g., if the rock mass is of a lower quality than indicated in the geotechnical investigation, or if the rock is badly fractured by blasting), then the rock displacements will be correspondingly higher.

The displacement patterns for Steps 1 and 2 (Figures 3.3 and 3.4) are exactly as expected: The vectors are directed toward the opening with the magnitude increasing with increasing proximity to the opening. At excavation Step 4, the most noteworthy features of the displacement patterns (Figure 3.5) are: 1) the general downward trend of the vectors at Sta. 20+35 , 20+50, and 20+65; 2) the radially outward displacements at the south end of the main station cavern, Figure 3.5e, (Sta. 21+30); and 3) the relatively large movements at Sta. 23+00, Fig.3.5f due to the station cavern excavation. These features are

further accentuated in the plots of the incremental displacement vectors from Step 2 to Step 4 (Figure 3.6).

3.3 SUMMARY OF INCLINOMETER, EXTENSOMETER, AND GENERAL CAVERN MOVEMENTS

The locations of the inclinometers and extensometers within the idealized geometry assumed for the finite element analyses are shown in Figure 3.7.* Extensometers E-1 through E-15 and inclinometers I-1 and I-2 measure the rock movements around the research chamber; extensometers A-1 through A-5, which measure the rock movements around the main station cavern, have been included since their movements were also determined as a by-product of the analysis and may be of interest during construction.

The predicted rock mass displacements for excavation Steps 2 and 4 are summarized in Figure 3.8 for the inclinometers and in Figures 3.9 through 3.12 for the extensometers. In these, as well as in most of the other displacement plots in this chapter, the displacement field existing in the rock mass at the end of Step 1 is the datum condition; all subsequent displacements are measured as increments from this datum.** Furthermore, the inclinometer and extensometer displacements are also

* The instrument locations shown in Figure 3.7 are based on the original contract drawings SE-002 and SE-266-2 and on the supplementary drawing WJEC-M-1.

** This assumption of Step 1 as datum also implies that the inclinometers and extensometers are installed at the end of Step 1, if not before.

measured with respect to their own "local" datum. This "local" datum is the reference anchor point farthest from the underground opening, which is always assumed to be far enough away to be considered stationary. Thus, the data plotted in Figures 3.8 through 3.12 are the predicted relative movements along the measurement device - movements relative to the location of the device's reference anchor point at Step 1.

Inclinometers

The inclinometer displacements (Figure 3.8) at Step 2 are very small, especially when the large magnitude of the in situ longitudinal stresses is considered ($K_z=5$). This is quite reasonable, since very little longitudinal movement usually occurs around a tunnel except in the region ahead of the face. However, in Step 4 the inclinometers are now in the region ahead of a "face" - in this case, the "face" is the southern wall of the excavated main station cavern (Sta. 21+30 - see Figure 3.7a for geometry). There are now much stronger (although still small in an absolute sense) movements toward the newly excavated station cavern, and these movements increase at locations closer to the station cavern (i.e., Sta. 20+65).

The results plotted in Figure 3.8 assume that the inclinometers are installed at the end of Step 1. However, the inclinometer installation was delayed until after Step 3 (test section enlargement). The situation has been further complicated by the excavation of some sections

of the running tunnels prior to test section enlargement; if the analysis were run again in another sequence and including Step 5 (excavation of running tunnels), the proper basis for comparison could be obtained. .

Extensometers Around Research Chamber

At excavation Step 2, the general pattern for the displacements of the walls of the research chamber is a very slight movement toward the opening on the order of 0.001 in., with larger displacements at the invert than at the crown (Figures 3.9 and 3.10) and comparatively smaller displacements at the invert-sidewall corner (Figure 3.11). The magnitude of these displacements and their variation with distance from the opening agree well with the results one would expect from approximate closed-form elastic solutions. Excavation Step 4, though, seems to produce some counterintuitive results: Excavation of the main station cavern appears to cause the walls of the research chamber to move outward - i.e., the relative displacements of the extensometers at Step 4 are smaller than at Step 2. This effect is more pronounced at the invert of the research chamber than at the crown.

This predicted outward movement of the research chamber walls as "measured" by the extensometers is misleading. Figure 3.13 illustrates the deformed position of the research chamber crown and invert along the centerline of the opening. As usual, the datum condition is Step 1 for this figure. At

Step 2, the figure shows a nearly equal convergence at the crown and invert; at Step 4, both the crown and invert settle, the crown by a relatively large amount and the invert by a much smaller quantity. Thus, based on the data in Figure 3.13b, at Step 4 one would expect a large increase in the extensometer displacements at the crown and a small or insignificant decrease at the invert. The curves in Figures 3.9 and 3.10 contradict this expected behavior, however. Where Figure 3.13b shows a slight outward incremental movement at the invert between Step 2 and Step 4, Figure 3.10 shows a rather substantial incremental displacement outward. Where Figure 3.13b shows a significant inward (or downward) incremental movement at the crown between Steps 2 and 4, Figure 3.9 shows an outward incremental movement - not only is the magnitude of the displacement wrong, but the direction of the movement is incorrect as well!

The cause of this apparent inconsistency in the extensometer displacements is suggested in Figure 3.14. This figure, which is based on the displacement vector plots presented in Section 3.2, shows (as the shaded region) the extent to which the excavation of the main station cavern induces significant (greater than 0.0001' in the vertical direction) displacements in the rock mass. The shaded "zone of influence" surrounds many of the reference anchors for the research chamber extensometers; in other words, these reference anchors are not stationary as originally assumed. Since the extensometers measure the relative movements between anchor points, a

nonstationary reference anchor makes these movements difficult to interpret. The extensometer displacements must now be considered as relative movements between two moving points.

The effects that the main cavern excavation have on the absolute displacements of the extensometer reference anchors are summarized in Table 3.1 for Steps 2 and 4. The reference anchors for the vertical crown extensometers (E-10, E-11, E-14) move the most, while the anchors for the vertical invert extensometers (E-1, E-4, E-7) shift a smaller but still significant amount. Paradoxically, the inclined extensometers at the invert of the research chamber (E-3, E-5, E-9), which are the shortest extensometers and should therefore be most affected by the excavation of the main station cavern, demonstrate the smallest reference anchor movement. However, Figure 3.6c illustrates that this is just a coincidence of their particular location in the rock mass displacement field. The reference anchors for these inclined anchors do shift laterally, but the component of this shift along the axis of the instrument (which is the component actually measured by the extensometer) is very small.

The movement of the extensometer reference anchors does not necessarily imply that the data from these instruments is useless. In many cases, the designer or contractor is interested only in the relative displacement between the moving anchor points nearest the opening. When absolute displacements are required, optical surveying can sometimes be used to

establish a reference point (although in this particular case, the magnitude of the movements is much too small for accurate surveying). What is most important is that the designer or contractor be aware of the type of movements being measured.

Note that the above description of the reference anchor shift for the extensometers applies equally well to the inclinometers; as shown in Table 3.1, the lateral movement of the reference end of the inclinometers I-1 and I-2 is quite substantial.

One last important conclusion that can be drawn from the data in Figure 3.13 is that the excavation of the main station cavern at Step 4 does not cause any tilting of the research chamber in the longitudinal direction; however, it does cause the research chamber to settle uniformly. Differential or tilting movements do occur north of Sta. 20+65 and increase rapidly near the main station cavern; at Sta. 21+30 (the south wall of the station cavern), the invert of the pilot tunnel settled 0.0068 inches as a result of the station cavern excavation versus a settlement of 0.0012 inches at Sta. 20+65 (the north end of the research chamber).

Extensometers Around the Main Station Cavern

The displacements of extensometers A-1 through A-5 located around the main station cavern at Sta. 23+00 are summarized in Figure 3.12. The displacements are much larger here because the opening is much larger. The reference anchor

movements are also very large for these instruments (Table 3.1); the reason in this case, though, is that the extensometers are just too short (length $\approx 40'$) for an opening as large as the main station cavern (equivalent diameter $\approx 45'$). The extensometers can measure differential movements near the cavern, but they cannot measure the total or absolute displacements.

Comparison with Plane Strain Analysis

A two-dimensional plane strain analysis of the transversal cross-section at Sta. 20+50 has been performed earlier by Kulhawy (1977). In addition to the assumptions inherent in 2-D versus 3-D analyses, the significant differences between Kulhawy's study and the present investigation are:

- 1) The research chamber geometry. The 2-D analysis modeled the chamber as a slightly wider opening with a flatter crown arch than in the 3-D case.
- 2) The longitudinal in situ stresses. In the 2-D analysis, these stresses are dictated by the plane strain assumption. In the 3-D analysis there is more control over this variable, so the initial longitudinal stresses were set equal to their measured values (i.e., $K_x=5$).
- 3) The rock mass homogeneity. The 2-D analysis was based on a slightly inhomogeneous and discontinuous rock mass, while the 3-D case assumed complete homogeneity. However, in the 2-D analysis nearly all of the rock near the openings is classified as

"medium modulus" and the discontinuities/ inhomogeneities are either small enough and/or far enough from the openings to be relatively insignificant.

The elastic modulus assigned to the "medium modulus" rock for the "intact rock" case was 5×10^6 psi in the 2-D analysis versus the value of 4.6×10^6 psi used for the homogeneous rock mass modulus in this 3-D study.

- 4) The excavation sequence. Because of the plane strain assumption, the 2-D analysis does not include any effects from the main station cavern excavation.

Despite the above differences, the 2-D and 3-D analyses are sufficiently similar that reasonable agreement between their results are expected at Sta. 20+50. Figure 3.15 shows the displacements of the research chamber walls that were derived from the two analyses at excavation Step 2 (Step 0 is datum for this figure); as anticipated, there is good correlation. The 2-D analysis gives slightly smaller movements at all locations except the crown; the smaller movements are due primarily to the higher modulus and lower longitudinal stresses in the 2-D analysis, while the larger movements at the crown are most likely attributable to the flatter crown arch.

Although the 2-D and 3-D analyses yield similar results for the radial displacements at Sta. 20+50, this correlation

will not, in general, be true at other locations. In particular, at locations closer to the main station cavern the longitudinal movements induced by the excavation of the main cavern have an increasingly important effect that cannot be modeled in the 2-D analysis because of the plane strain assumption. Similarly, the 2-D analysis is incapable of predicting the inclinometer movements along the centerline of the research chamber.

Comparison with Field Data

Prior to and during construction of the pilot tunnel (excavation Step 1), a total of 23 extensometers were installed in the rock mass. Five of these instruments were in the region around the research chamber, at Sta. 20+50; the details of their location, installation, and reading are given in the "Report of Geology and Instrumentation - Peachtree Center Station Pilot Tunnel (Construction Unit CN-124)" prepared by the Law Engineering Testing Company (1977).

Several difficulties were encountered with these extensometers. Much of the displacement data is very erratic as a result of problems with the electronics and with the back-up mechanical measurement systems. A more serious problem, though, is the damage caused by blasting; 30 percent of the extensometers were adversely affected. Many of the anchors near the pilot tunnel were either dislodged or destroyed by the blasting, and the accuracy of many of the remaining intact instruments may have been seriously impaired. Of the five extensometers at Sta. 20+50, only two were unaffected by either

of these problems.

A comparison of the measured movements of the east horizontal extensometer at Sta. 20+50 with the displacements predicted by the 3-D finite element analysis at excavation Step 1 is presented in Figure 3.16 (Step 0 to datum for this figure).

The comparison is not satisfactory; although the general character of the movement is the same for both curves, the measured displacements are much larger - by approximately an order of magnitude - than the predictions. Moreover, this discrepancy is even larger when one realizes that the predictions assume the extensometer to be in place before excavation while in fact this instrument can only be installed in the tunnel after some excavation - and some movement of the rock mass - has already occurred.

The next question, obviously, is what is the cause for this discrepancy. A combination of the following factors may be responsible: 1) the wrong rock properties were used in the finite element analysis (e.g., the elastic modulus was too high); 2) the actual in situ stresses are higher than those used in the analysis; and 3) the instruments were inaccurate. The first of these factors, the incorrect rock properties, is quite possible; it is always very difficult to extrapolate rock mass properties from the results of laboratory tests on small specimens. However, to completely eliminate the discrepancies in the displacements, the rock mass elastic modulus would have to be reduced by an order of magnitude;

this seems unreasonable if any confidence is placed in the results from the geotechnical investigation. Another possibility is strongly discontinuous behavior of the rock mass - i.e., movements along discontinuities. However, the horizontal orientation of the extensometer minimizes the effects of partings along the bedding planes, although the opportunity for deformation across a near-vertical joint still exists.

Again based on some confidence in the findings from the geotechnical investigation, it is unlikely that an error in the assumed in situ stresses is solely responsible for the discrepancies between the predicted and measured extensometer data. To completely eliminate these differences, the stresses would have to be increased by approximately an order of magnitude.

The final factor that may be responsible for the poor correlation is instrument failure and/or measurement error. Since excessive blasting severely damaged 30 percent of the extensometers, including one in the crown at Sta. 20+50, and since the blasting at this location was strong enough to cause excessive loosening of the 6' of rock nearest the tunnel (as determined by the engineer - see note on Figure 3.16), it is conceivable that all of the anchor points along the extensometer may have been jarred and that a component of this movement is being included in the displacements plotted in Figure 3.16. However, more measurement data is needed, preferably under more controlled blasting procedures, before the

validity of this hypothesis can be established.

At this point, it is very difficult to determine the degree to which each of the above factors is responsible for the differences between the measured and predicted displacements and to determine what is the best correction. If the assumed rock mass properties or in situ stresses are found to be in error, the analysis results can be approximately corrected by scaling. If instrument errors are the problem, the necessary corrections will involve more careful installation and reading procedures and more controlled blasting techniques. The measurements that are made at excavation Step 2 will aid in pinpointing the correct approach.

As mentioned several times, it was not possible to perform the most valuable comparison, that of predicted movements with those measured after enlargement of the chamber, excavation of the main station cavern (and excavation of the running tunnels). The contractor decided to excavate the two running tunnels prior to enlarging the research cavern (and consequently prior to installation of extensometers E-1 to E-15 and inclinometers I-1, 2). This would, however, still have allowed us to compare measured and predicted displacements using the previously installed extensometers at Station 20+50 and by running the analysis corresponding to the modified sequence. However, no, or insignificant, movements were measured with these extensometers as the running tunnels "passed by". The extensometers were later destroyed as the research cavern was enlarged.

At the time of final writing of this report (May 1979), no measurement from the research chamber instruments E-1 to E-15 and I-1 are available. The comparison must thus conclude with this rather limited discussion.

3.4 SUMMARY OF RESULTS FROM THE 3-D ANALYSIS

The significant findings from the 3-D finite element analysis are as follows:

- 1) A tensile stress zone forms at the south wall of the main station cavern (Sta. 21+30). These tensile stresses may cause problems (such as excessive overbreak) during construction of the running tunnels at this location.
- 2) Radial tensile stresses form at the flat parts of the main station cavern's crown, sidewall, and invert. These tensile stress zones are small (reaching a maximum value of about 50 psi) and may be due in part to the high longitudinal stresses in the rock.
- 3) The magnitude of the rock mass displacements is very small. At the walls of the main station cavern, the rock displacements reach a maximum of 0.025 in. radially and 0.06 in. longitudinally; at the walls of the research chamber, the respective movements are 0.0048 and 0.018 in.
- 4) The research chamber does not tilt measurably in the longitudinal plane as a consequence of the main station cavern excavation; however, the research chamber does settle uniformly.

4. COST AND SIZE OF THE ANALYSIS

Table 4.1 gives an idea of the size of the Peachtree Center Station problem. The analysis involved 4757 degrees of freedom with a mean half band width equal to 398. The analysis was performed on MIT's IBM 370/168 computer, used 840 kilobytes of core and required about 81,000 kilobytes of secondary storage. Table 4.2 gives a solution timelog for the analysis of one step which indicates that over 90% of the time is used for solution of equations. The computer cost of each one of the three steps performed was about \$1,200.* A breakdown of this cost is given below:

<u>Item</u>	<u>Percent of Total Cost</u>
1. Use of 840 K of core for 162 minutes	84%
2. Central Processing Unit, CPU, charges for 139 minutes	13%
3. Input/output operations (Total of 47,461 operations)	2%
4. Input of data and output of results	1%

The total computer cost of the complete analysis amounted to about \$11,000. A breakdown of this cost is given below:

* Analyses were performed on Sundays to make full use of MIT's 50% cost reduction policy available for weekend jobs. Hence, the actual cost would have been \$2400.

<u>Item</u>	<u>Percent of Total Cost</u>
1. Program modification and implementation	30%
2. Input preparation, which includes mesh generation and debugging runs	20%
3. Actual analysis (3 steps)	33%
4. Interpretation and analysis of results	17%

A total of four-man months by highly qualified engineering personnel was spent on the analysis, broken down in approximately the same way as the computer costs. Since 50% of the cost and time was devoted to problem preparation (items 1 and 2), any further analysis can be conducted at a lower incremental cost. It should also be noted that a substantial part of item 1 consisted of general (non-project specific) modification and implementation of the ADINA program. These expenses will not be incurred in future applications.

5. SUMMARY AND CONCLUSIONS

This study presents the results of the three-dimensional finite element analysis of the Peachtree Center Station cavern in Atlanta. Analyses were performed to examine the ground behavior due to various stages of excavation and to predict excavation-induced movements within the rock mass. These predictions were then compared with the displacements measured during construction. The major findings from this study are:

1. Deformation Characteristics:

a) The magnitude of the rock mass displacements is very small. At the walls of the main station cavern, the rock displacements reach a maximum of 0.025 inches radially and 0.06 inches longitudinally. At the walls of the research chamber, the respective movements are 0.0048 and 0.018 inches. The small magnitude of displacements is a consequence of the low deformability of the rock and the comparatively low in situ stresses.

b) The excavation of the main station cavern induces relatively large longitudinal movements in the rock surrounding the research chamber. However, the research chamber does not tilt measurably in the longitudinal plane as a consequence of the main station cavern excavation; instead, it settles uniformly.

c) The comparison between rock displacements measured during the excavation of the pilot tunnel and movements

predicted by this analysis is unsatisfactory. The discrepancies in these results may either be due to the use of incorrect rock mass properties and in situ stresses in the analysis or to malfunctions of the field instruments resulting from excessive blasting. More field measurements are needed to determine the exact cause.

d) Due to changes in excavation sequence and unavailability of measurements from the research chamber instruments, no further comparison can be made at this time.

2. State of Stress:

a) The maximum compressive stresses around the openings are low relative to the strength of the rock mass.

b) A tensile stress zone forms at the south wall of the main station cavern which may cause problems, such as excessive overbreak, during construction of the running tunnels at this location. Furthermore, radial tensile stresses form at the flat parts of the main station cavern's crown, sidewall, and invert.

c) In the transverse cross-sections through the research chamber, the major and minor principal stresses are approximately tangential and radial with a maximum tangential stress concentration (relative to the in situ vertical stress) of about 2.

3. Overall Evaluation of Three-Dimensional Finite Element Analysis:

This study has shed some light on the use of three-dimensional finite element analysis as a tool in the analysis and design of underground structures. Several features of the

analysis and results obtained herein could not have been modeled or predicted had a two-dimensional finite element model been used. These features are:

- 1) The complex geometry of the station;
- 2) The longitudinal in situ stresses. In the 2-D model, these stresses are dictated by the plane strain assumption. In the 3-D model, the measured values of stresses can be easily incorporated in the analysis. As was clearly illustrated, the longitudinal stresses have an overriding effect on the instrument movements, and they also induce tensile stresses in the rock which may have practical construction consequences.

3. The excavation sequence. Because of the plane strain assumption, the 2-D model cannot include any effects from the main station cavern excavation.

4. Inclinator movements. Because inclinometers are approximately located in the y-z plane of symmetry, a 2-D model is incapable of predicting their movements.

On the other hand, the effectiveness of the 3-D finite element analysis is constrained by the significant time and high cost required to prepare input, conduct the analysis, and interpret the results. However, this cost is not usually a major limitation when compared to the total cost of a subway station. For example, for this case it is estimated that the cost of a 3-D analysis (computer and manpower) would represent a maximum of 0.25 percent of the total project cost.

(The analysis performed herein cost less because it did not take into consideration all aspects required in design.) The computer cost is only about one-third of the analysis costs, the rest being salary costs for highly qualified personnel. The availability and time commitment of such personnel may be a more stringent problem than the cost in dollars. This evaluation of 3-dimensional analyses is only a limited one. The limited objectives (comparison with measurements) and high quality rock conditions de-emphasize the advantages of 3-dimensional finite element analysis compared to simpler ones. For ground structure interaction in lower quality rock and complex geometries, 3-D analyses will become essential. It is conceivable that the incremental cost of 3-D analyses will be only a fraction of the cost savings made possible by them through reduced supports and modified construction sequences.

6. FIGURES REFERENCED IN SECTIONS 2 AND 3

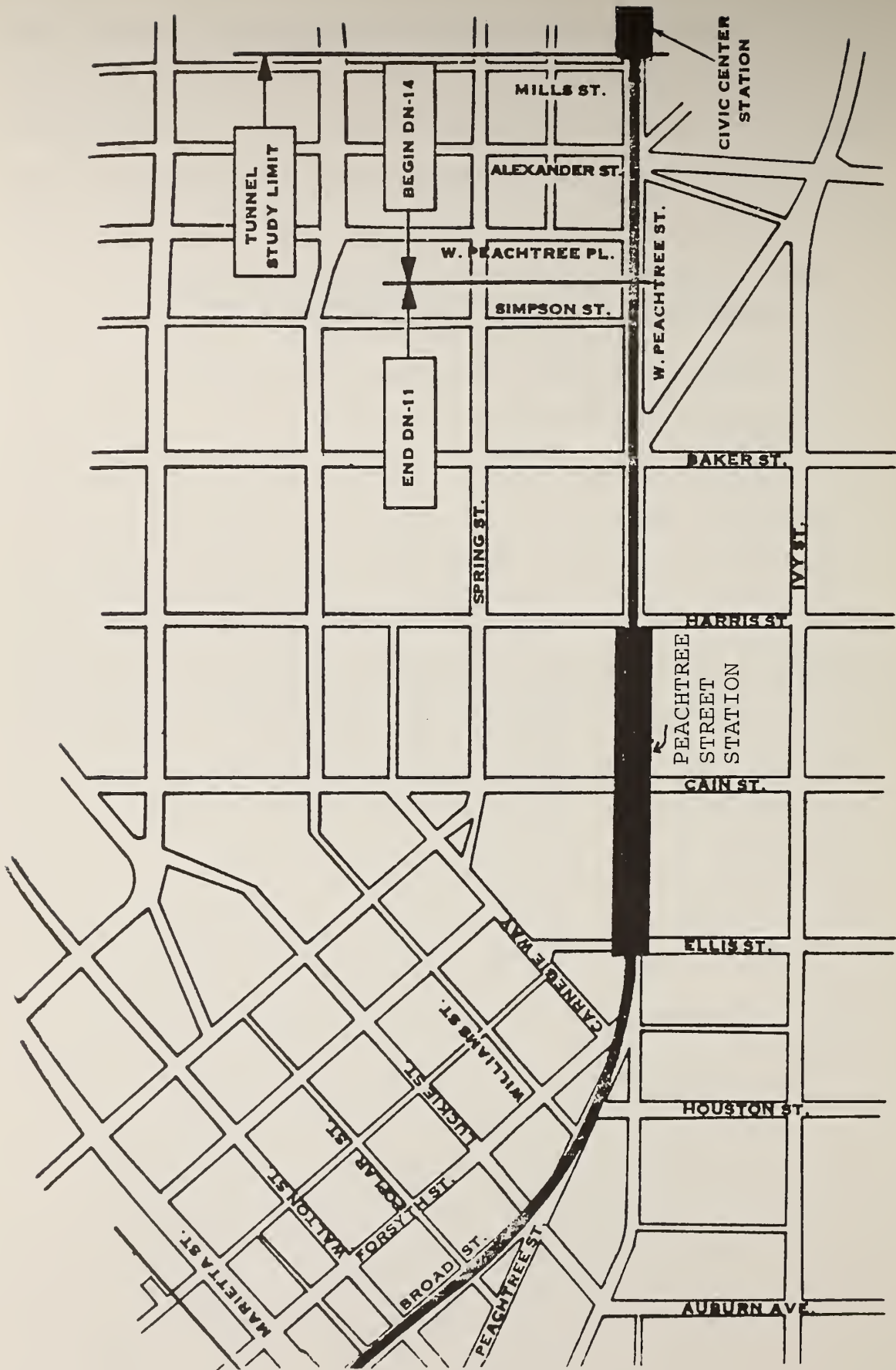


FIGURE 2.1. PROJECT LOCATION PLAN (FROM LAW ENGINEERING TESTING COMPANY, 1976)

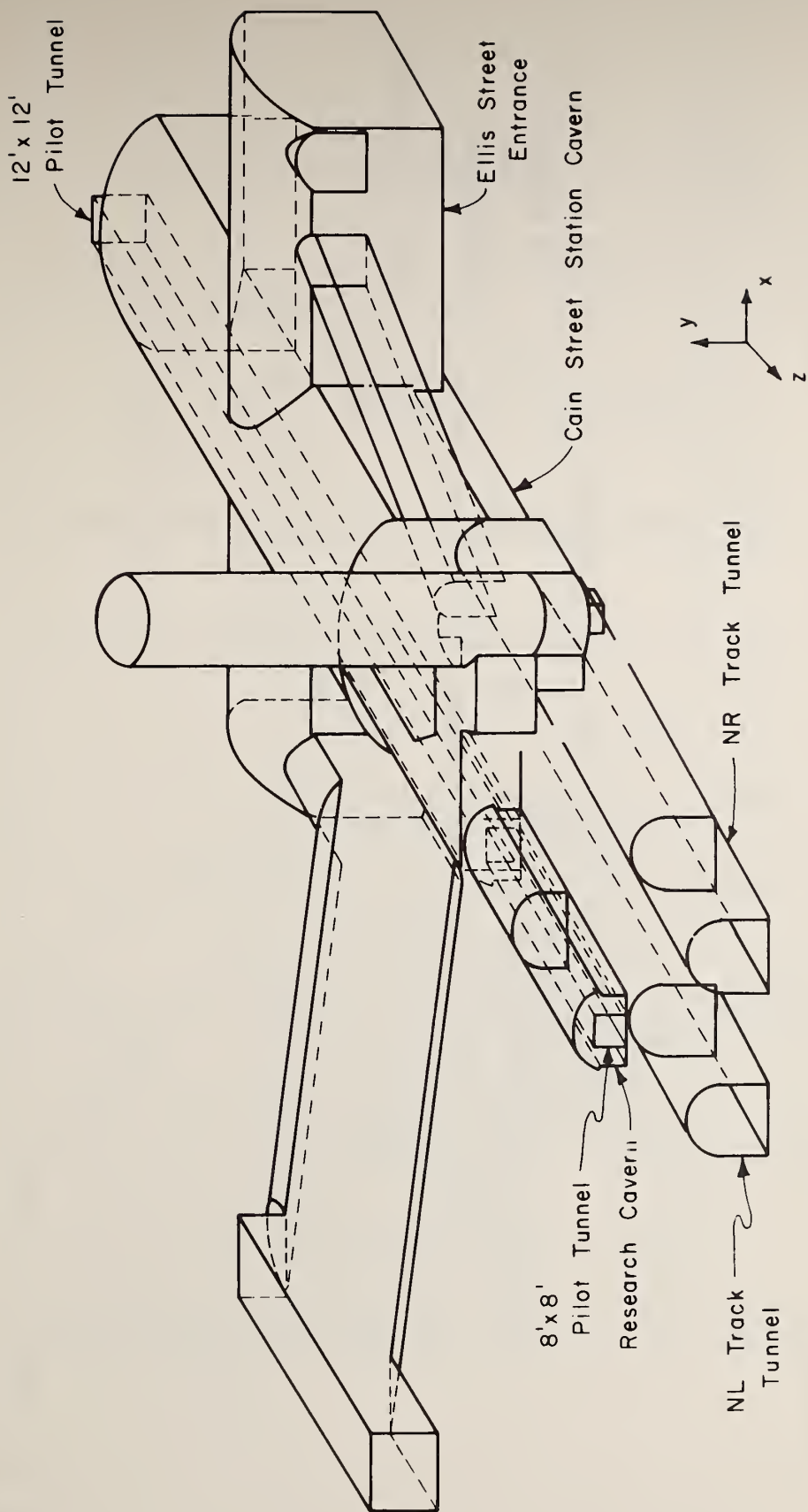


FIGURE 2.2. OBLIQUE VIEW OF THE PEACHTREE CENTER STATION AREA (AFTER KULHAWY, 1977)

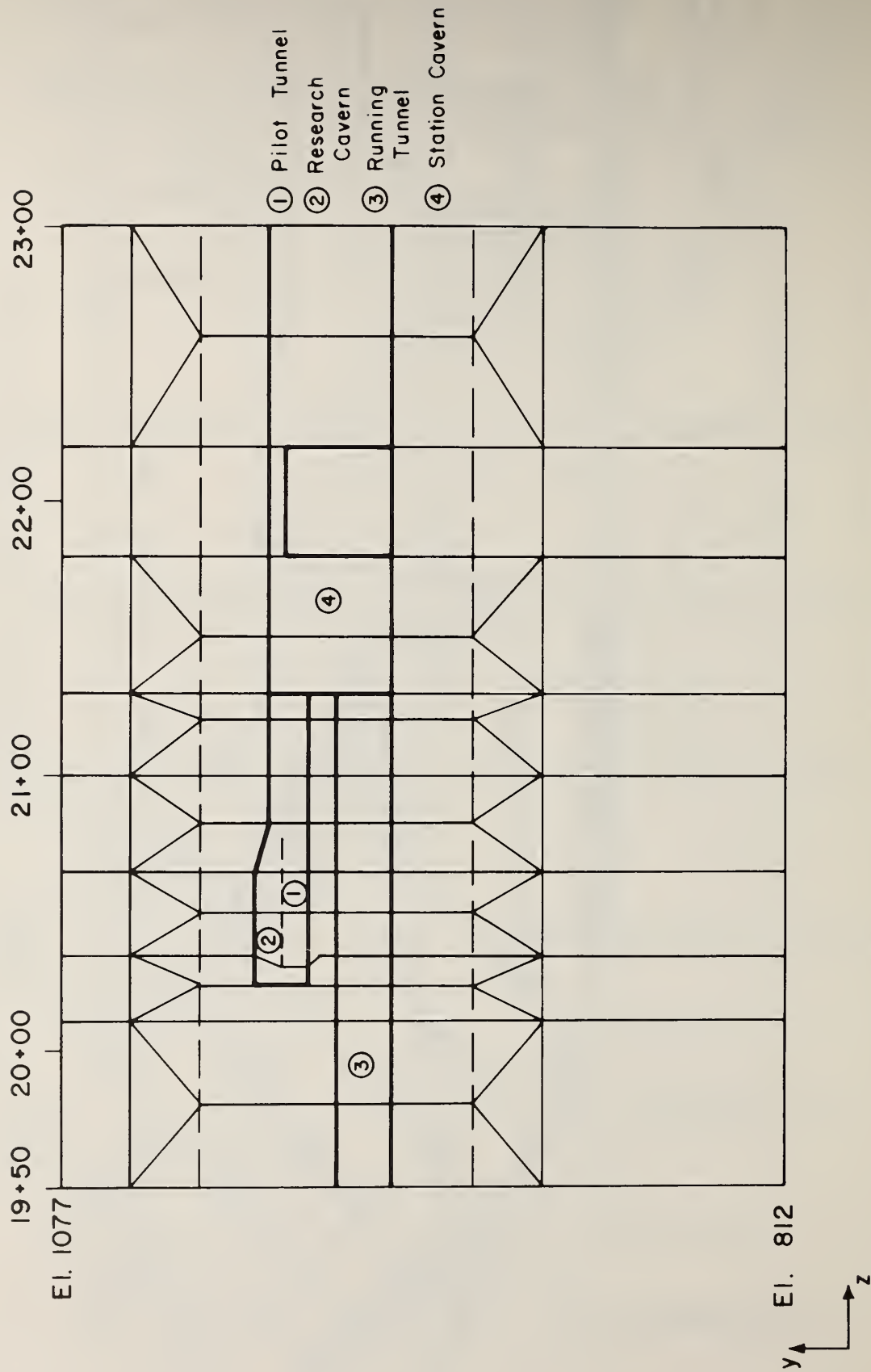
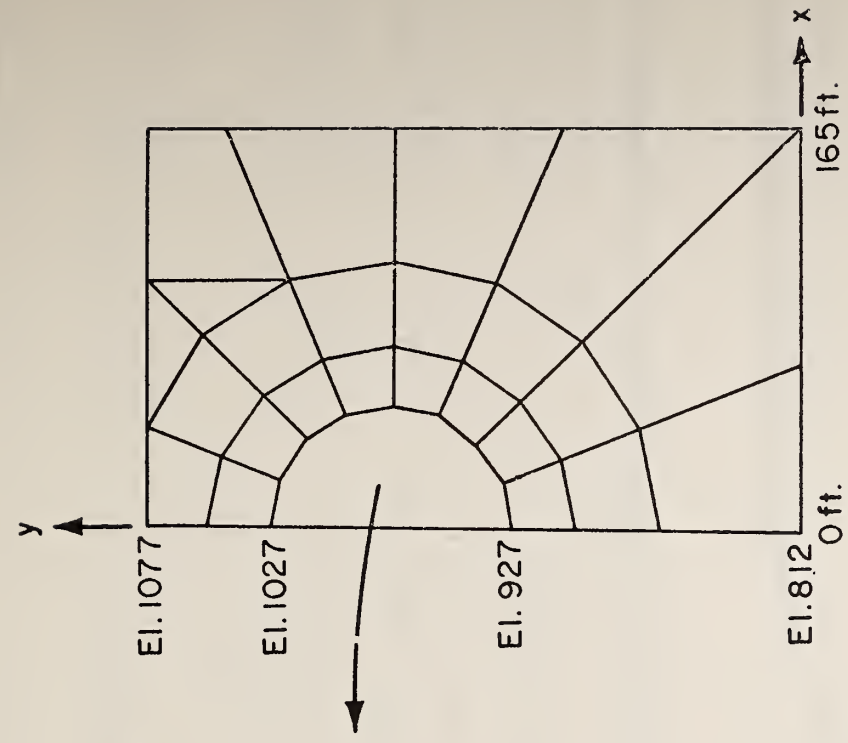


FIGURE 2.3. CROSS-SECTIONAL ELEVATION ALONG THE Y-Z PLANE OF SYMMETRY

50 ft.
Scale: 50 ft.



10 ft.
Scale: 10 ft.

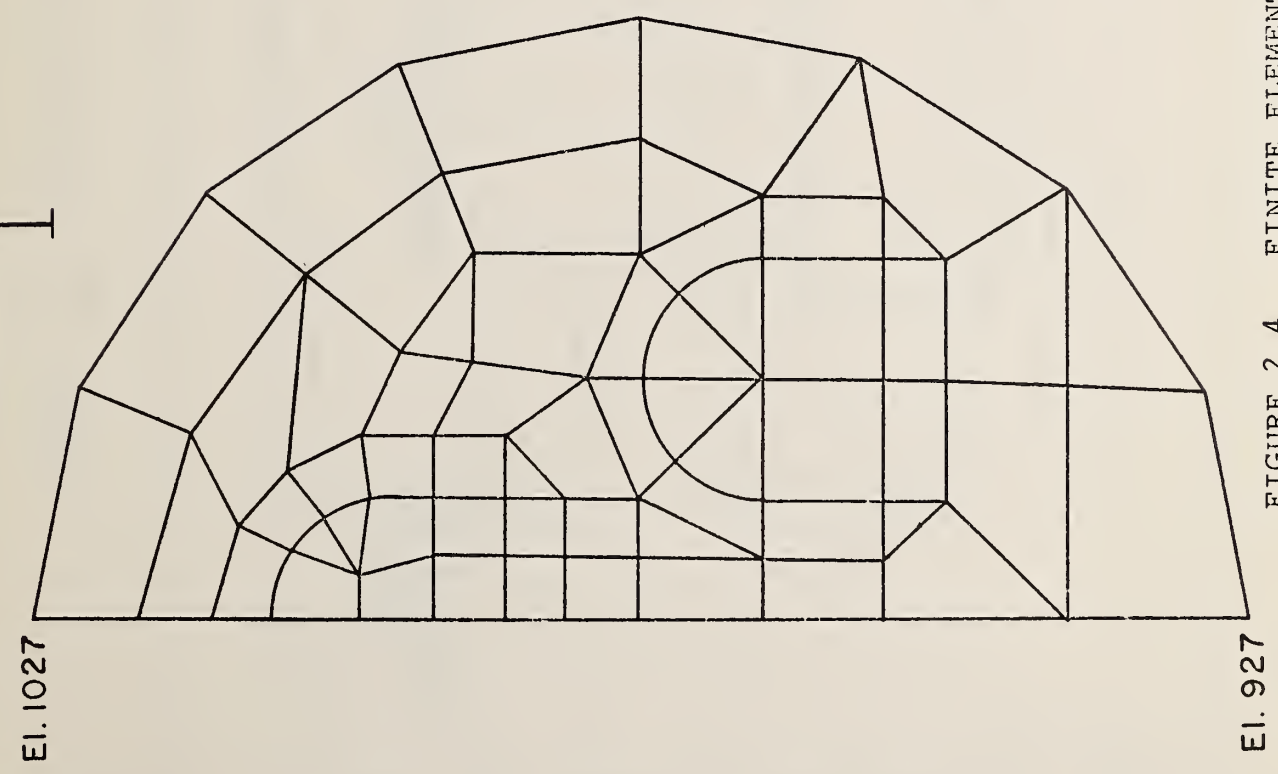


FIGURE 2.4. FINITE ELEMENT MESH FOR A TYPICAL CROSS-SECTION

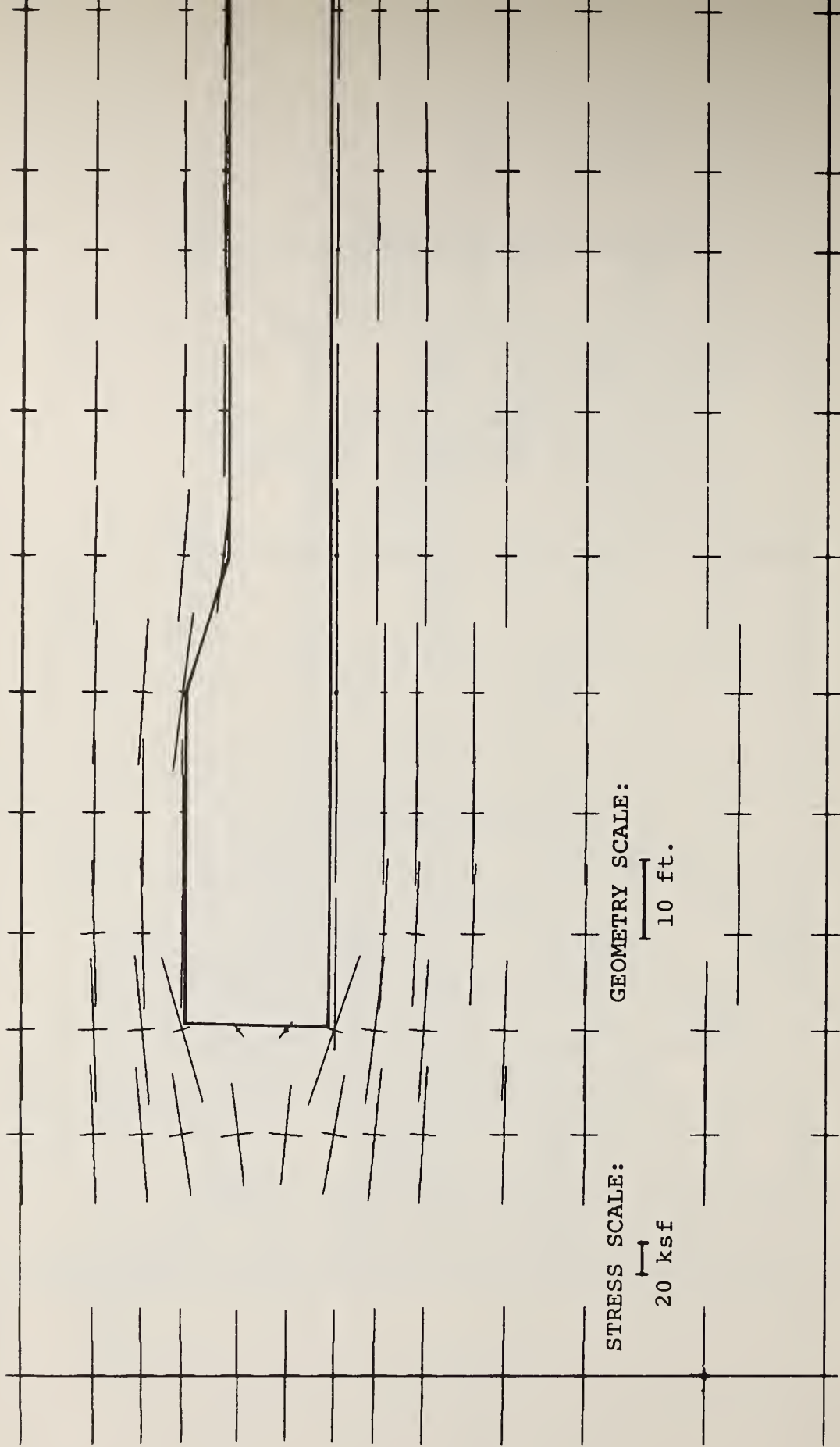


FIGURE 3.1a. PRINCIPAL STRESSES ALONG PLANE OF SYMMETRY -- STEP 2

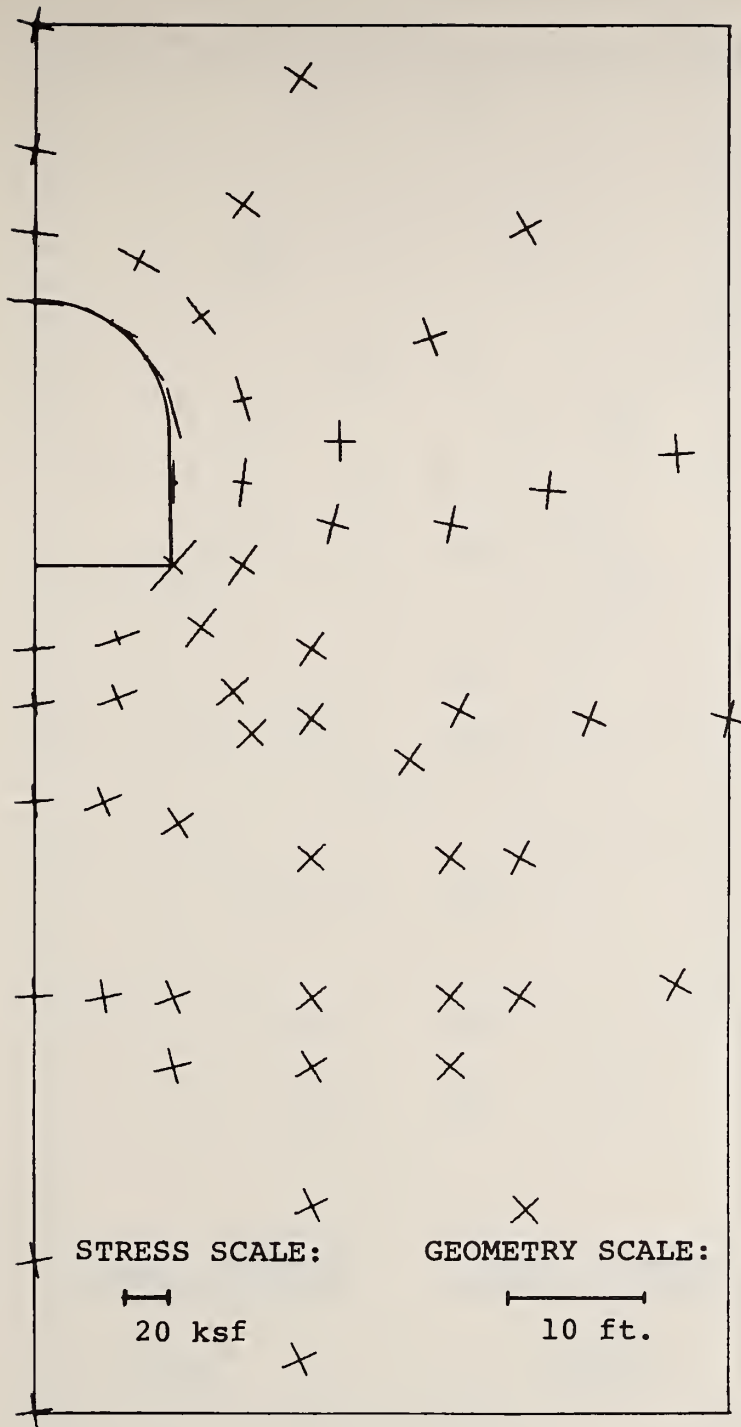


FIGURE 3.1b. PRINCIPAL STRESSES AT STATION 20+35 -- STEP 2

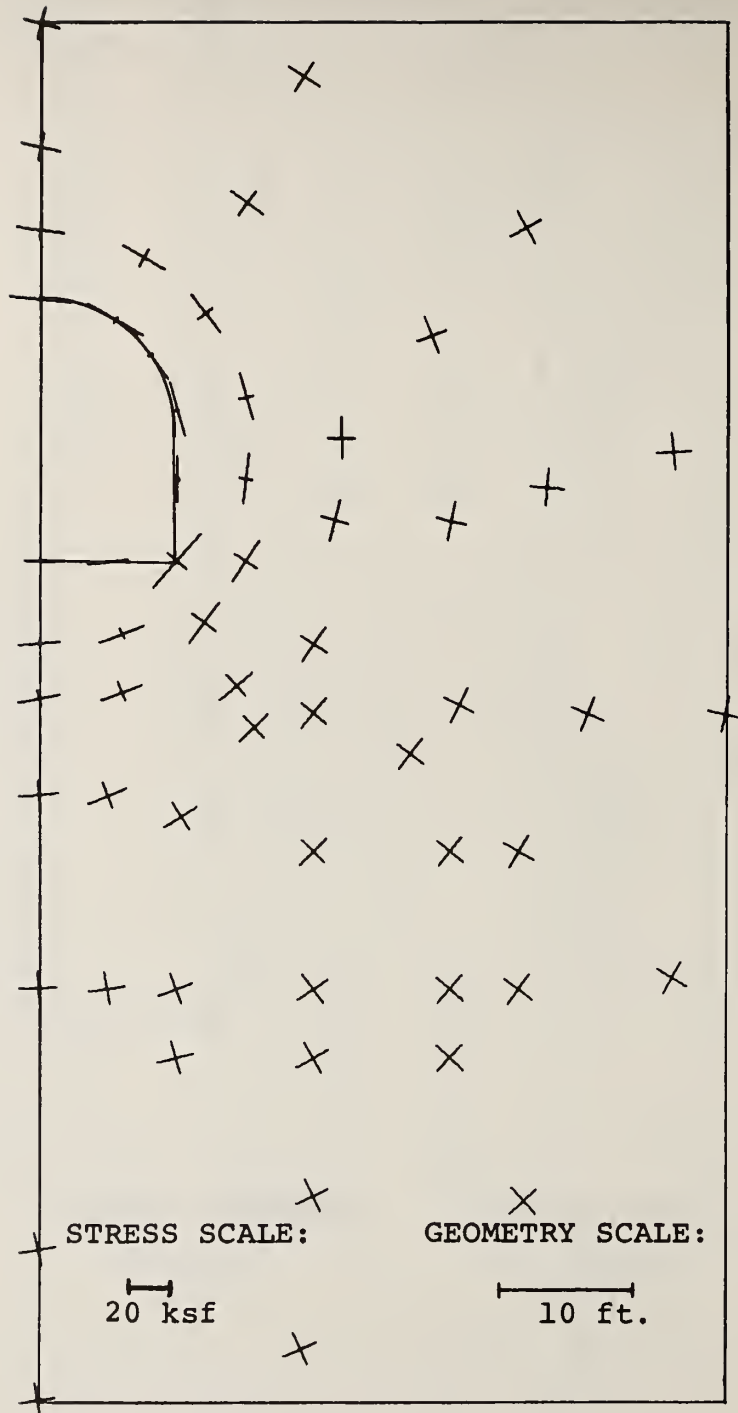


FIGURE 3.1c. PRINCIPAL STRESSES AT STATION 20+50 -- STEP 2

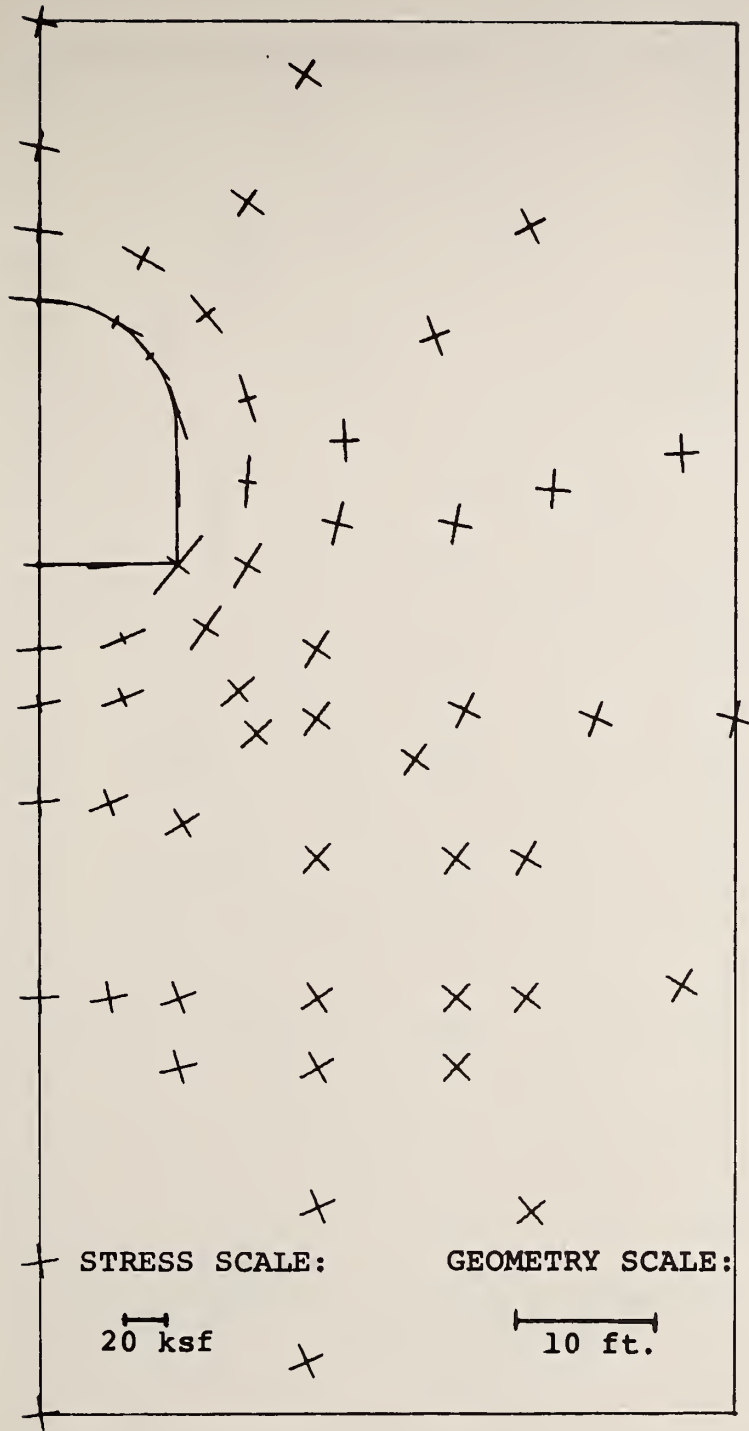


FIGURE 3.1d. PRINCIPAL STRESSES AT STATION 20+65 -- STEP 2

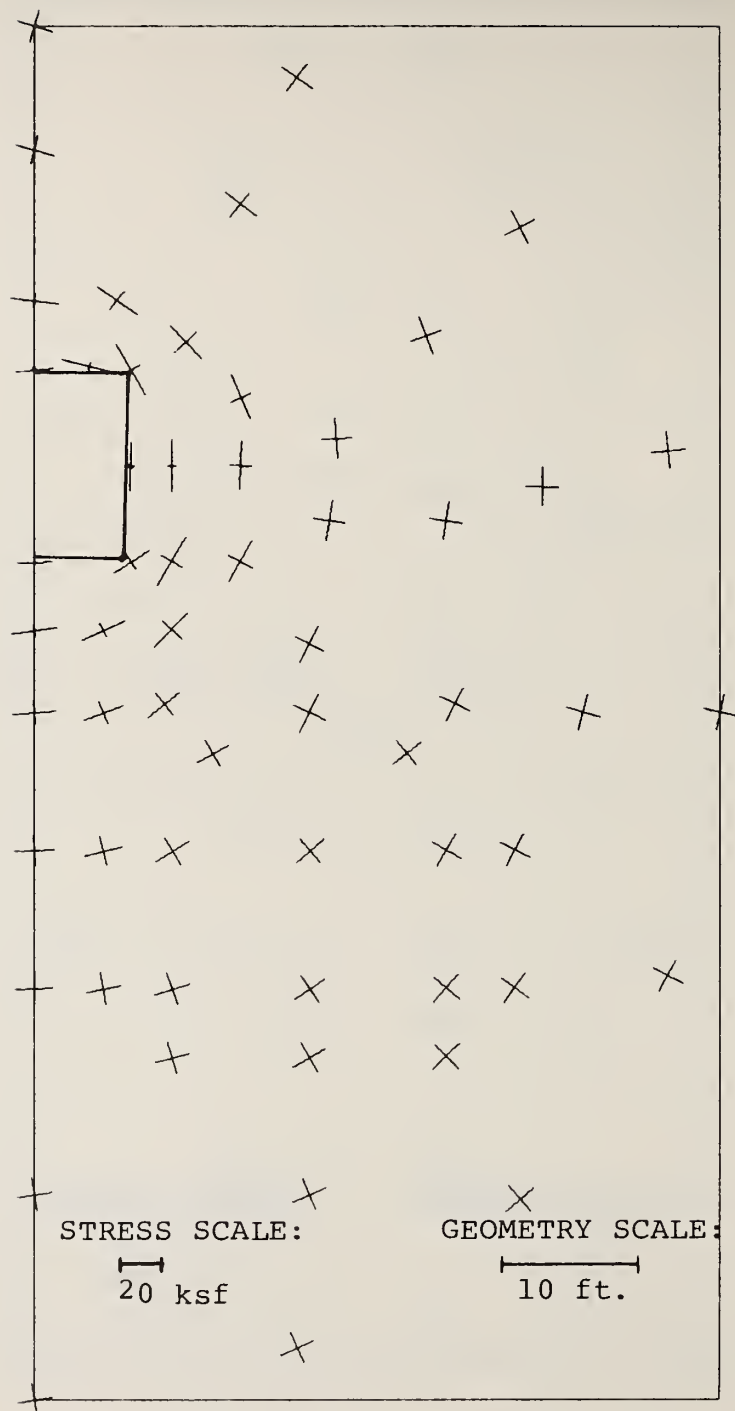


FIGURE 3.1e. PRINCIPAL STRESSES AT STATION 21+30 -- STEP 2

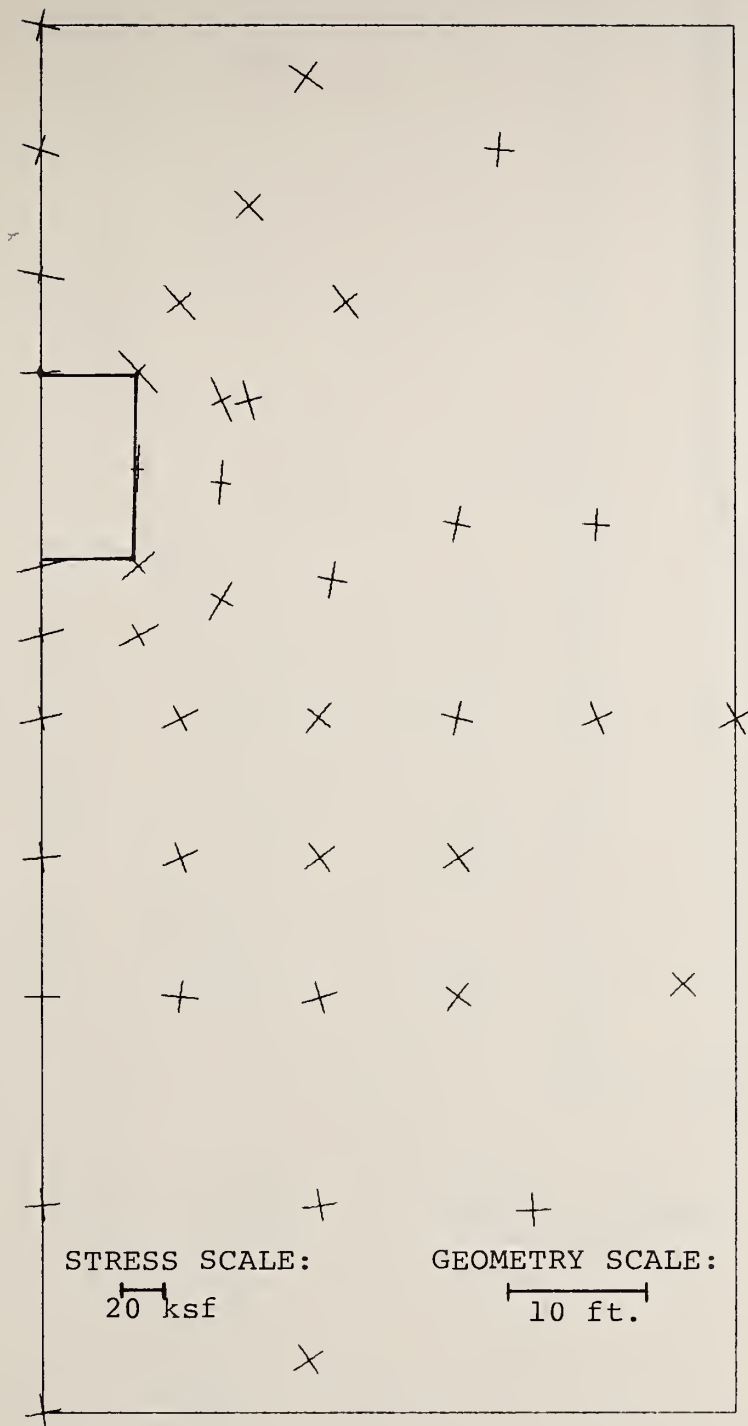


FIGURE 3.1f. PRINCIPAL STRESSES AT STATION 23+00 -- STEP 2

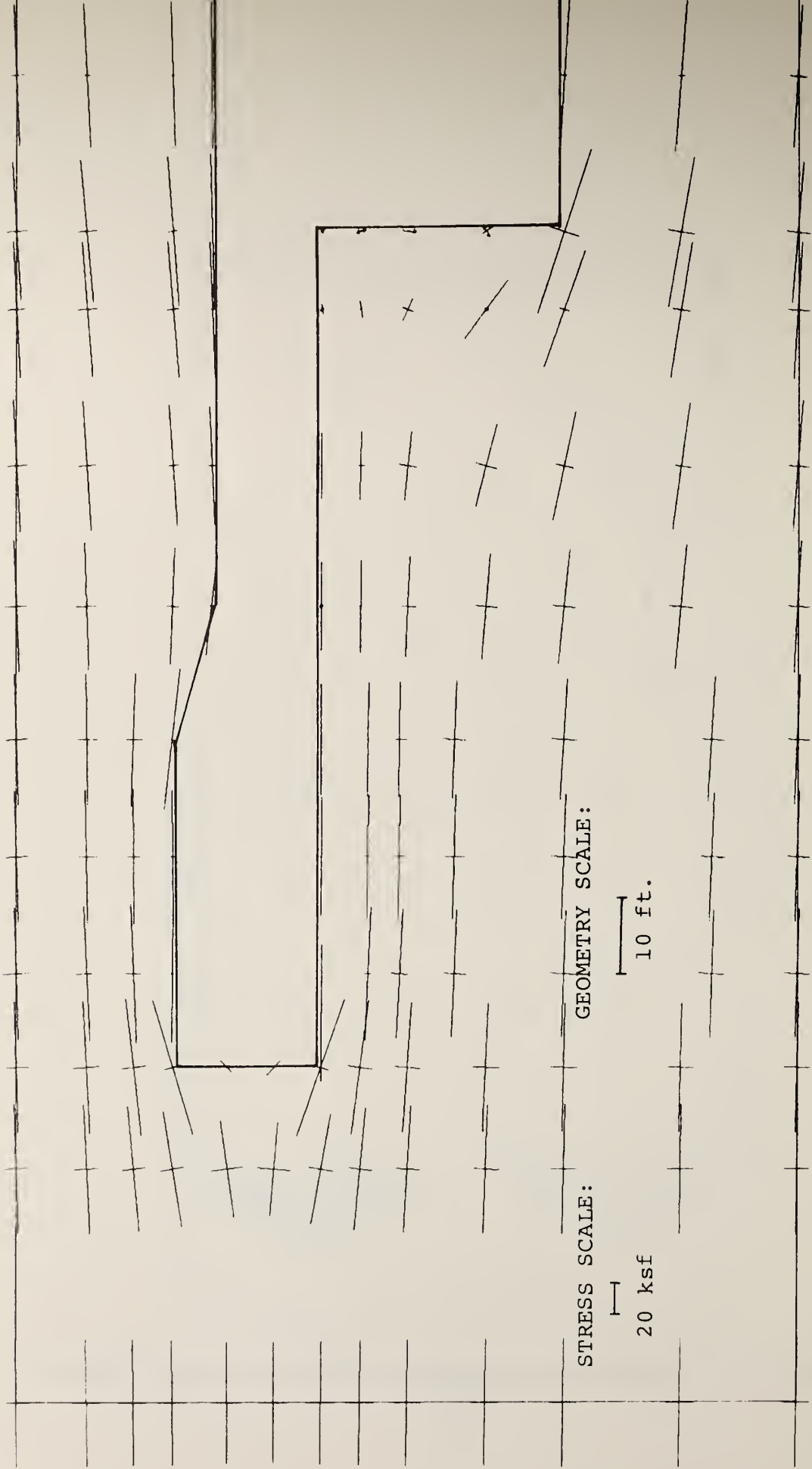


FIGURE 3.2a. PRINCIPAL STRESSES ALONG PLANE OF SYMMETRY -- STEP 4

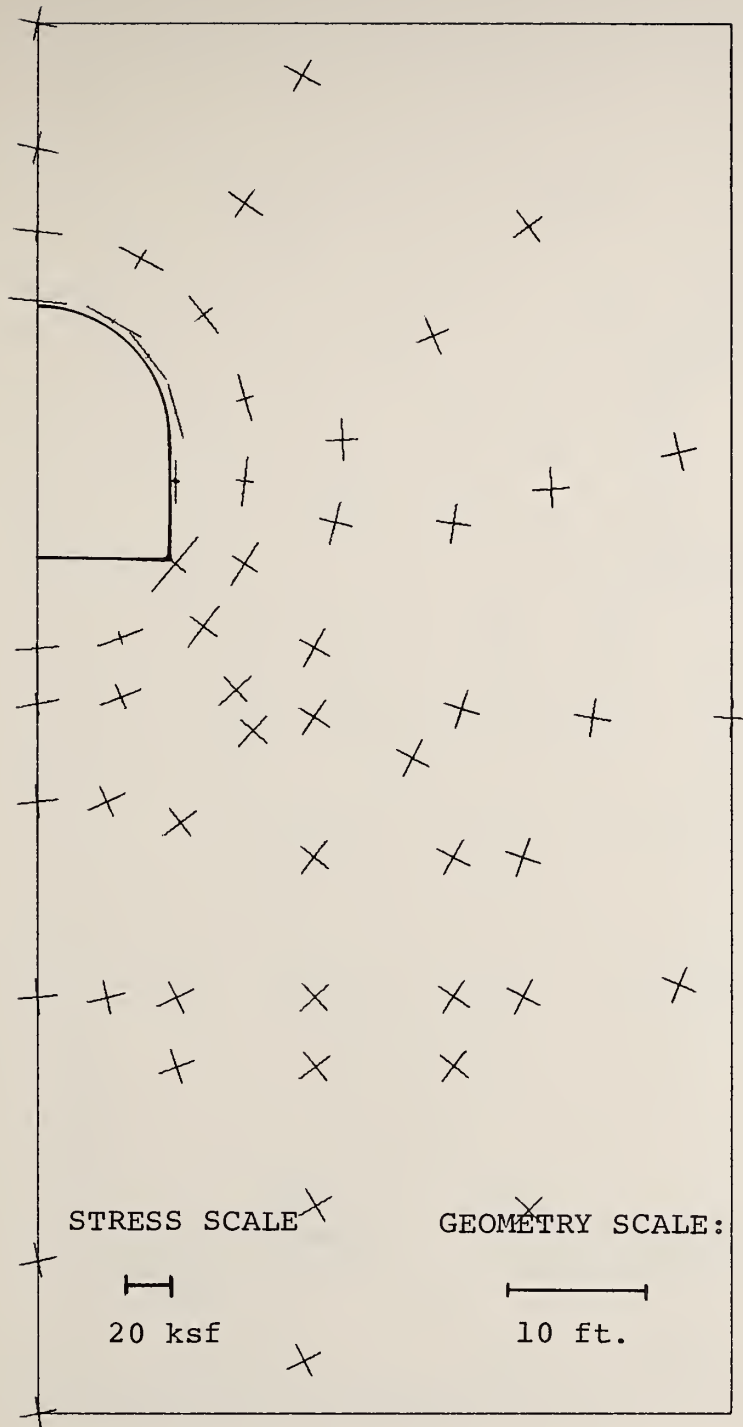


FIGURE 3.2b. PRINCIPAL STRESSES AT STATION 20+35 -- STEP 4

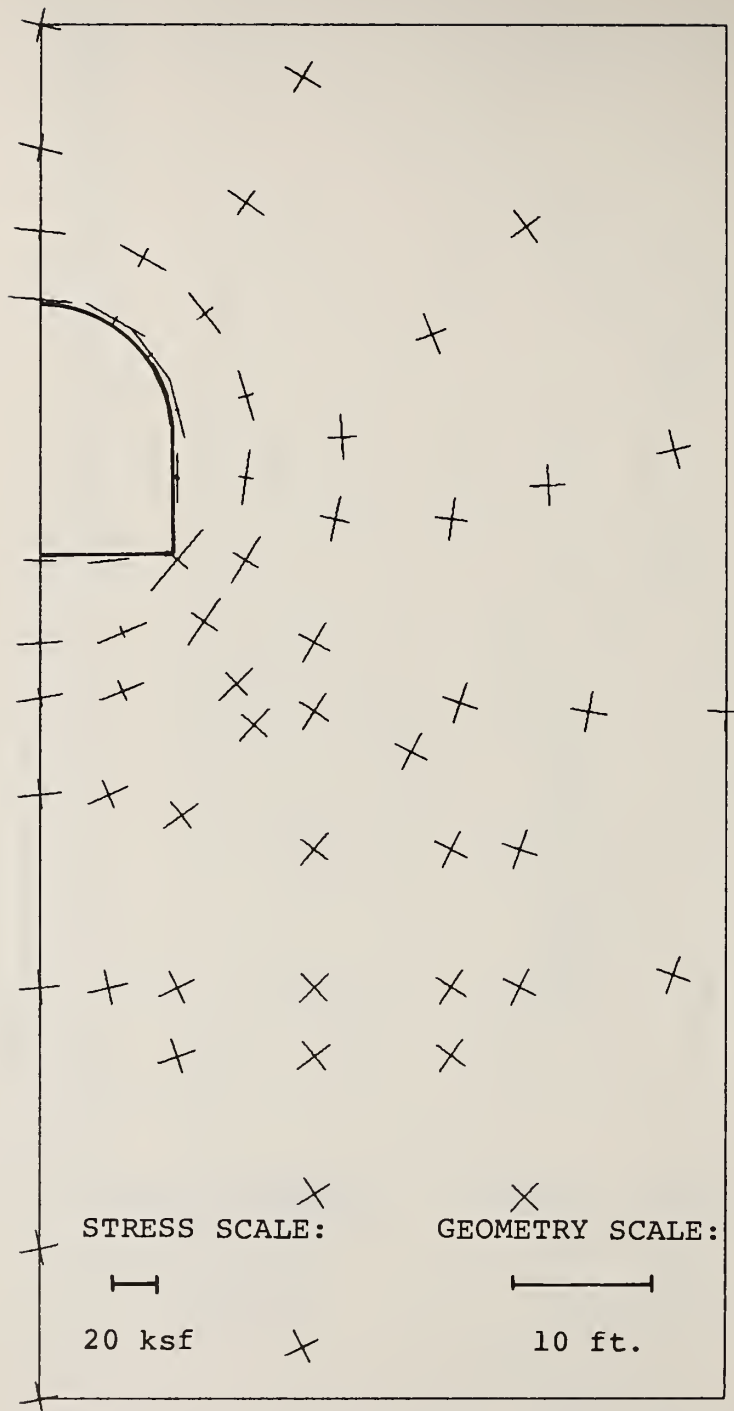


FIGURE 3.2c. PRINCIPAL STRESSES AT STATION 20+50 -- STEP 4

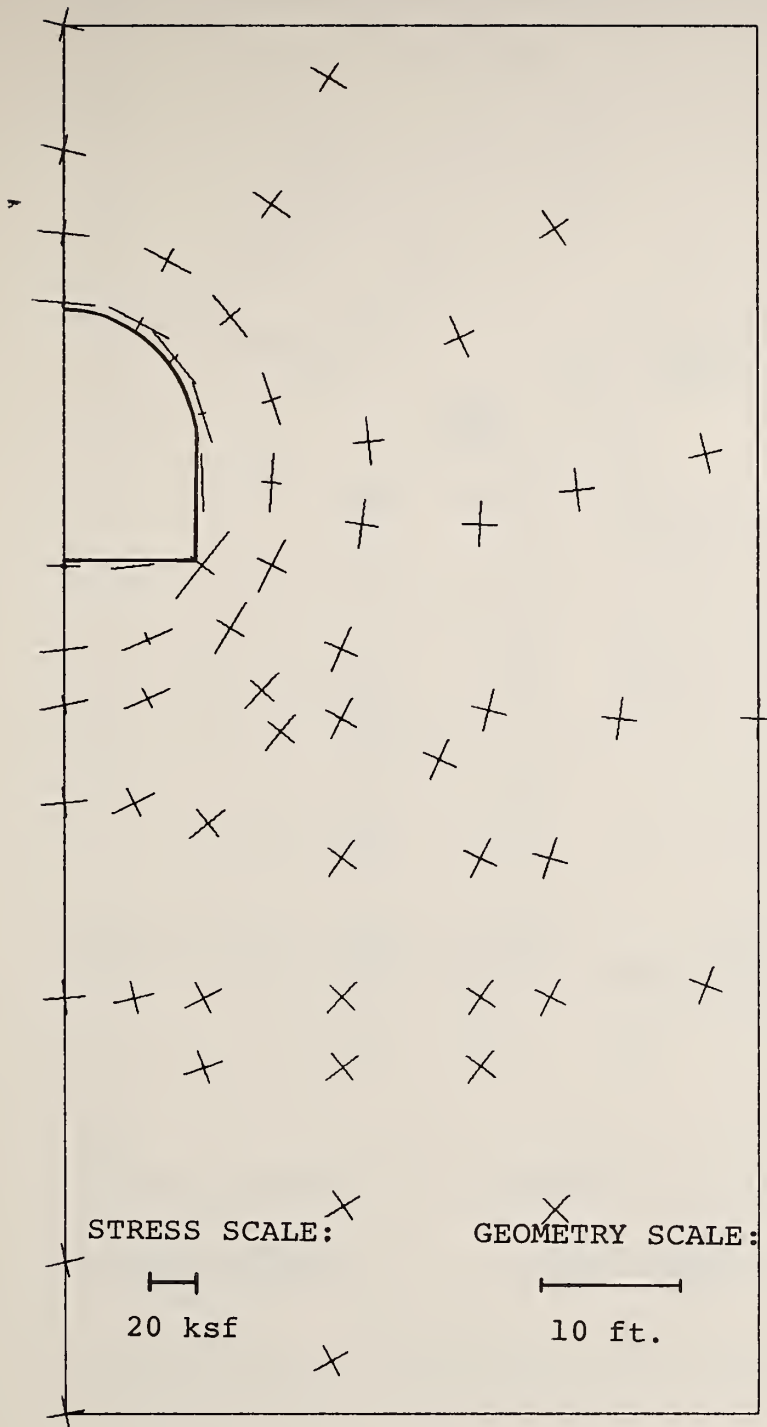


FIGURE 3.2d. PRINCIPAL STRESSES AT STATION 20+65 -- STEP 4

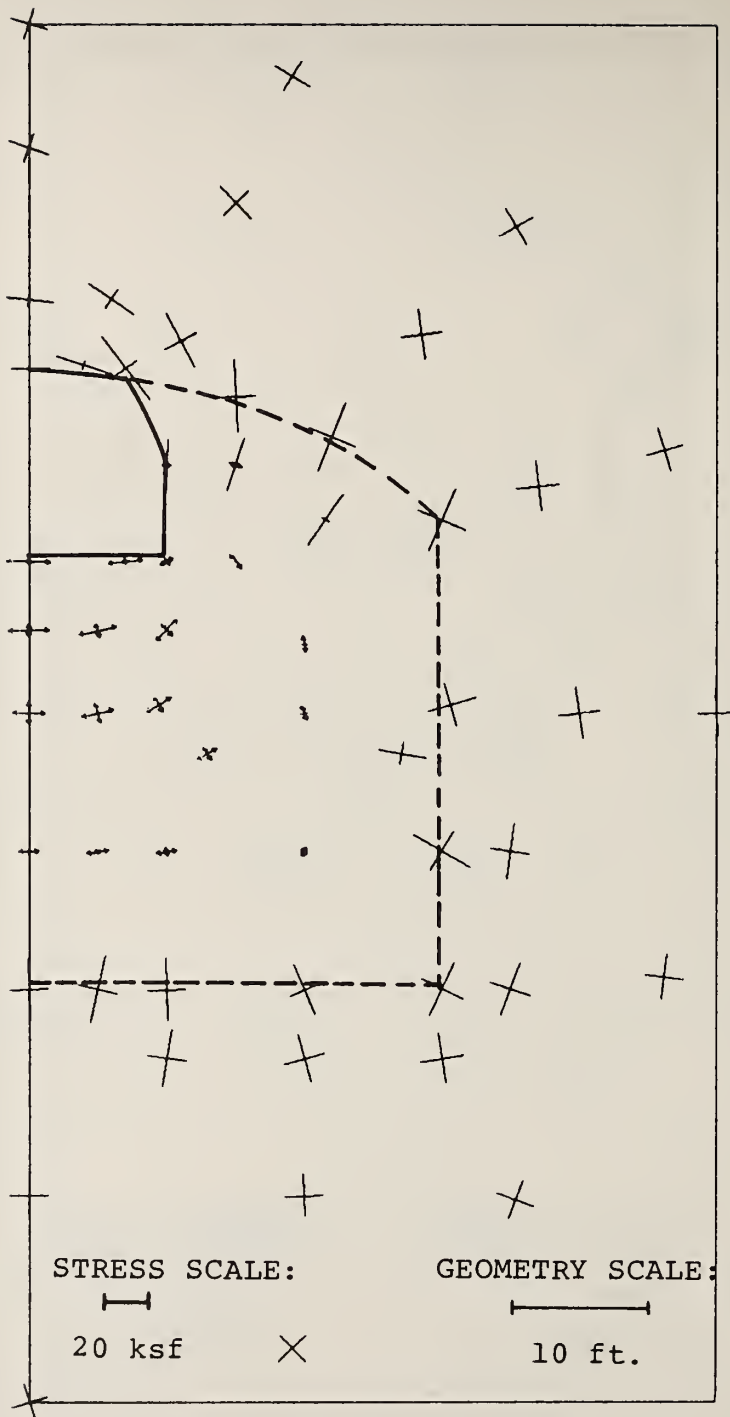


FIGURE 3.2e. PRINCIPAL STRESSES AT STATION 21+30 -- STEP 4

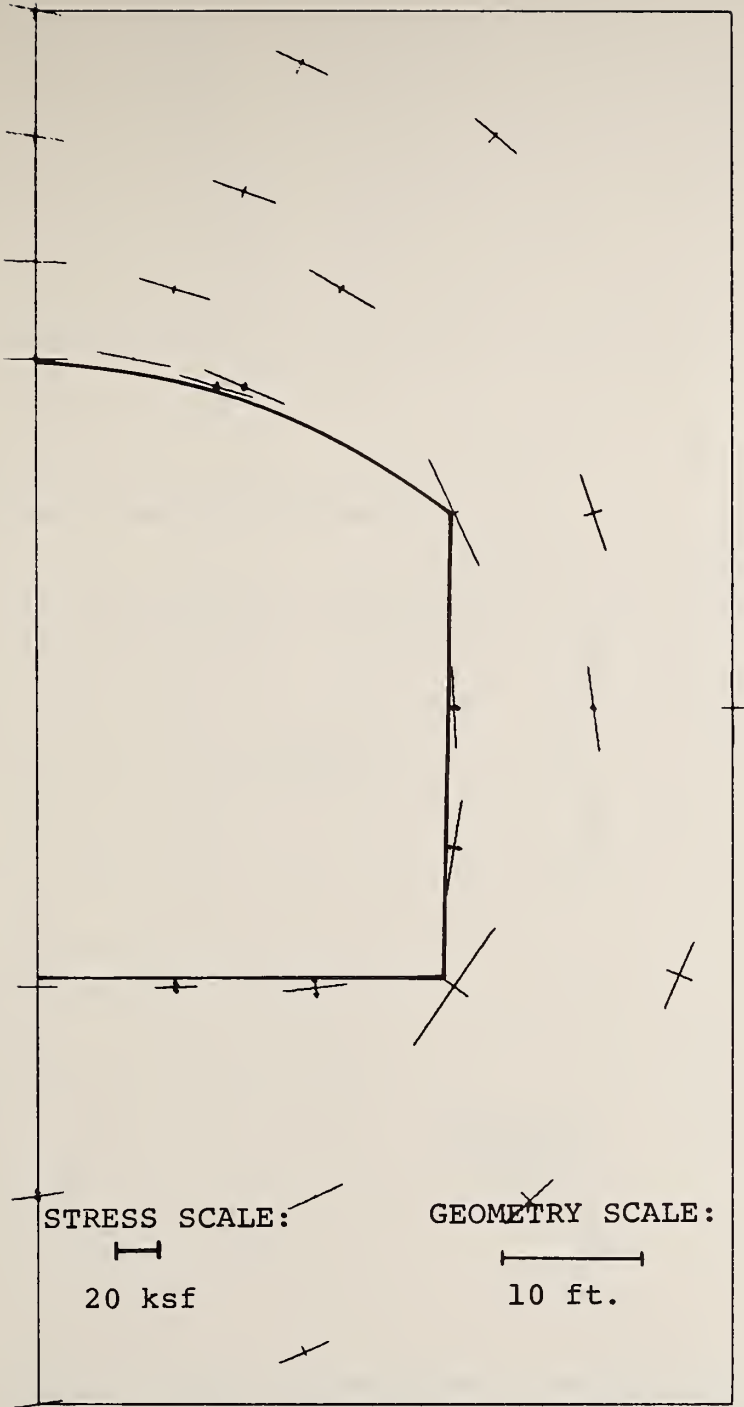
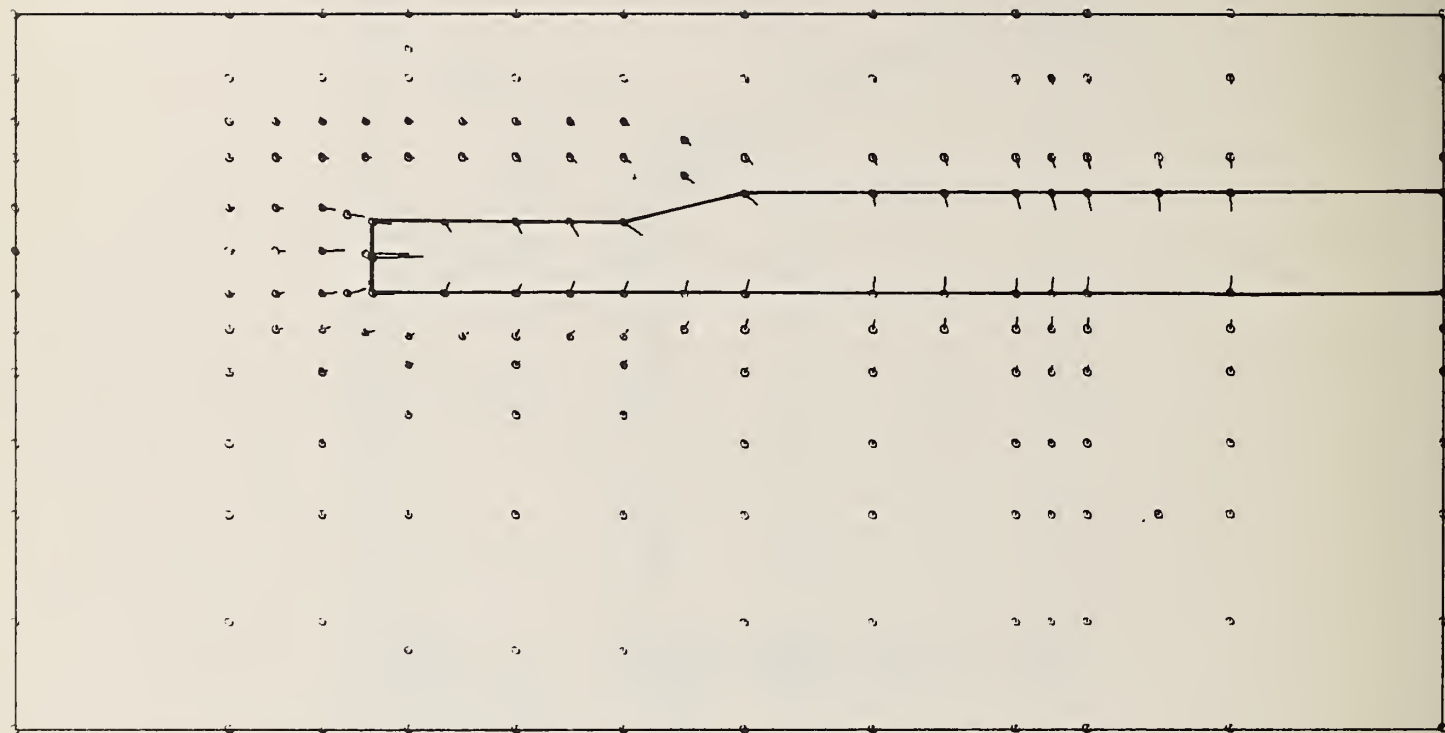
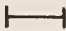


FIGURE 3.2f. PRINCIPAL STRESSES AT STATION 23+00 -- STEP 4



DISPLACEMENT
SCALE:

 0.001 ft.

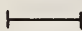
GEOMETRY
SCALE:

 10 ft.

FIGURE 3.3a. INCREMENTAL DISPLACEMENTS ALONG PLANE OF SYMMETRY
STEP 1

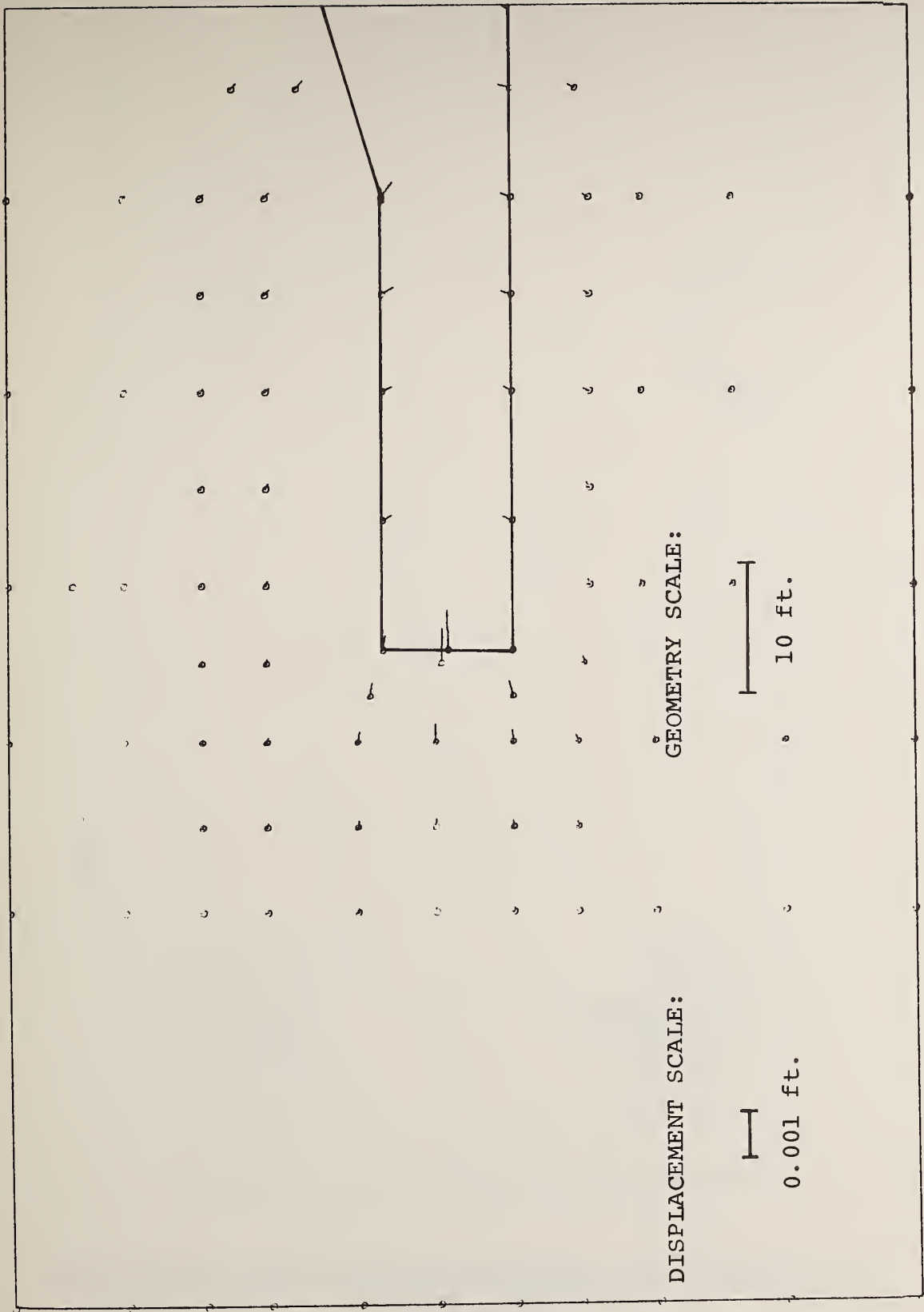


FIGURE 3.3b. INCREMENTAL DISPLACEMENTS OF THE FRONT END OF THE RESEARCH CHAMBER ALONG PLANE OF SYMMETRY -- STEP 1

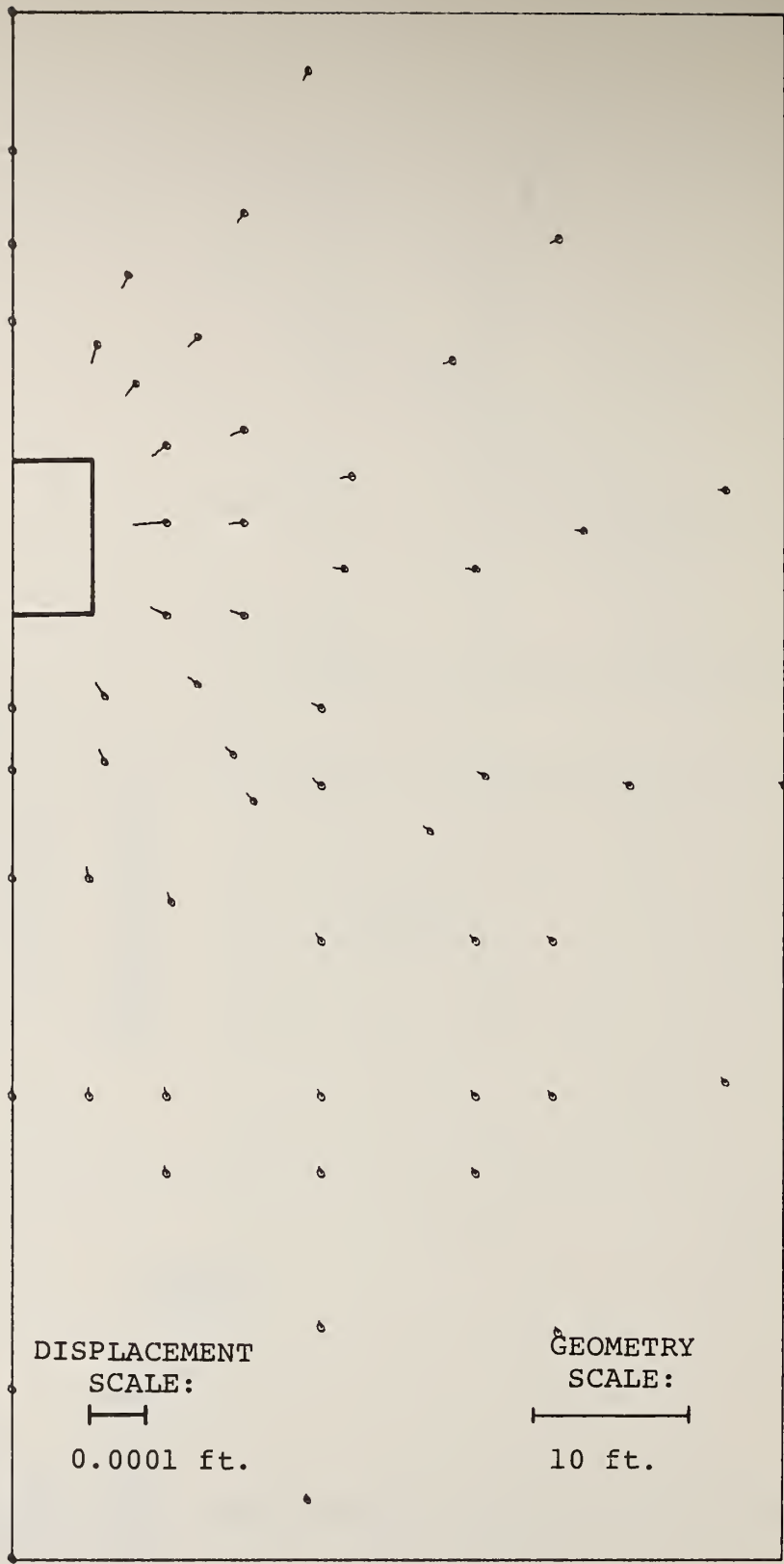


FIGURE 3.3c. INCREMENTAL DISPLACEMENTS AT STATION 20+35 -- STEP 1

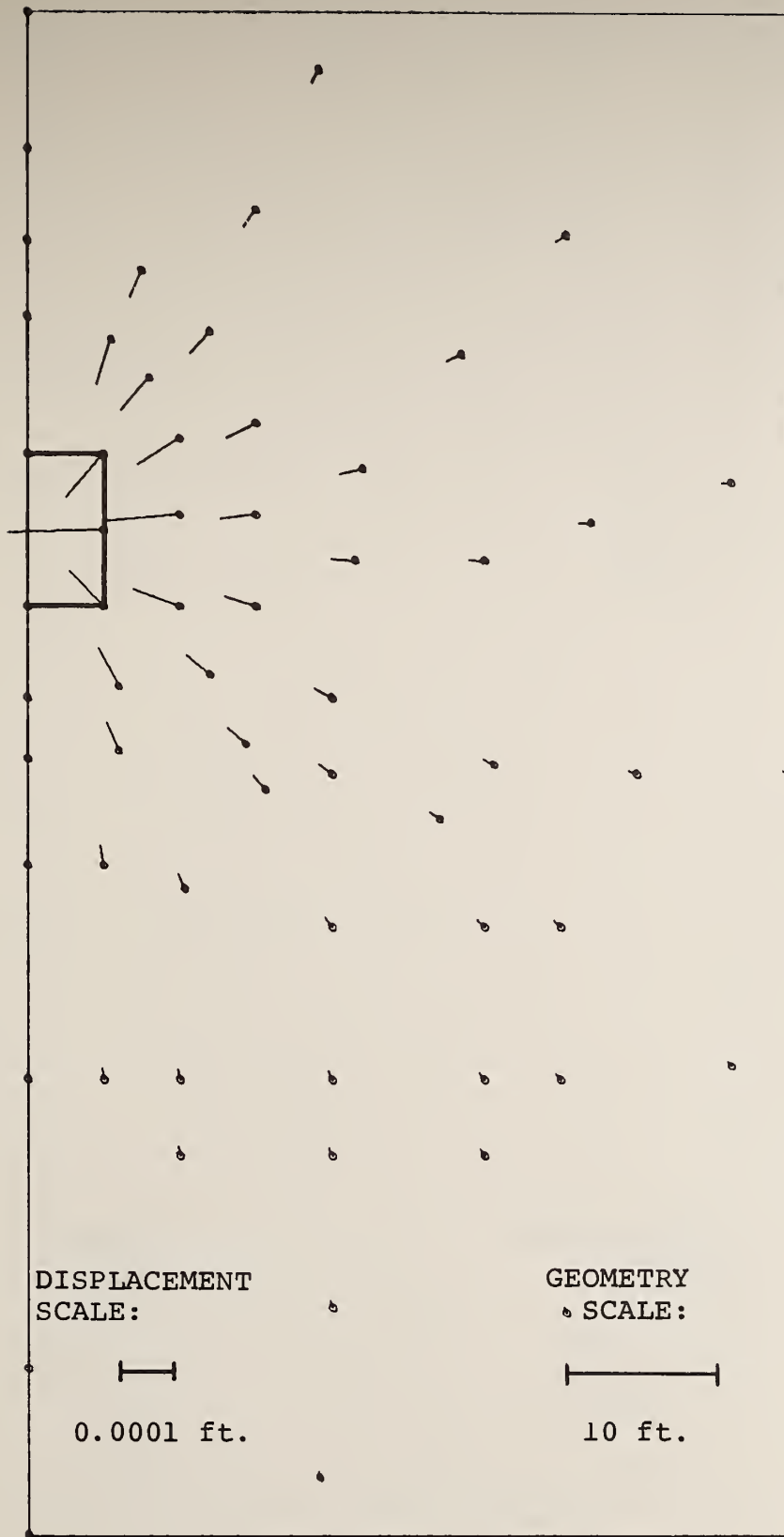


FIGURE 3.3d. INCREMENTAL-DISPLACEMENTS AT STATION 20+50 -- STEP 1

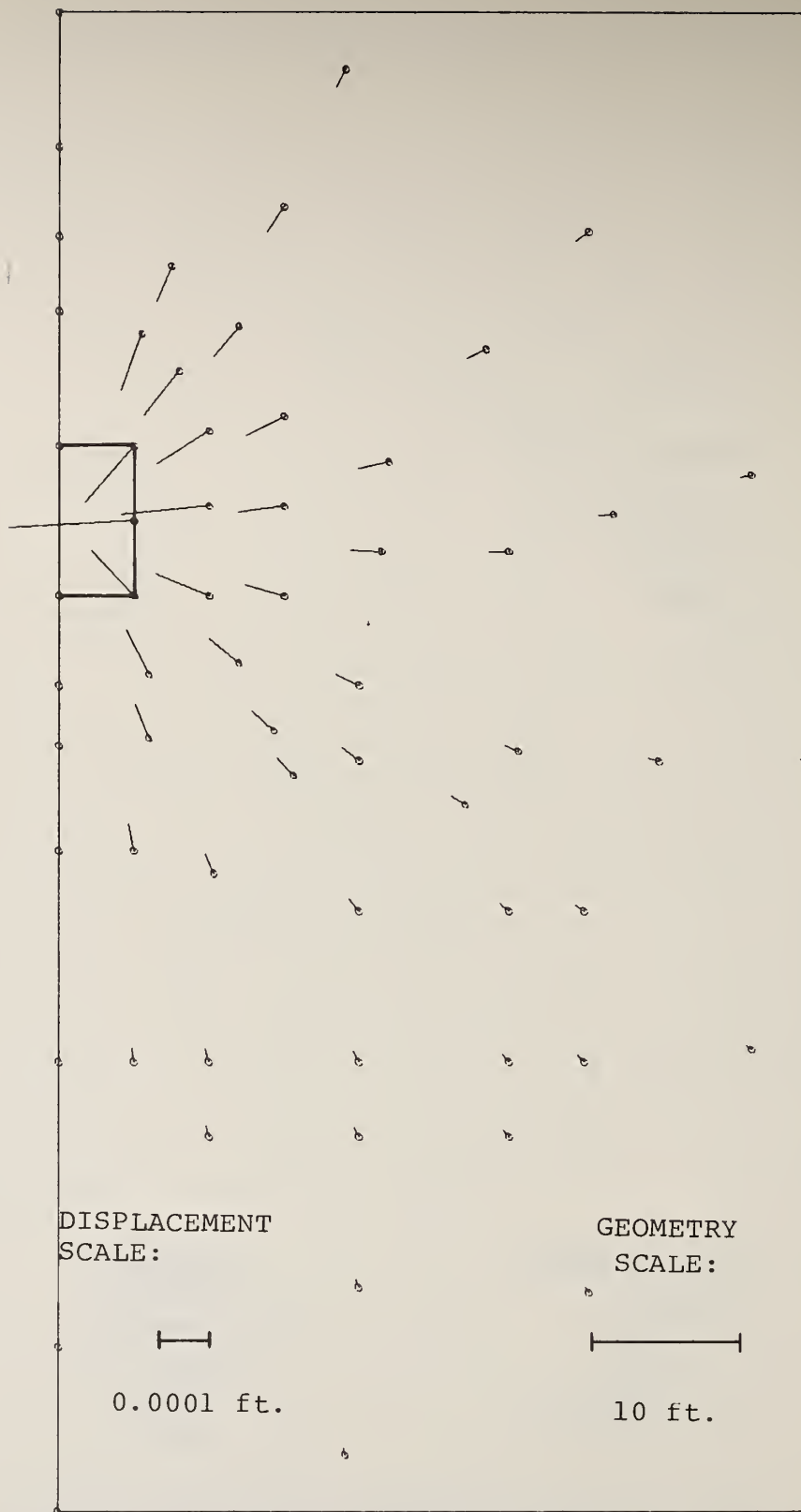


FIGURE 3.3e. INCREMENTAL DISPLACEMENTS AT STATION
20+65 -- STEP 1

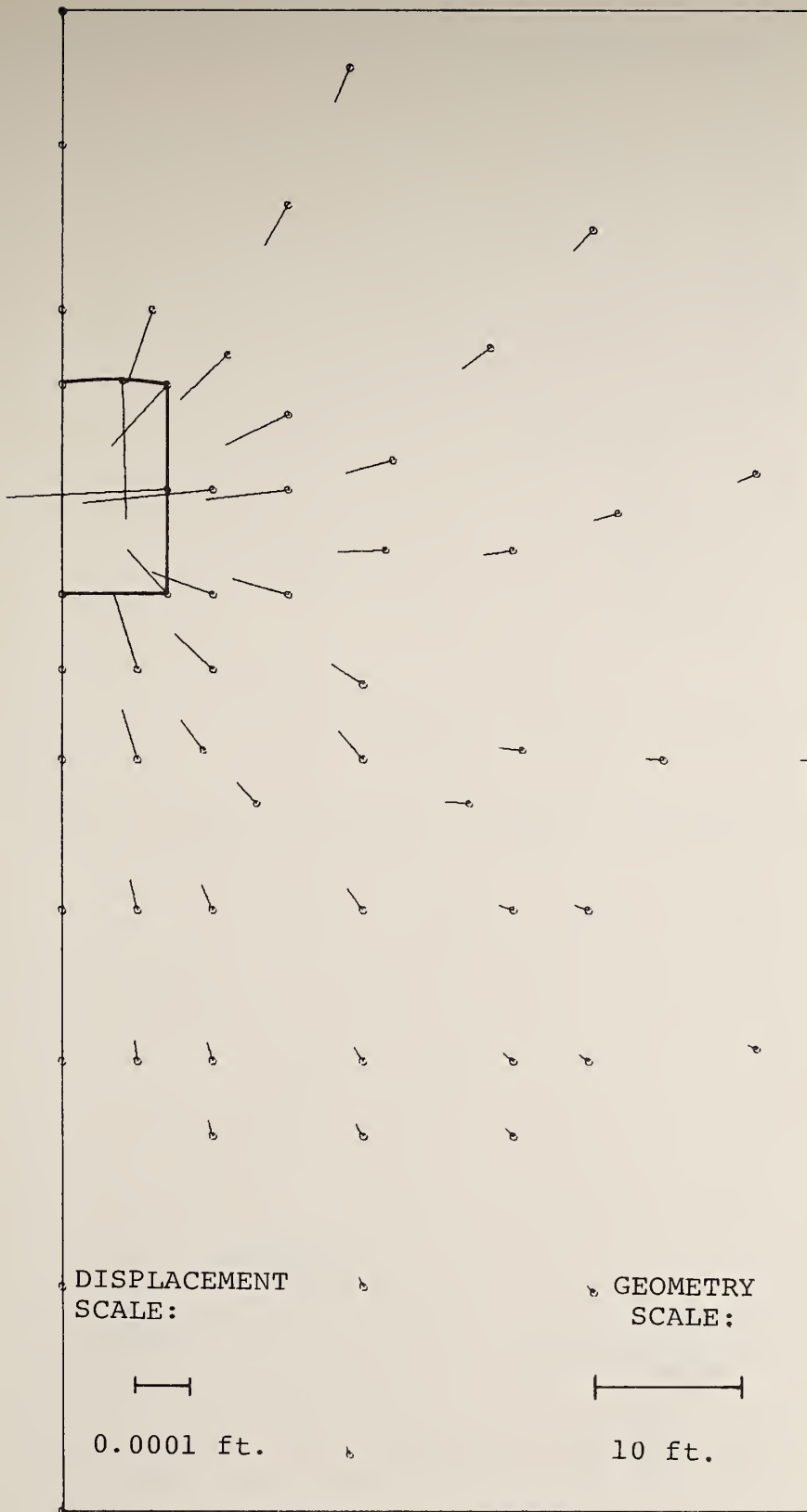


FIGURE 3.3f. INCREMENTAL DISPLACEMENT AT STATION 21+30 -- STEP 1

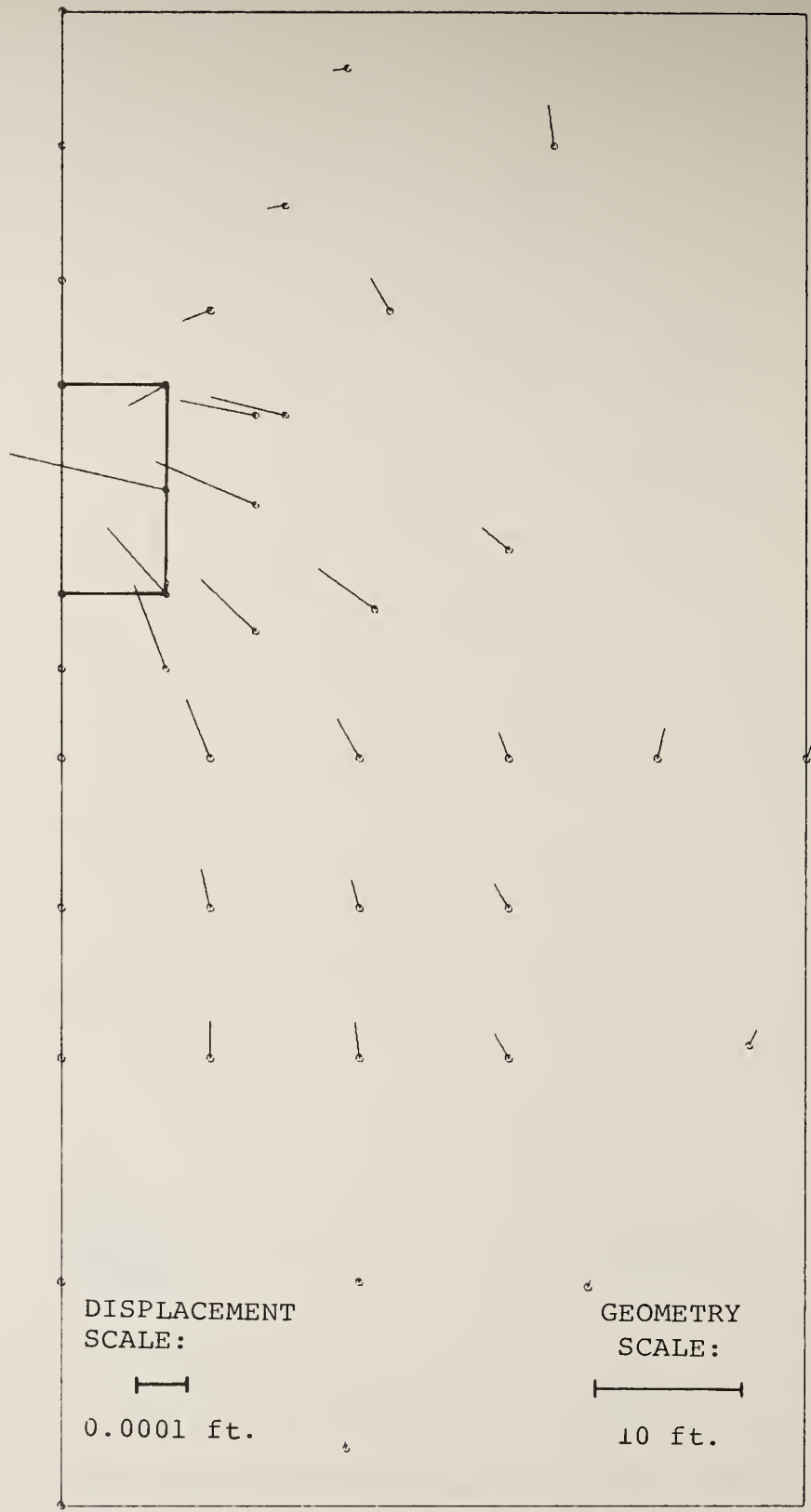
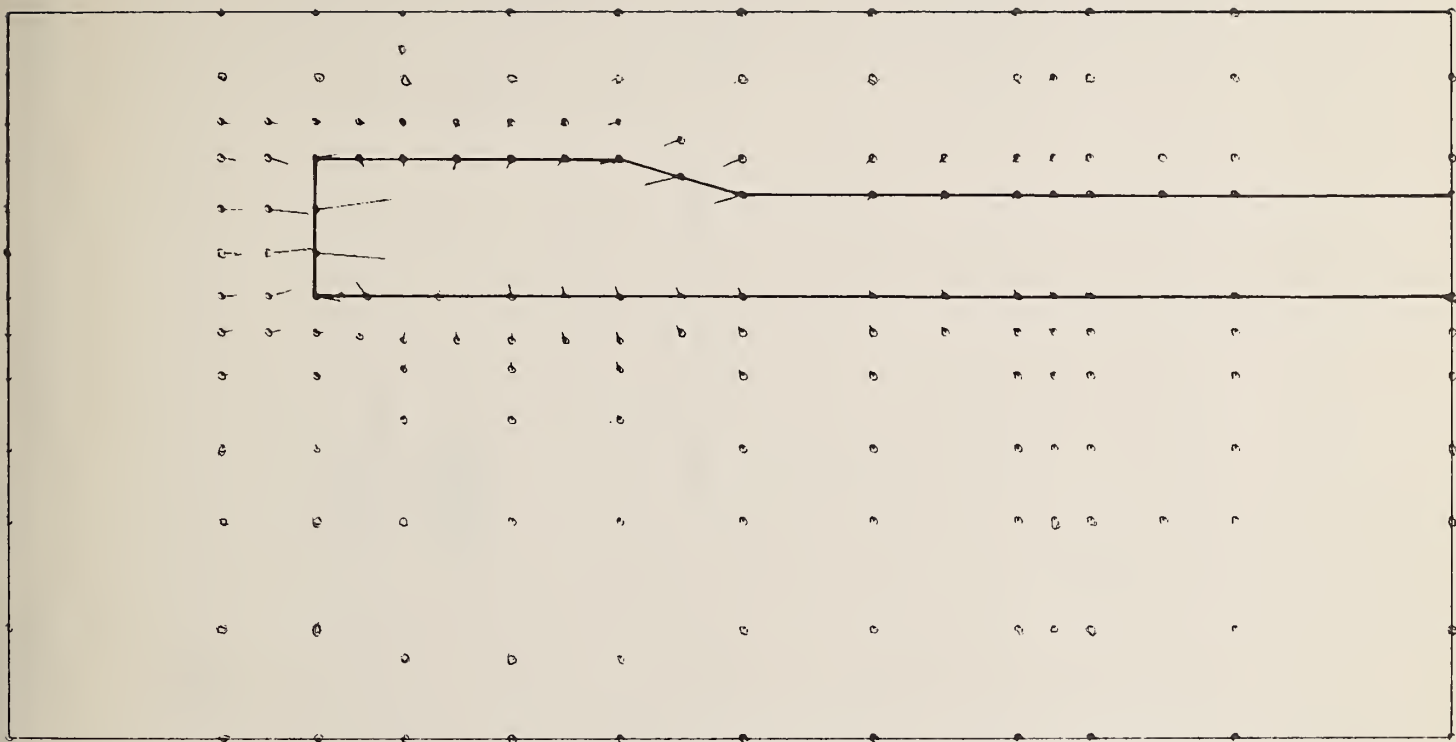


FIGURE 3.3g. INCREMENTAL DISPLACEMENT AT STATION 23+00 -- STEP 1



DISPLACEMENT
SCALE:



0.001 ft.

GEOMETRY
SCALE:



10 ft.

FIGURE 3.4a. DISPLACEMENTS ALONG PLANE OF SYMMETRY -- STEP 2

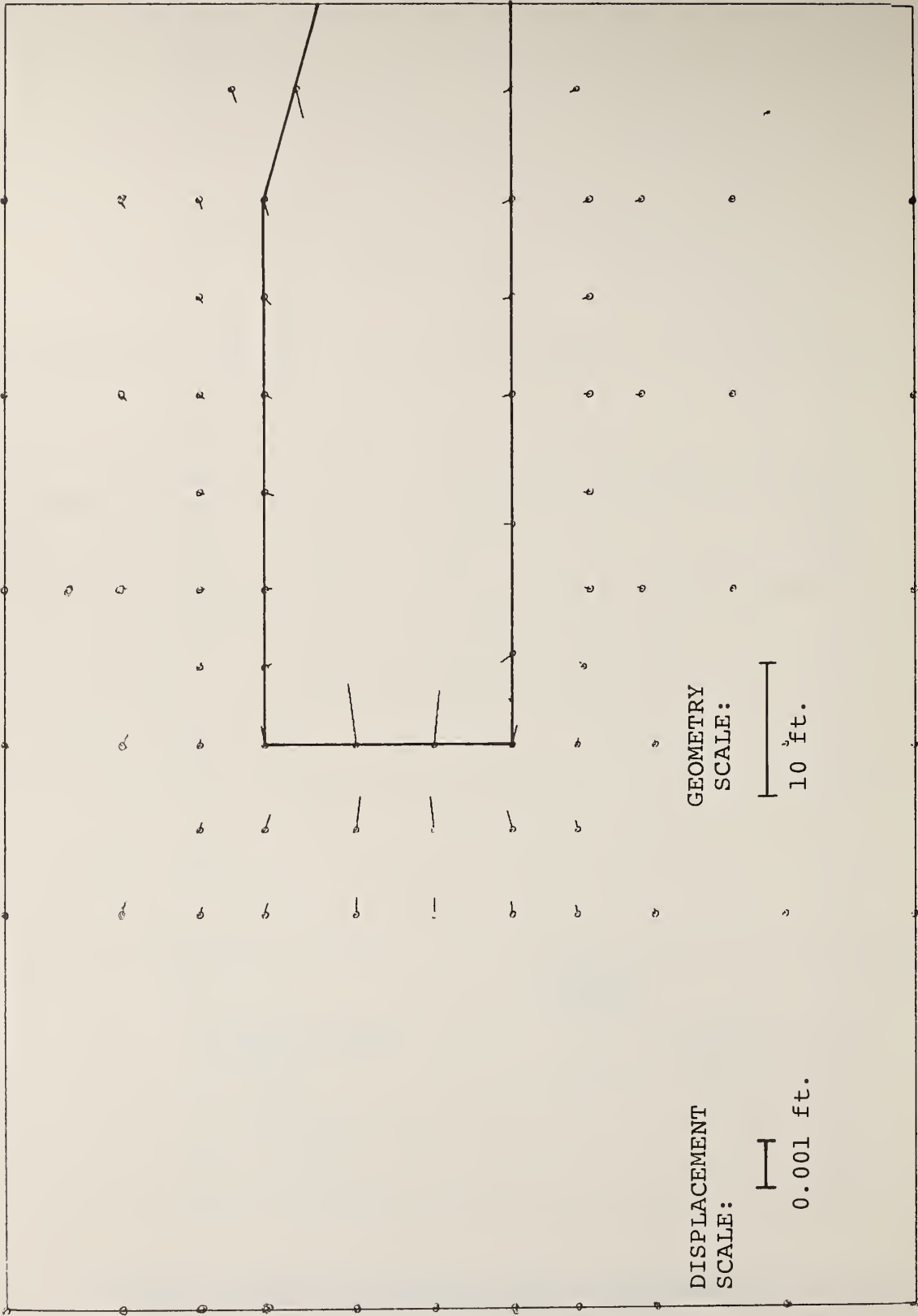


FIGURE 3.4b. DISPLACEMENTS AT THE FRONT END OF THE RESEARCH CHAMBER ALONG PLANE OF SYMMETRY -- STEP 2

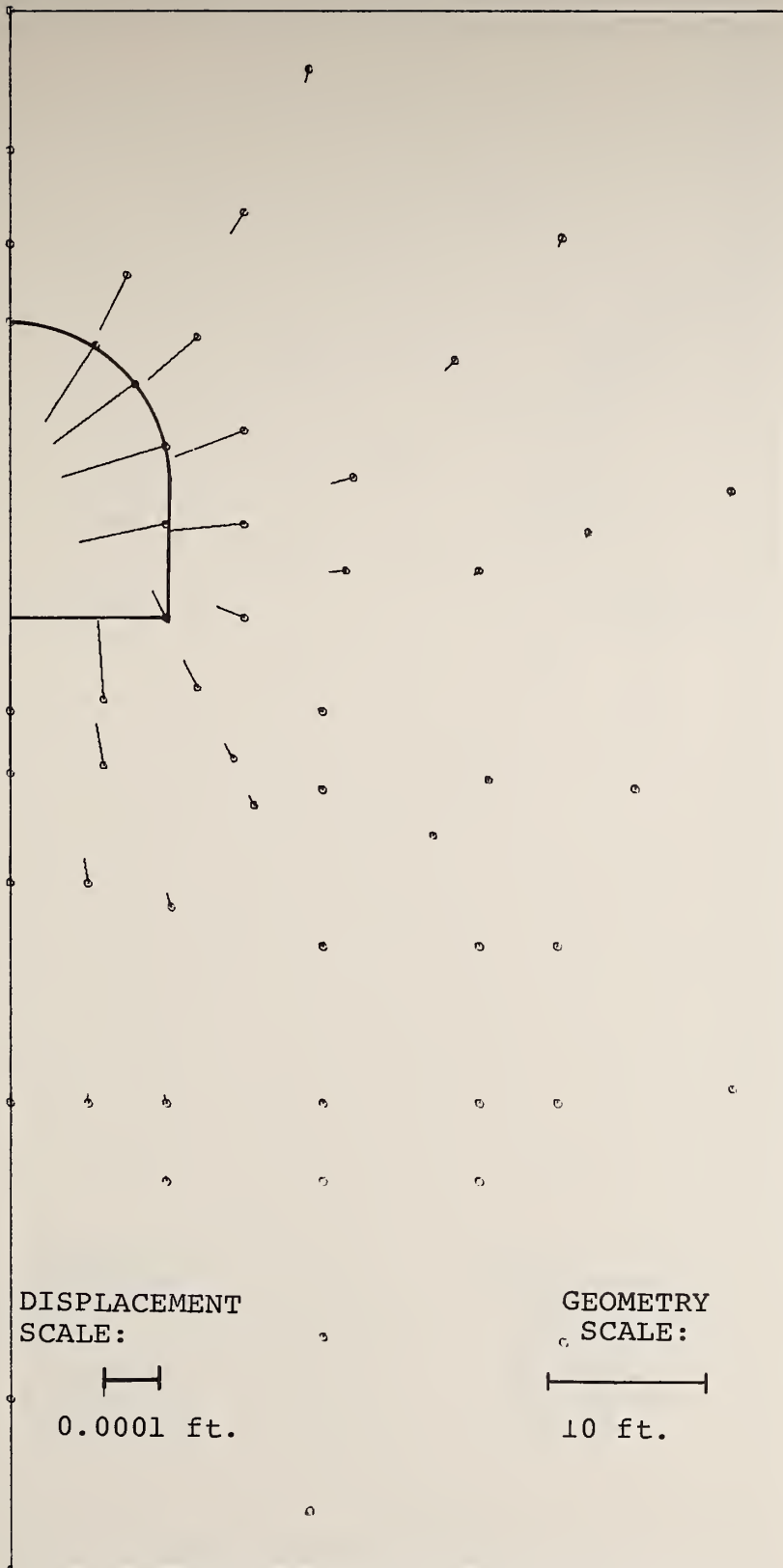


FIGURE 3.4c. DISPLACEMENTS AT STATION 20+35 -- STEP 2

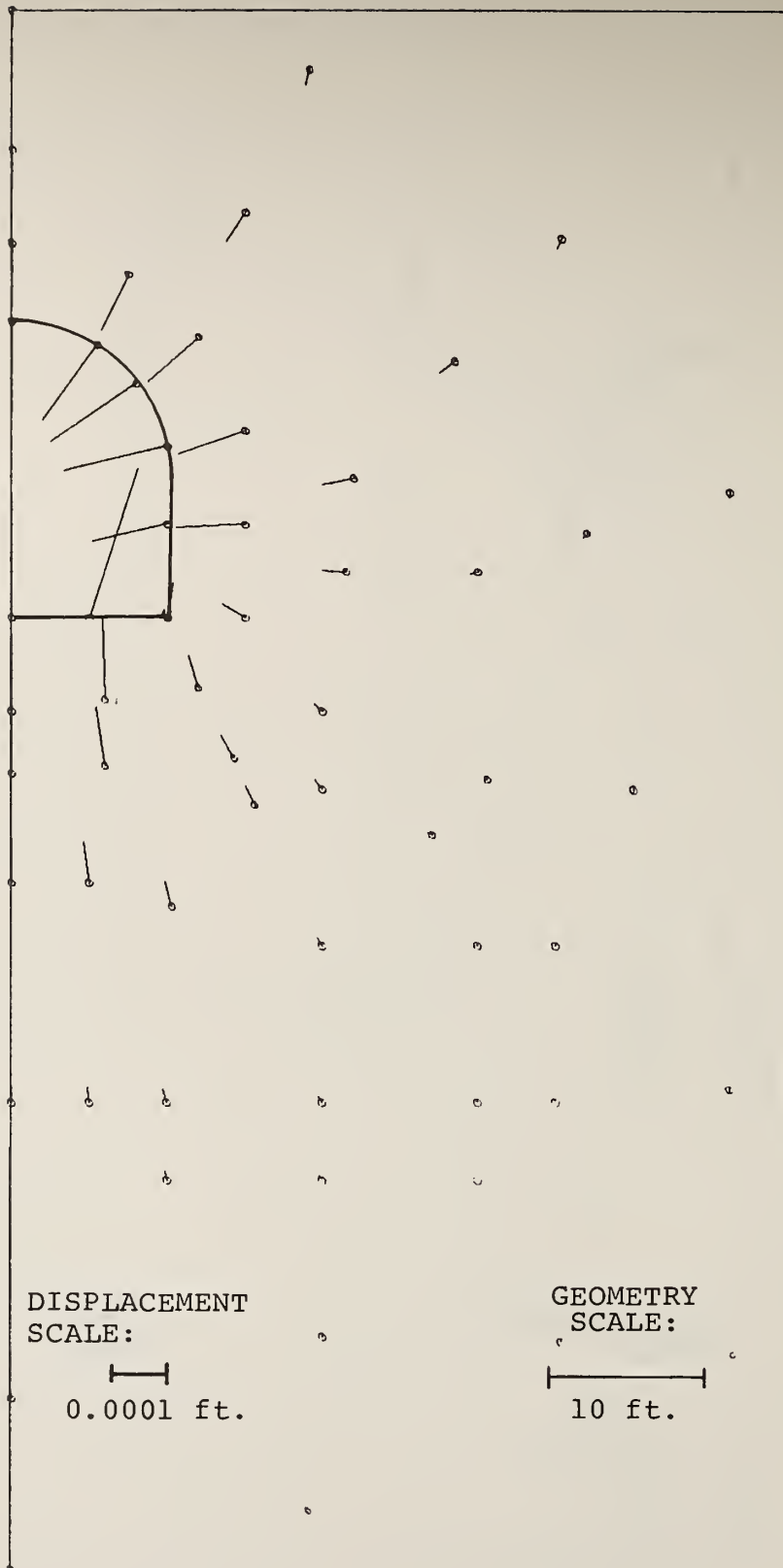


FIGURE 3.4d. DISPLACEMENTS AT STATION 20+50 -- STEP 2

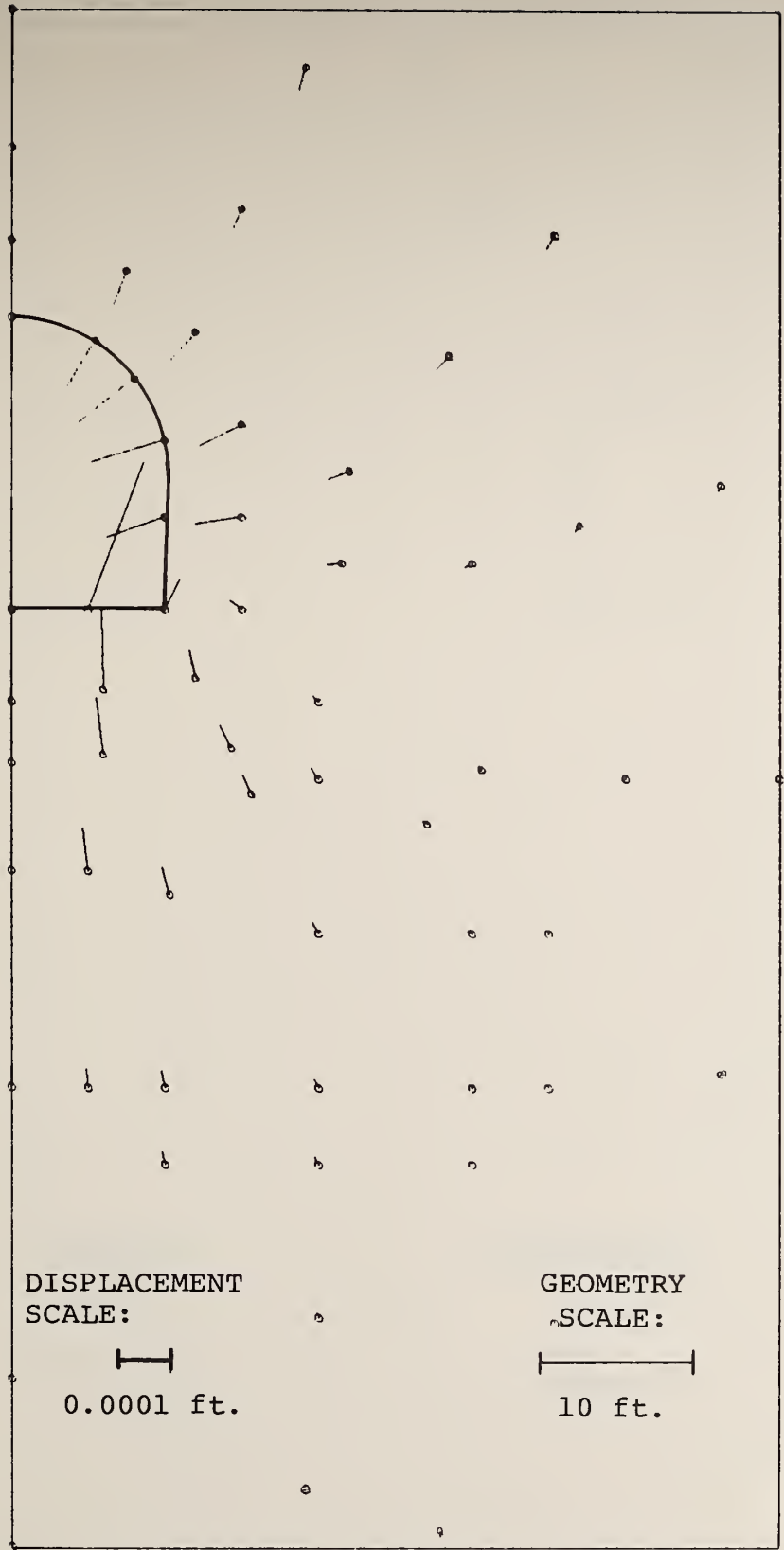


FIGURE 3.4e. DISPLACEMENTS AT STATION 20+65 -- STEP 2

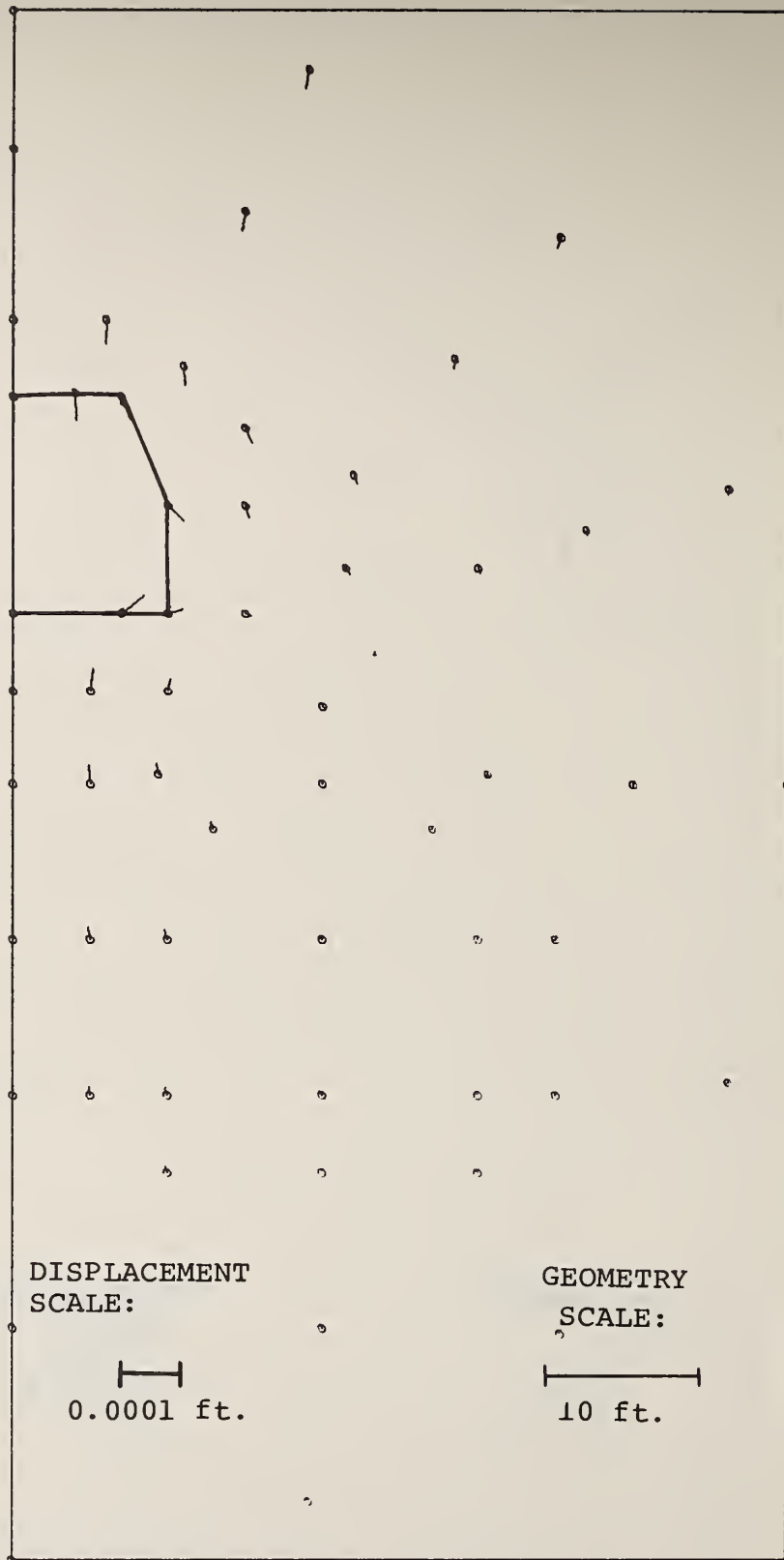


FIGURE 3.4f. DISPLACEMENTS AT STATION 21+30 -- STEP 2



FIGURE 3.4g. DISPLACEMENTS AT STATION 23+00 -- STEP 2

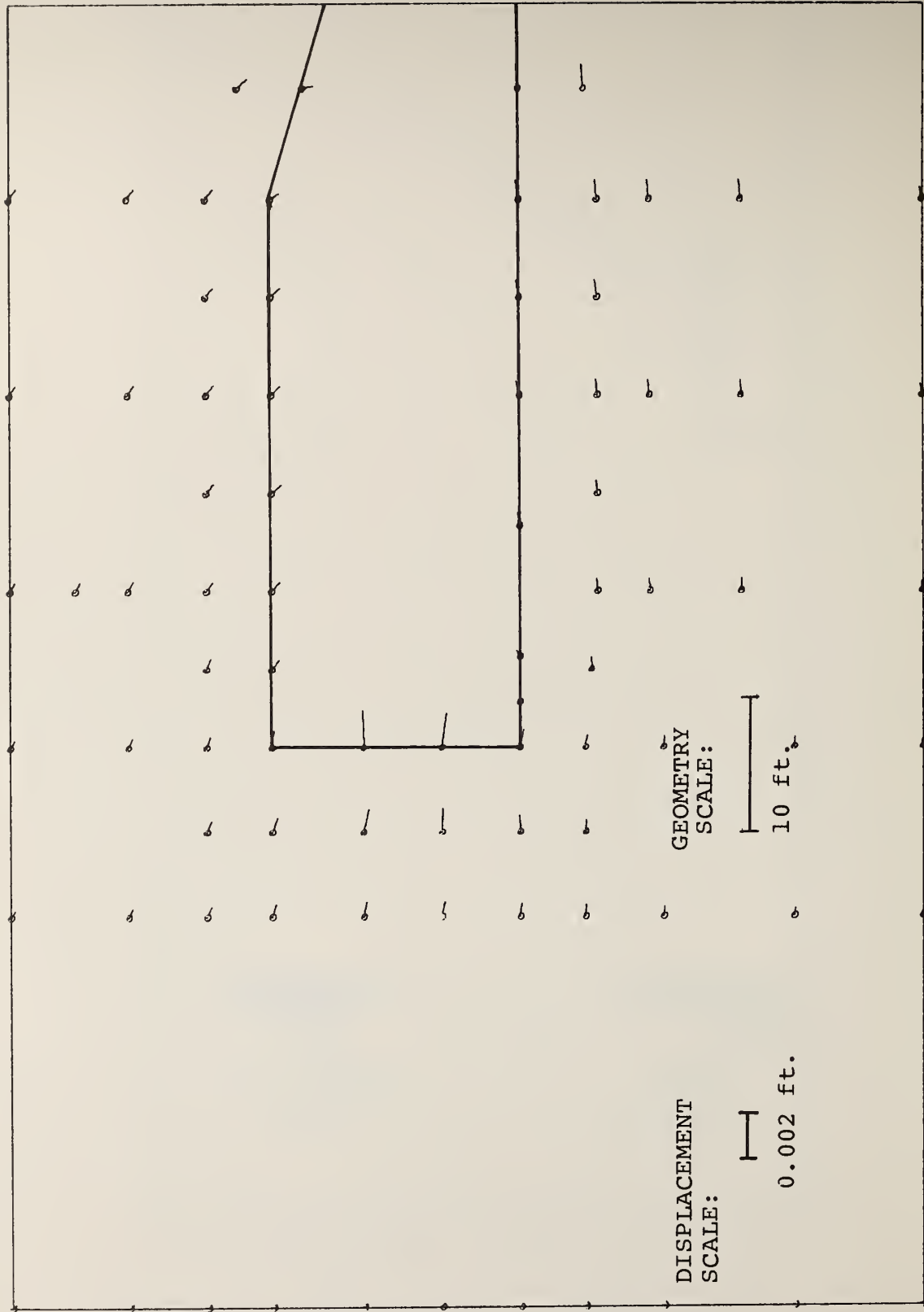


FIGURE 3.5a. DISPLACEMENTS AT THE FRONT END OF THE RESEARCH CHAMBER ALONG PLANE OF SYMMETRY -- STEP 4



FIGURE 3.5b. DISPLACEMENTS AT STATION 20+35 -- STEP 4

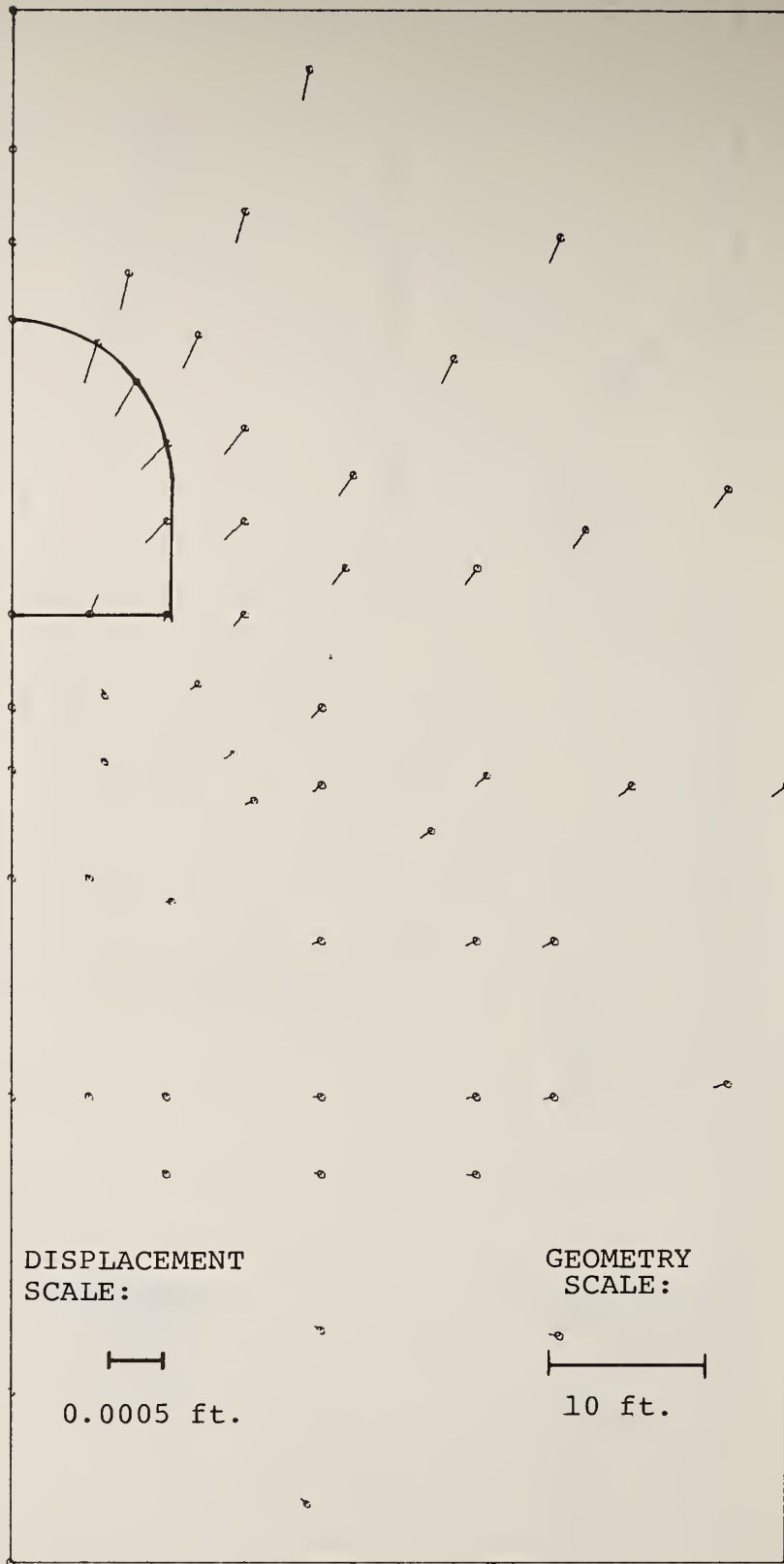


FIGURE 3.5c. DISPLACEMENTS AT STATION 20+50 -- STEP 4



FIGURE 3.5d. DISPLACEMENTS AT STATION 20+65 -- STEP 4

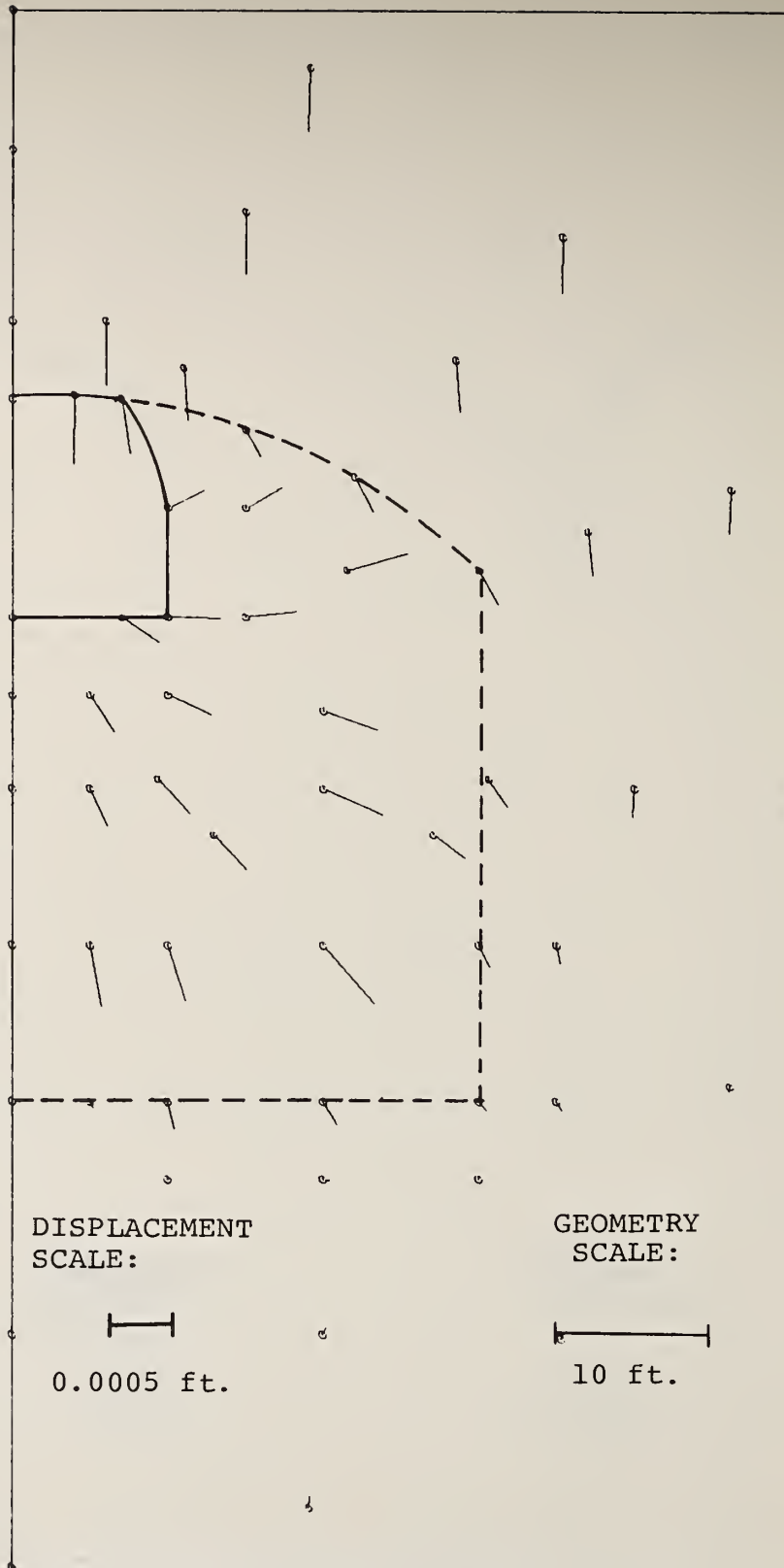


FIGURE 3.5e. DISPLACEMENTS AT STATION 21+30 -- STEP 4

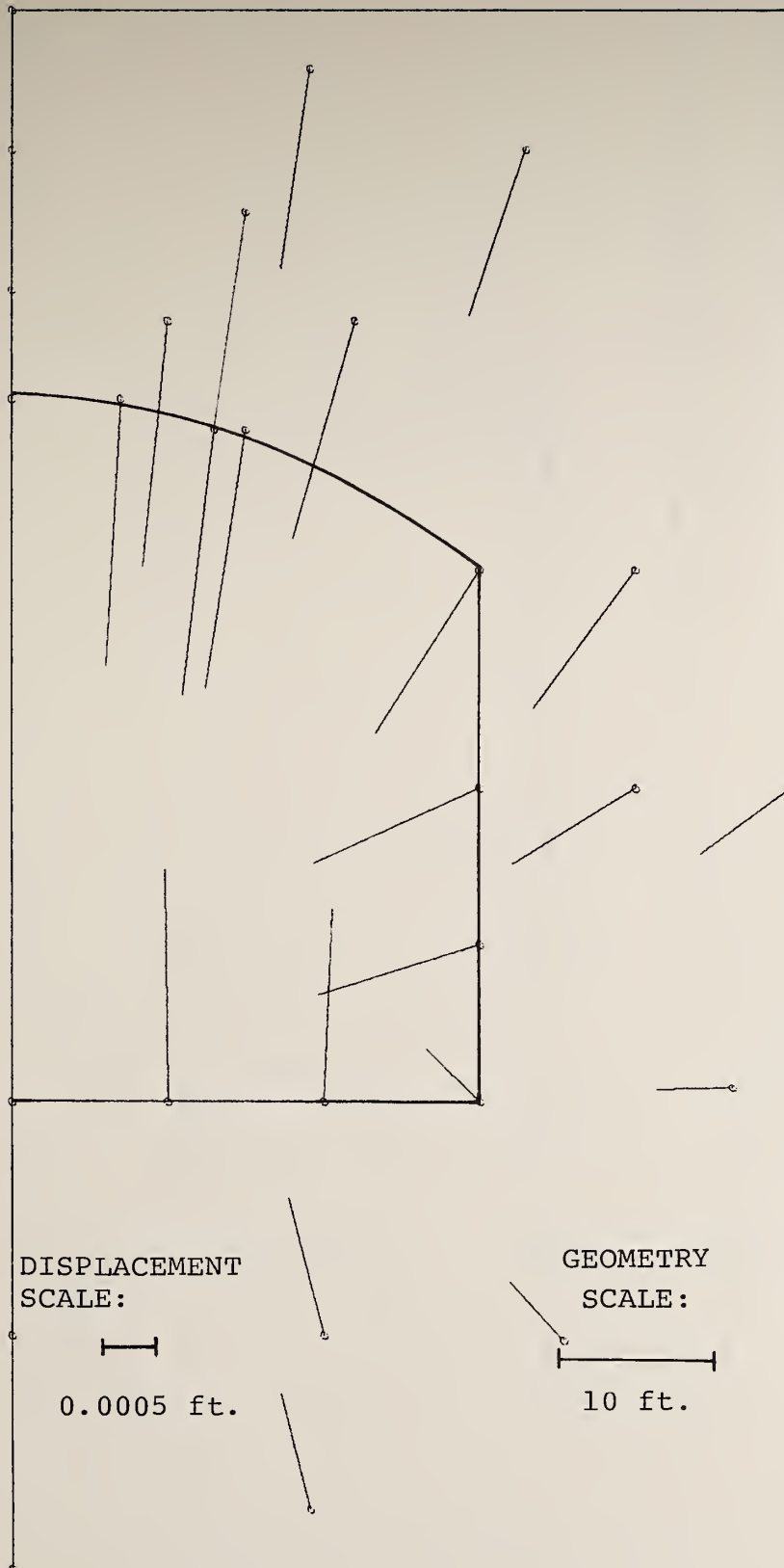


FIGURE 3.5f. DISPLACEMENTS AT STATION 23+00 -- STEP 4

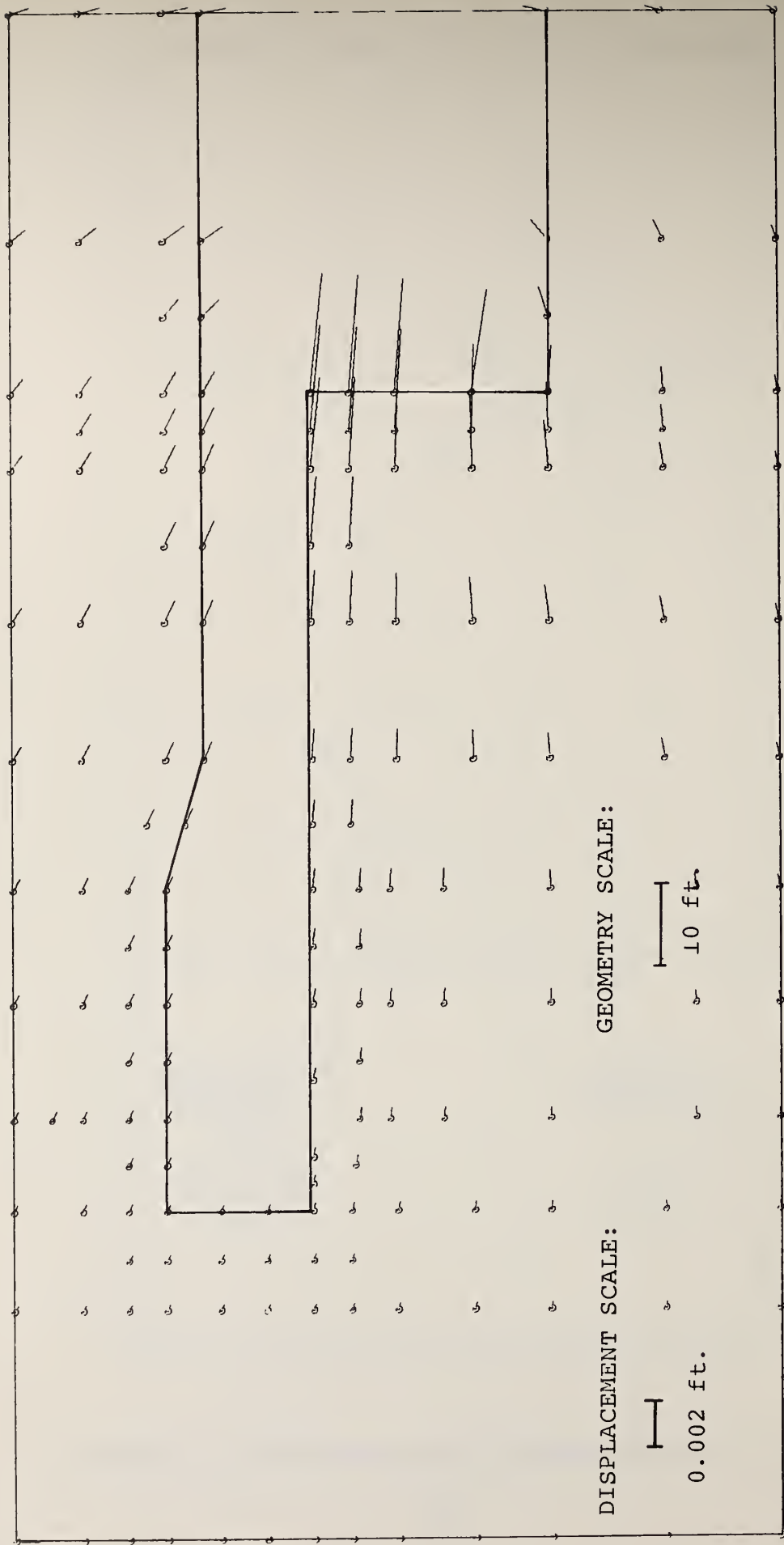


FIGURE 3.6a. DISPLACEMENTS ALONG PLANE OF SYMMETRY -- INC 24



FIGURE 3.6b. DISPLACEMENTS AT STATION 20+35 -- INC 24

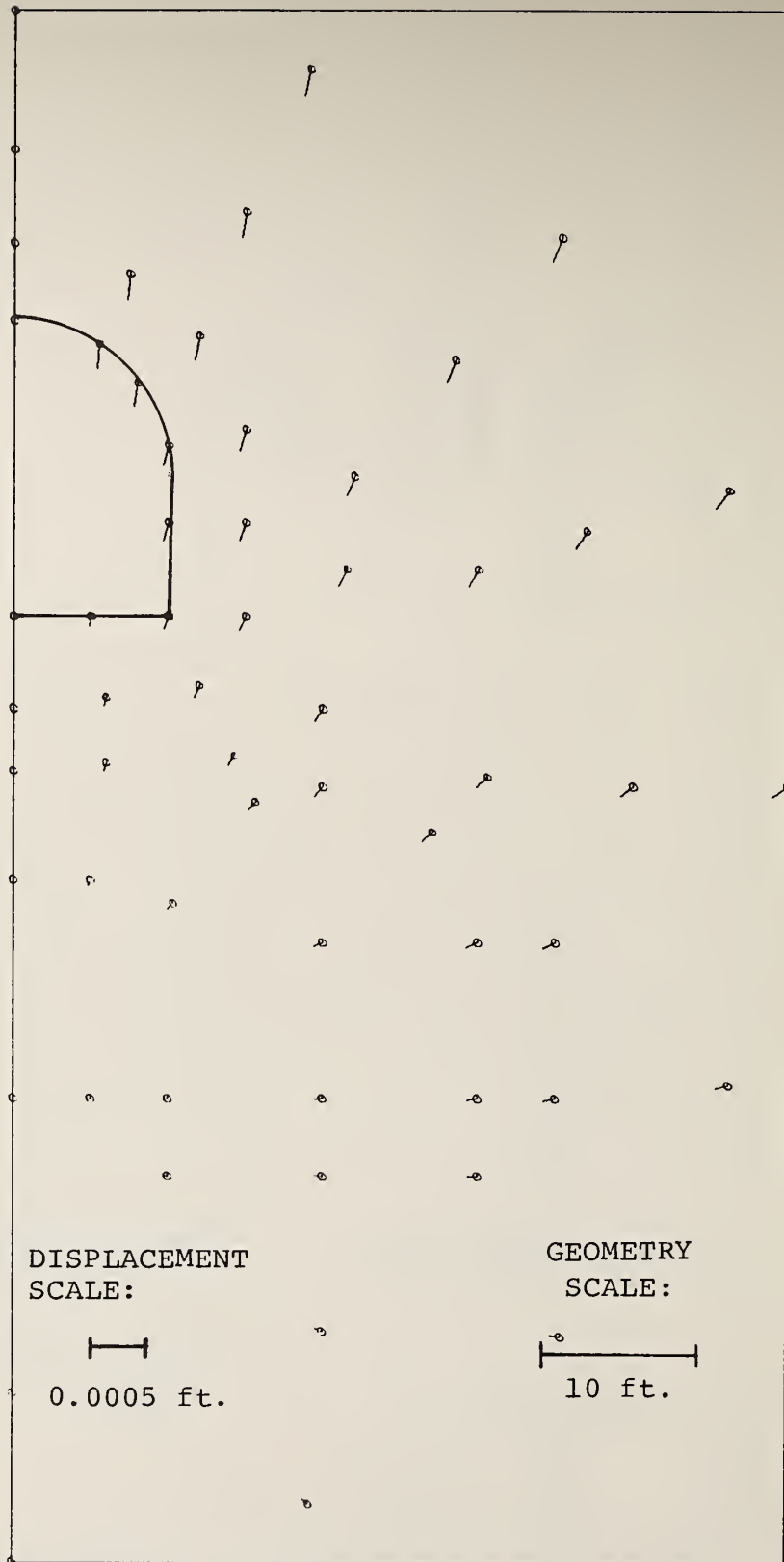


FIGURE 3.6c. DISPLACEMENTS AT STATION 20+50 -- INC 24

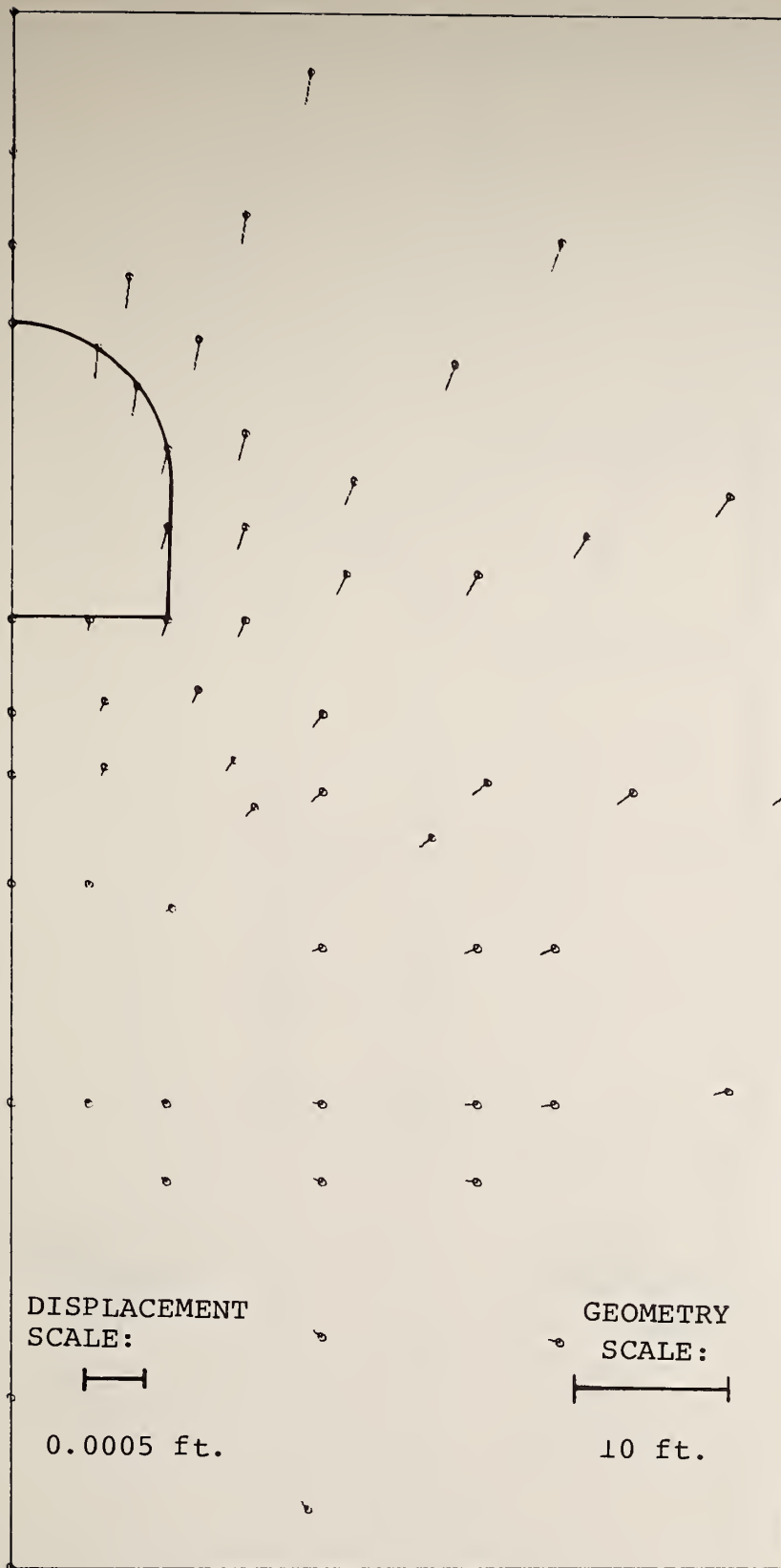


FIGURE 3.6d. DISPLACEMENTS AT STATION 20+65 -- INC 24

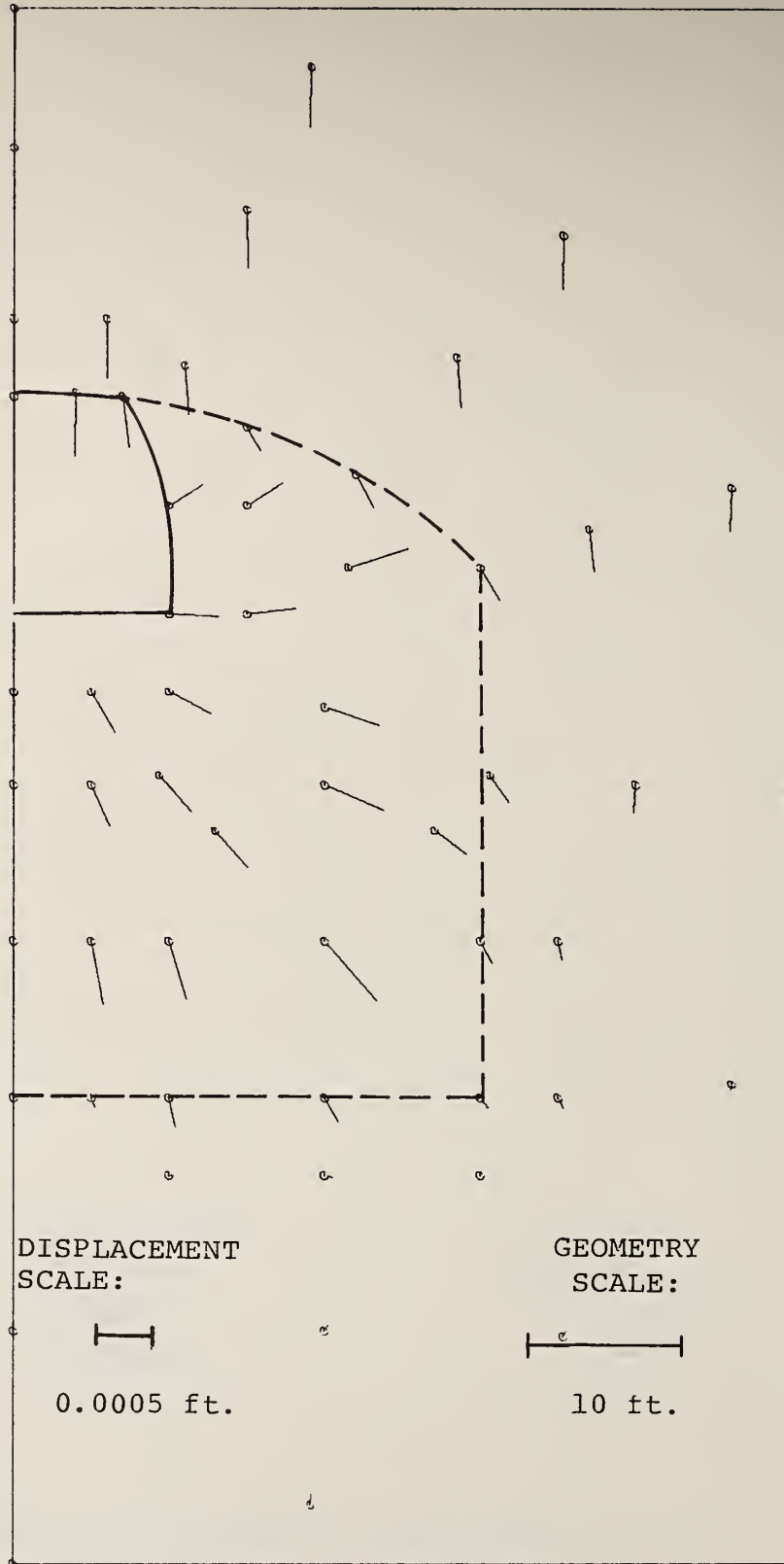


FIGURE 3.6e. DISPLACEMENTS AT STATION 21+30 -- INC 24

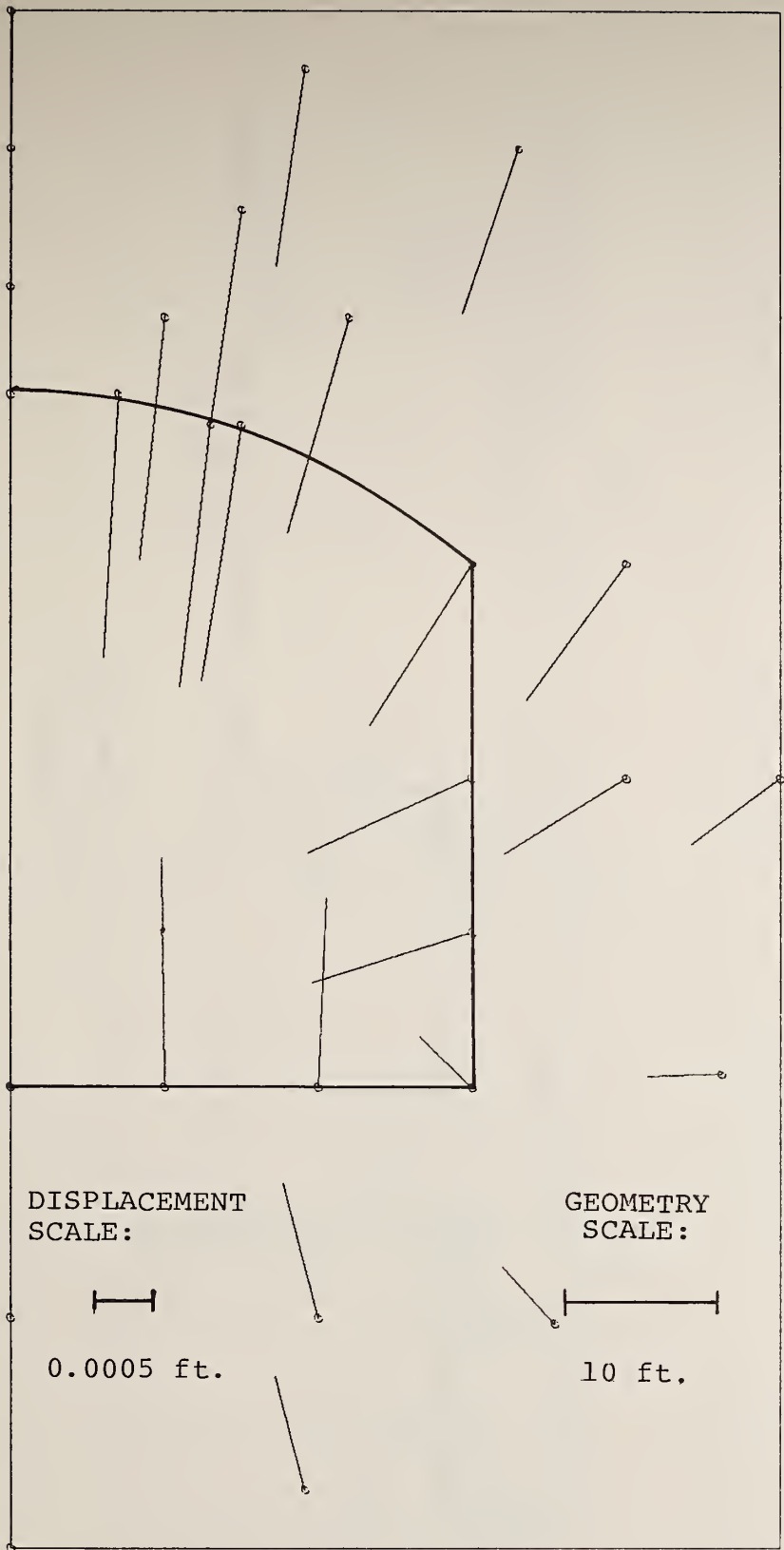


FIGURE 3.6f. DISPLACEMENTS AT STATION 23+00 -- INC 24

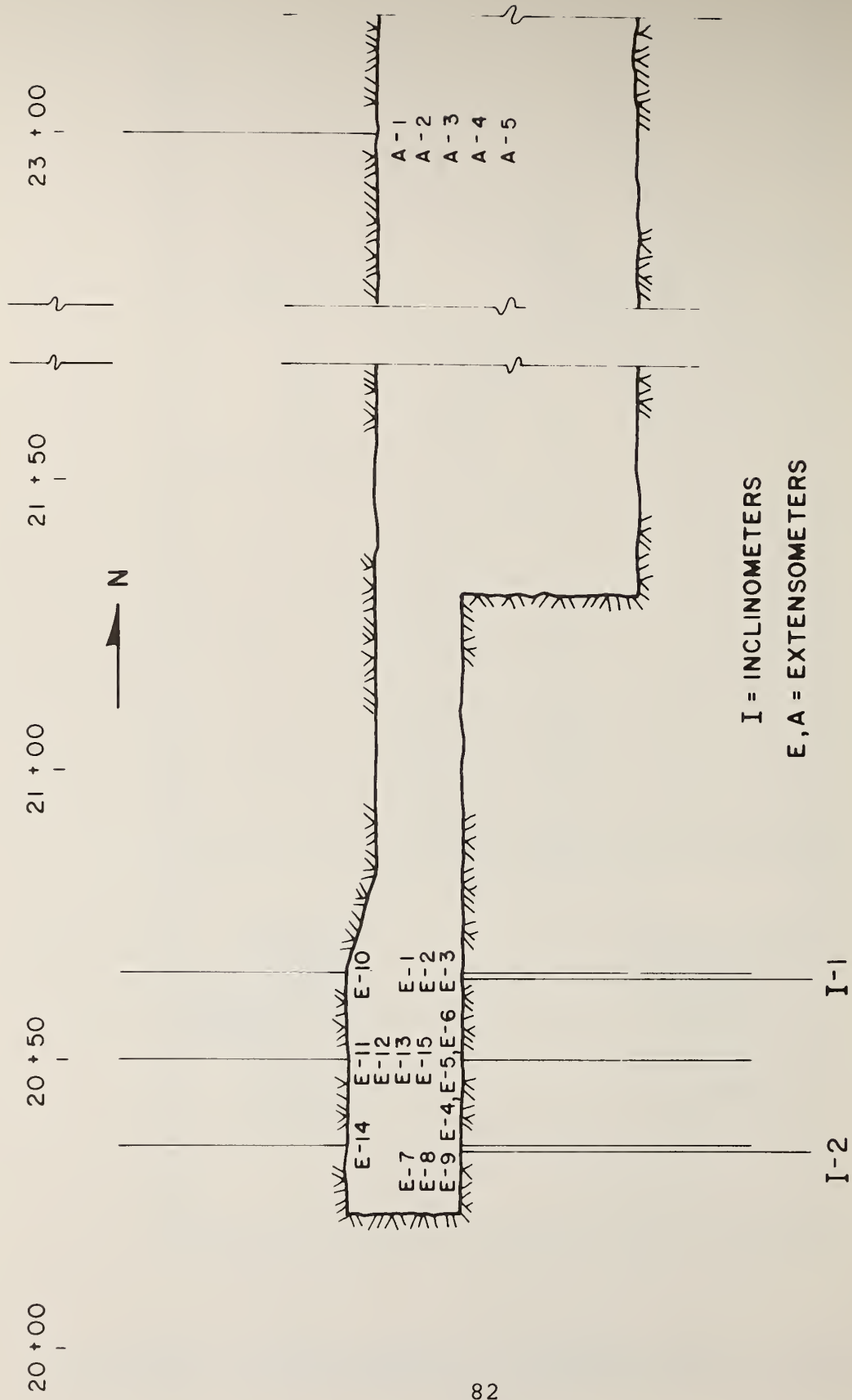
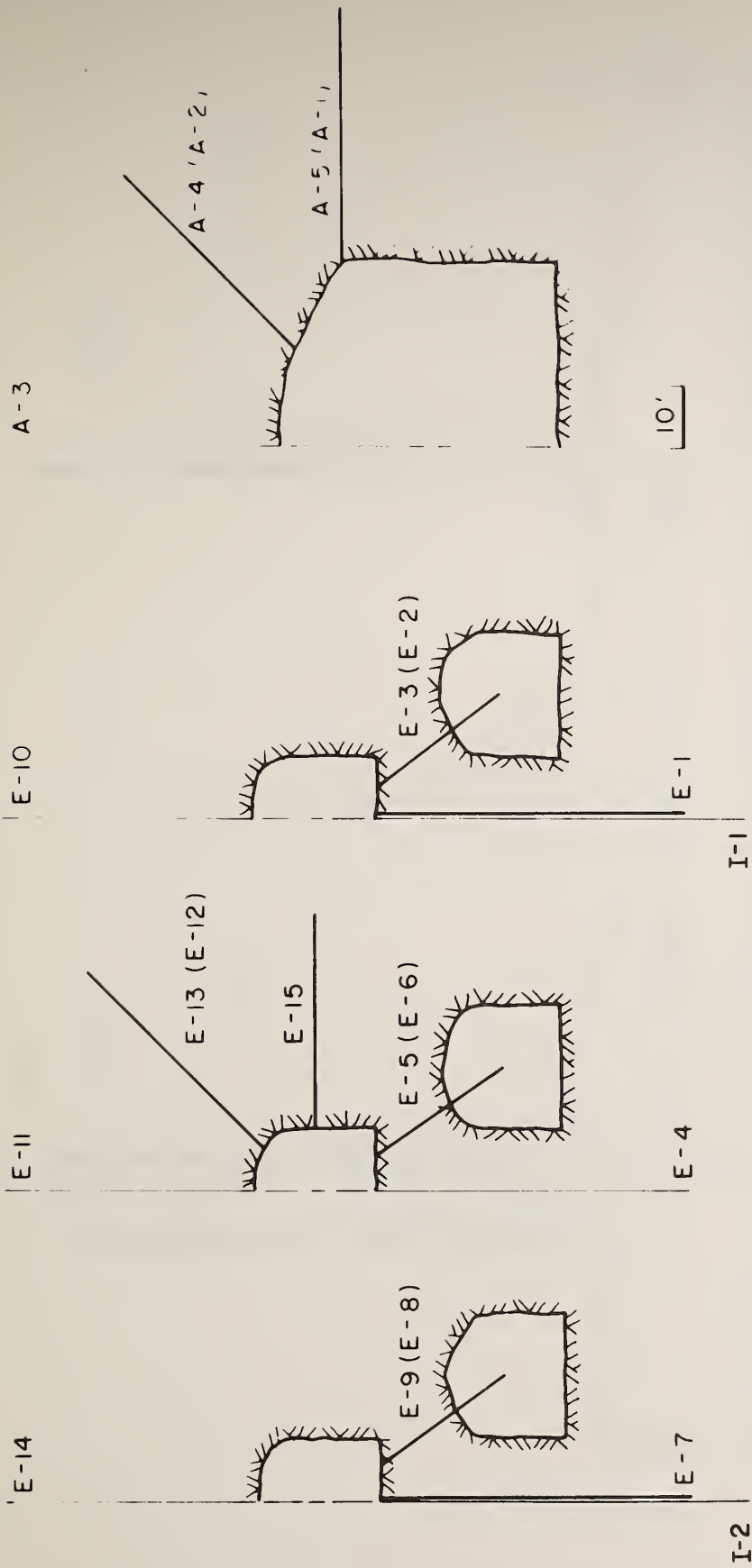


FIGURE 3.7a. INSTRUMENT LOCATIONS



STA. 23+00

STA. 20+65

STA. 20+50

STA. 20+35

FIGURE 3.7b. INSTRUMENT LOCATIONS (LOOKING NORTH)

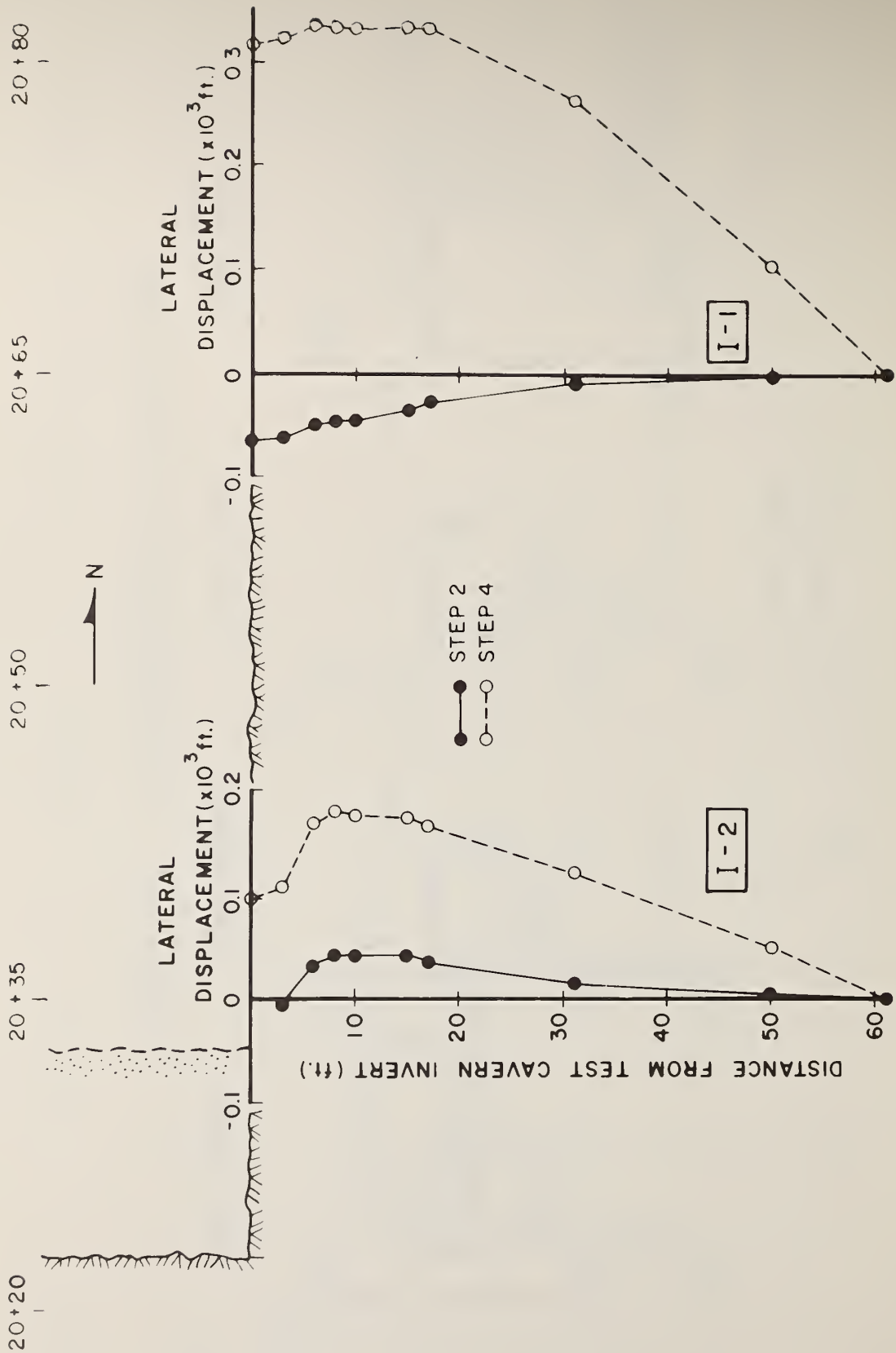


FIGURE 3.8. RELATIVE LATERAL DISPLACEMENTS ALONG INCLINOMETERS

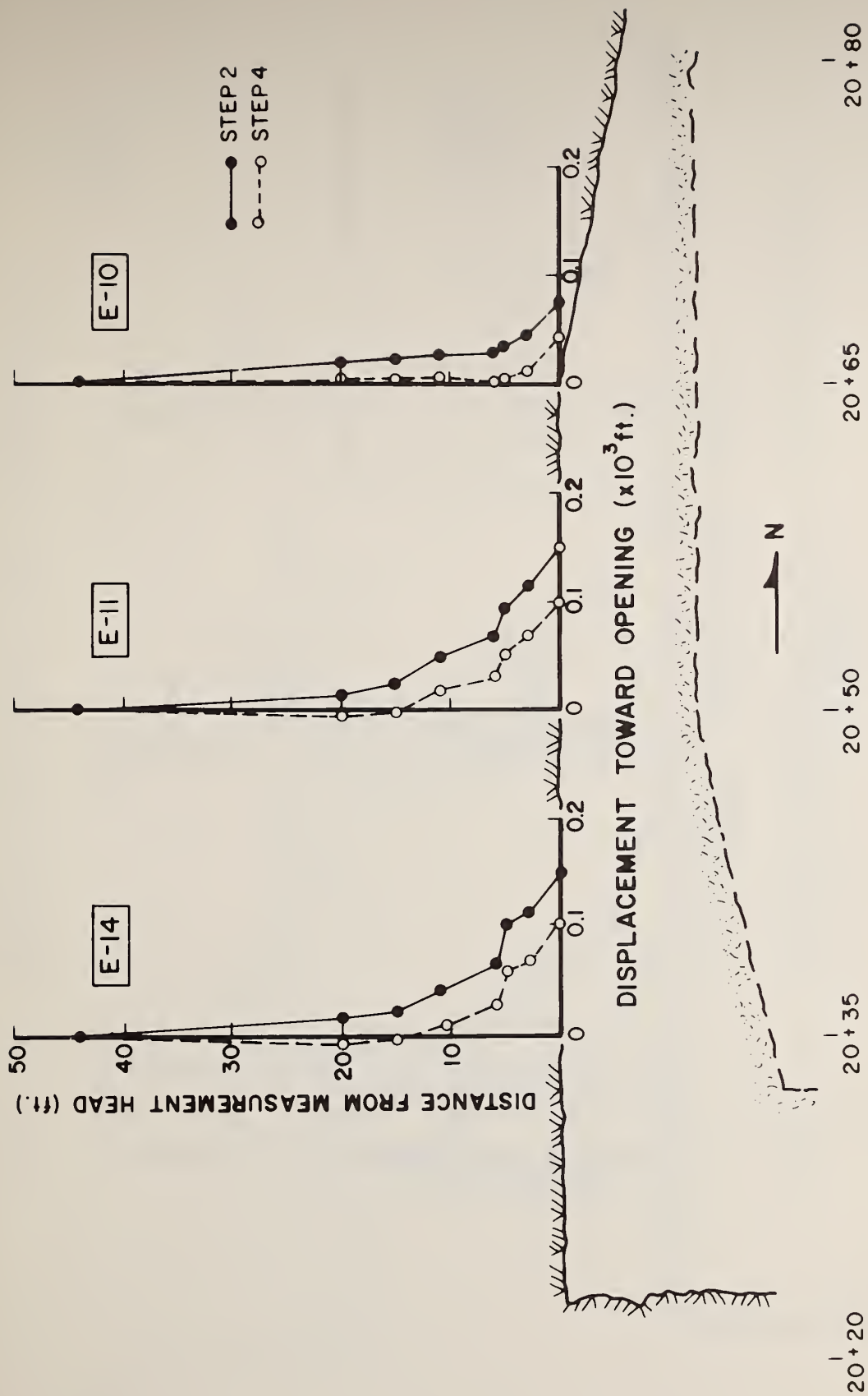


FIGURE 3.9. RELATIVE DISPLACEMENTS ALONG EXTENSOMETERS AT CROWN CENTERLINE OF RESEARCH CHAMBER

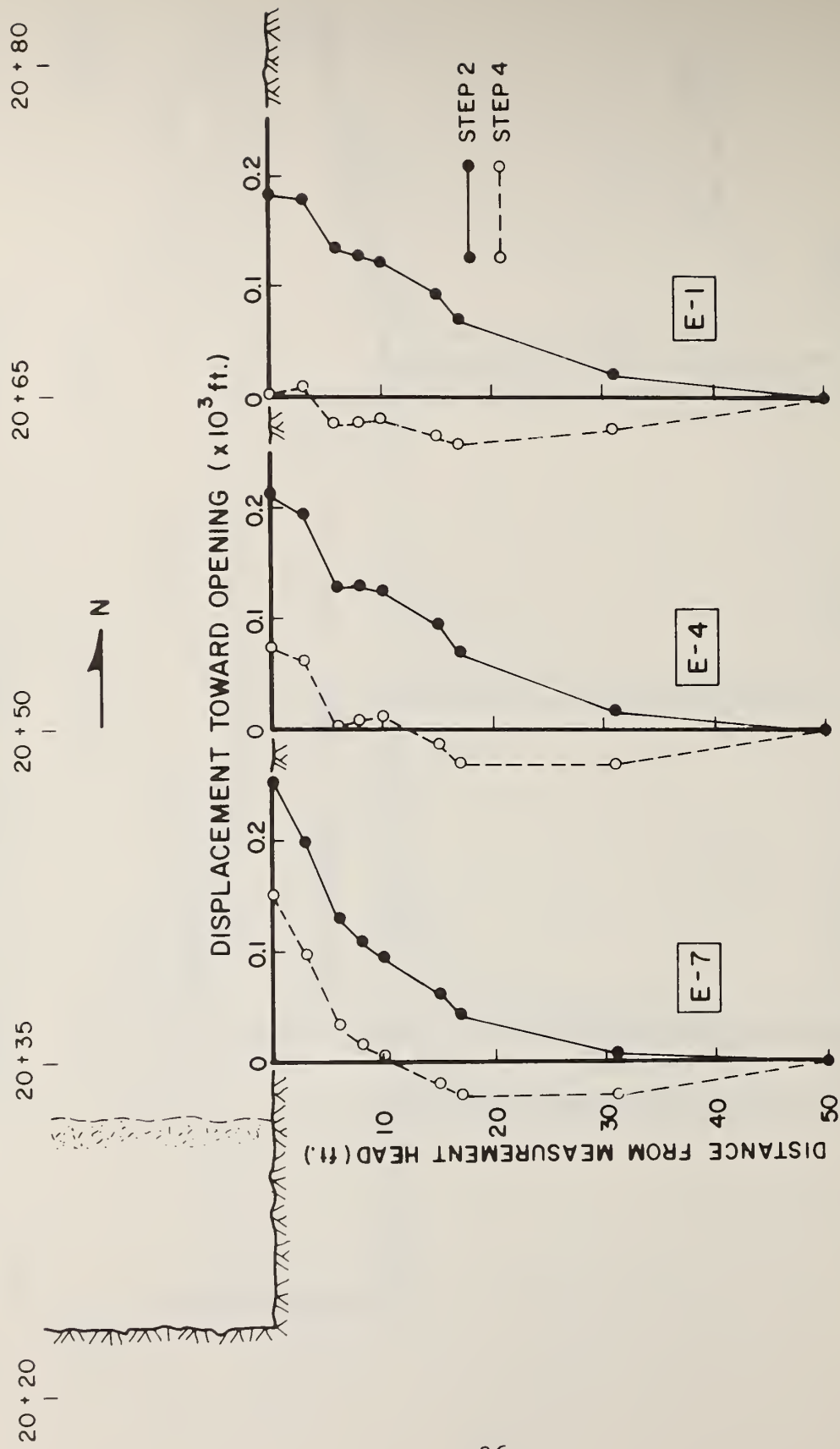


FIGURE 3.10. RELATIVE DISPLACEMENTS ALONG EXTENSOMETERS AT INVERT CENTERLINE OF RESEARCH CHAMBER

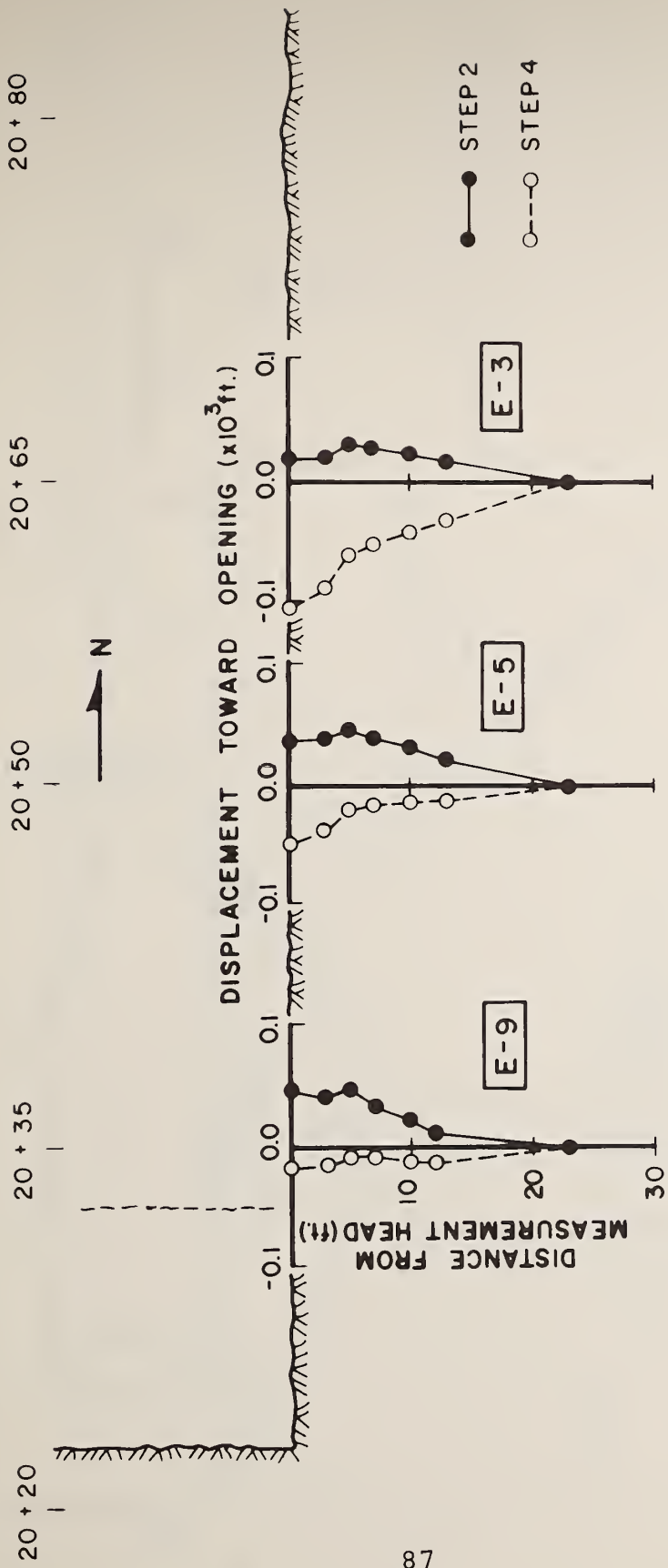


FIGURE 3.11. RELATIVE DISPLACEMENTS ALONG INCLINED EXTENSOMETERS AT INVERT OF RESEARCH CHAMBER

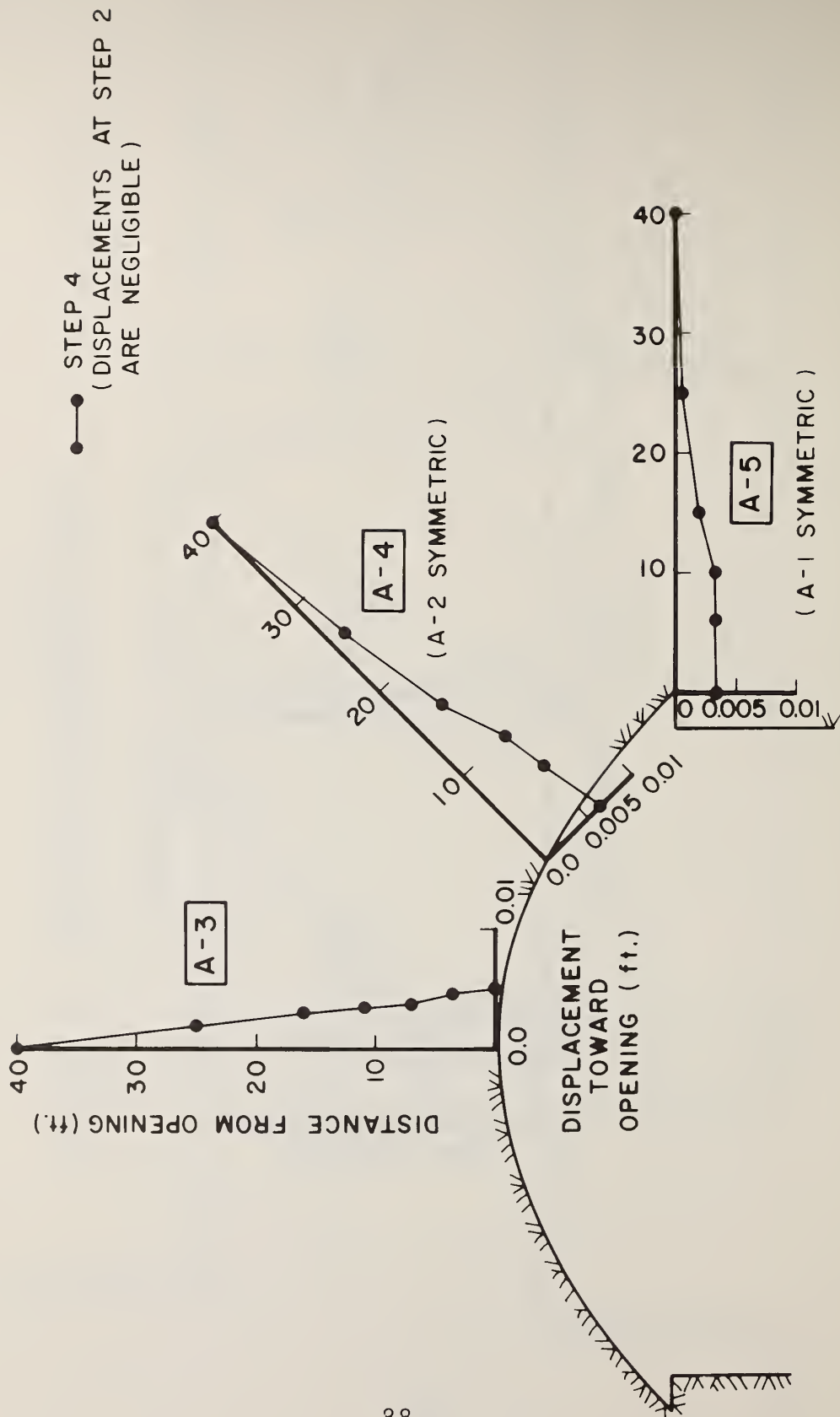


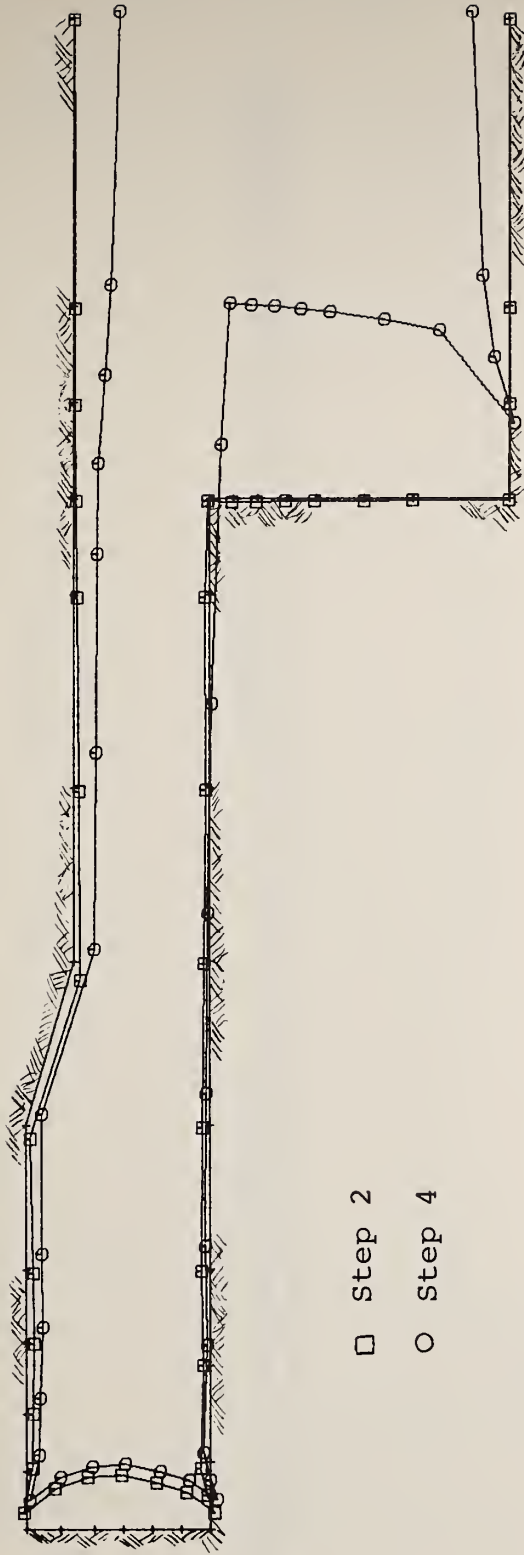
FIGURE 3.12. RELATIVE DISPLACEMENTS ALONG EXTENSOMETERS AROUND MAIN STATION CAVERN -- STATION 23 + 00

20+50

21+00

21+50

22+00

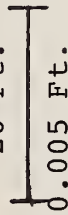


□ Step 2

○ Step 4

Scale:

20 Ft. (Geometry)



0.005 Ft. (Displacements)

FIGURE 3.13a. DEFORMED GEOMETRY OF OPENINGS

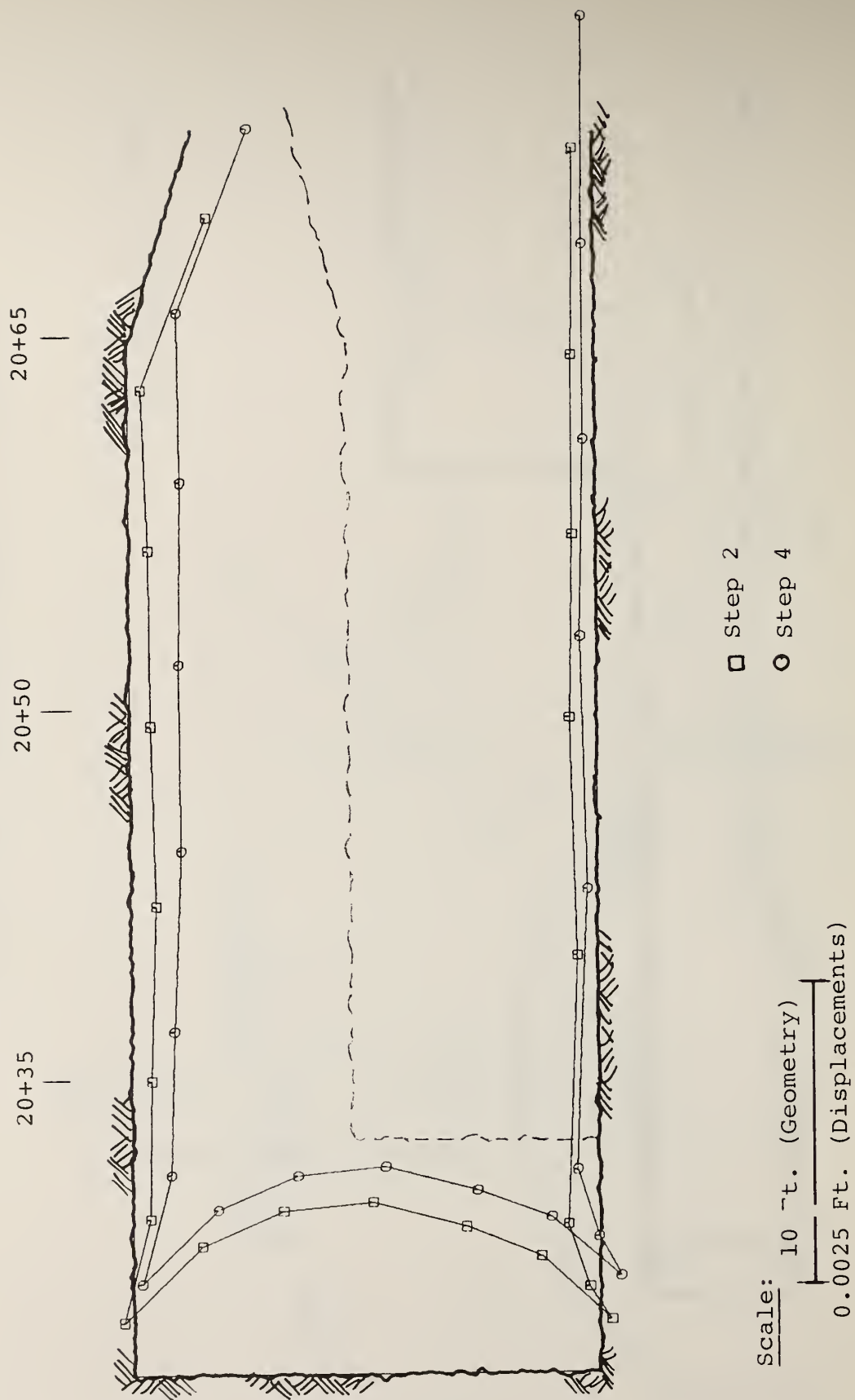


FIGURE 3.13b. DEFORMED GEOMETRY OF OPENINGS

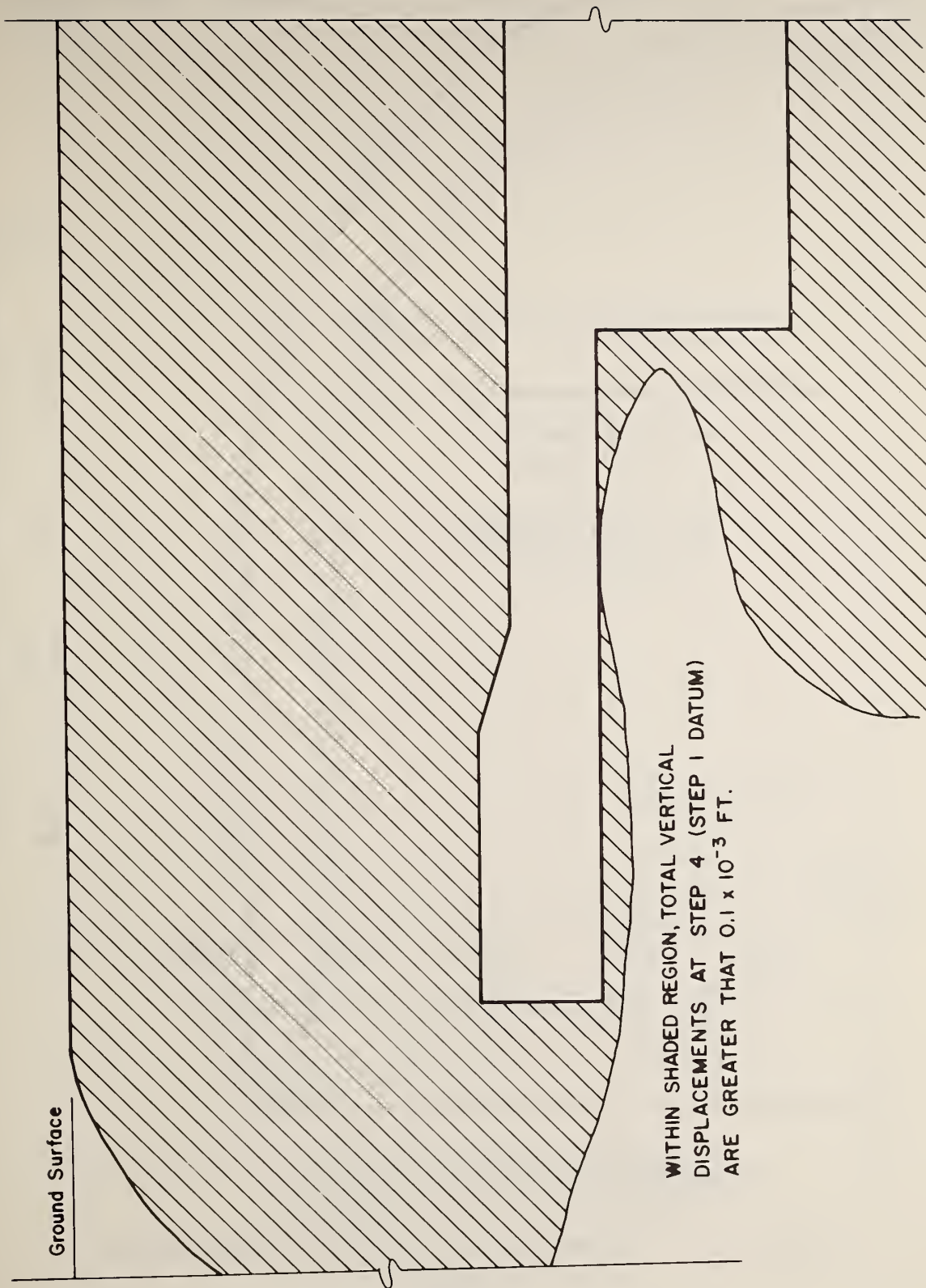


FIGURE 3.14. "ZONE OF INFLUENCE" AROUND OPENINGS

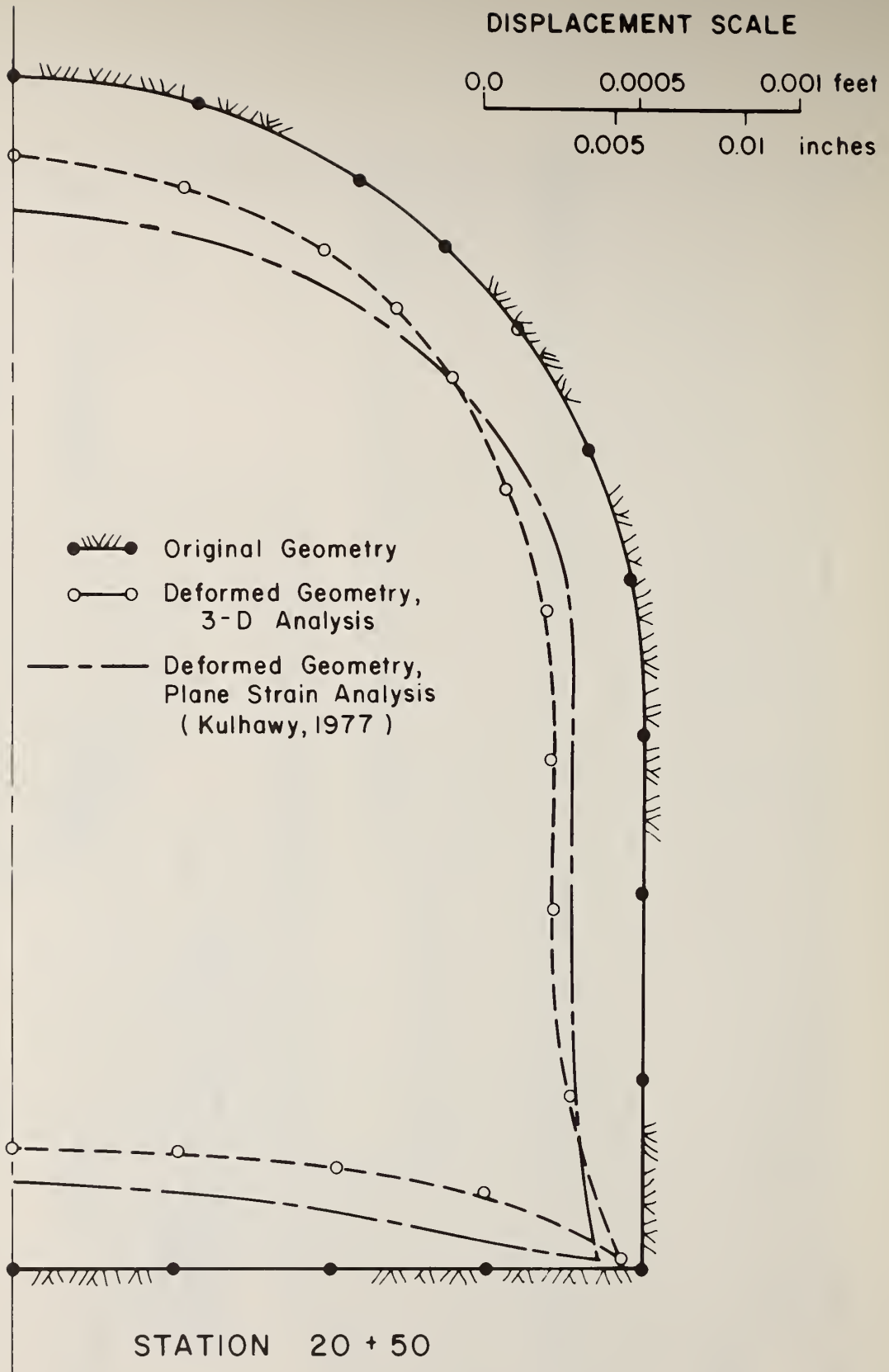


FIGURE 3.15. COMPARISON OF 3-D AND PLANE STRAIN ANALYSIS RESULTS

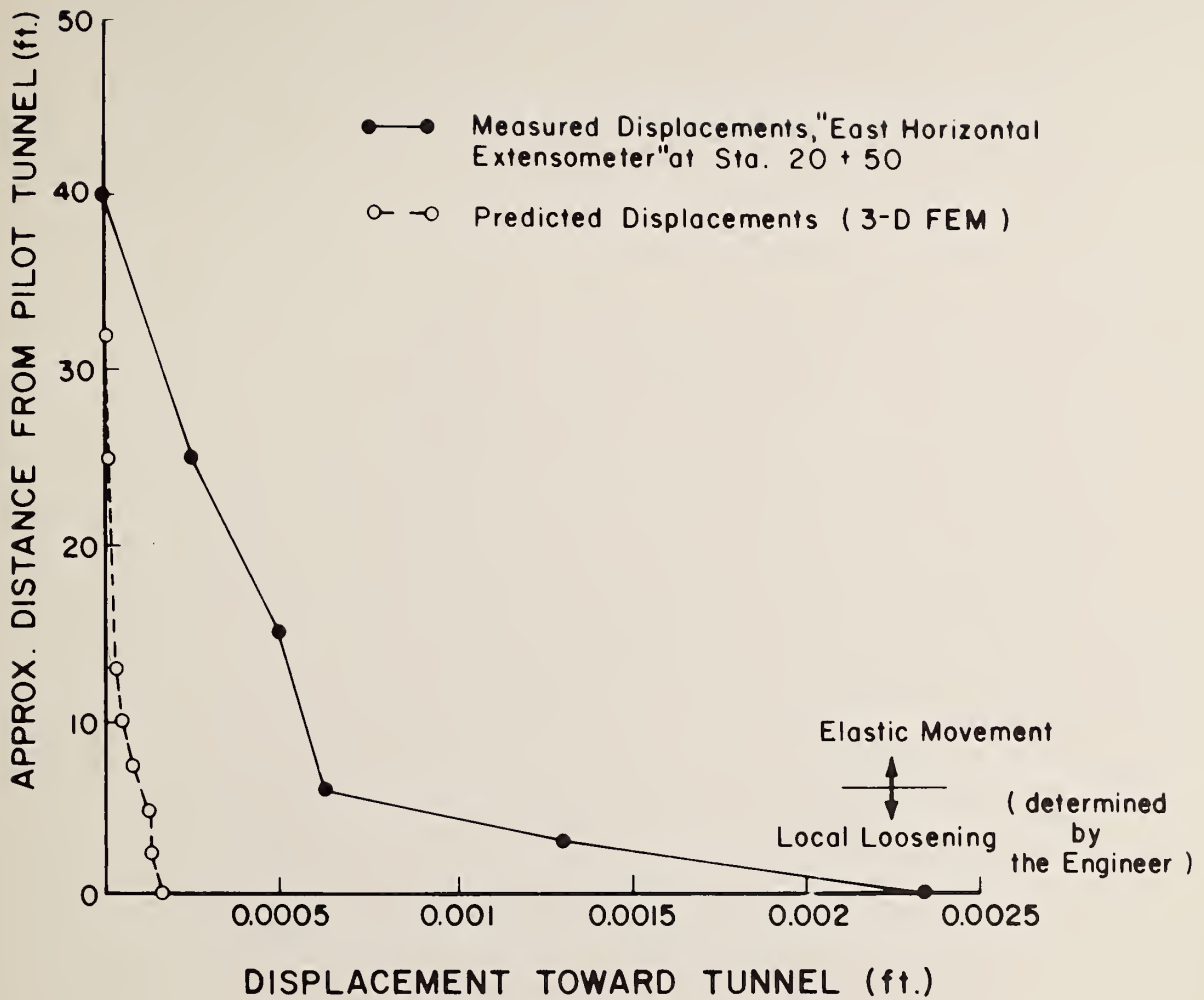


FIGURE 3.16. COMPARISON OF MEASURED ROCK DISPLACEMENTS WITH PREDICTIONS FROM THE 3-D FINITE ELEMENT ANALYSIS

7. TABLES REFERENCED IN SECTIONS 3 AND 4

TABLE 3.1 MOVEMENTS OF INSTRUMENT REFERENCE ANCHORS

INSTRUMENT	REFERENCE ANCHOR DISPLACEMENT (x 10 ³ ft)		SHIFT OF REFERENCE ANCHOR (x 10 ³ ft)
	STEP 2	STEP 4	
E-1	0.0149	0.0981	0.0832
E-2, E-3	0.0230	0.0319	0.0089
E-4	0.0108	0.0607	0.0499
E-5, E-6	0.0177	0.0077	-0.0100
E-7	0.0071	0.0309	0.0238
E-8, E-9	0.0076	-0.0116	-0.0192
E-10	0.0294	0.3641	0.3347
E-11	0.0210	0.3061	0.2851
E-12, E-13			
E-14	0.0127	0.2481	0.2354
E-15			
I-1	-0.0131	0.5106	0.5237
I-2	-0.0046	0.3517	0.3563
A-3	-0.0106	1.7535	1.7641
A-4, A-2	-0.0045	1.3045	1.3090
A-5, A-1	0.0046	0.5817	0.5771

NOTES:

1. Datum is step 1
2. Positive extensometer displacements indicate movements towards opening.
3. Positive inclinometer displacements indicate movements towards station cavern.

TABLE 4.1. SUMMARY OF THE SIZE OF THE FINITE ELEMENT ANALYSIS OF THE PEACHTREE CENTER STATION

Number of degrees of freedom	=	4757
Maximum half bandwidth	=	1076
Mean half bandwidth	=	398
Number of Matrix elements	=	1891278
High speed storage allocations	=	840 kilobytes
Low speed storage allocations	=	81000 kilobytes

TABLE 4.2. SOLUTION TIME LOG IN SECONDS FOR ONE STEP OF THE FINITE ELEMENT ANALYSIS OF THE PEACHTREE CENTER STATION

INPUT PHASE	12.81
ASSEMBLAGE OF LINEAR STIFFNESS, EFFECTIVE STIFFNESS, MASS MATRICES AND LOAD VECTORS	515.21
STEP-BY-STEP SOLUTION (1 TIME STEPS)	
CALCULATION OF EFFECTIVE LOAD VECTORS	57.26
UPDATING EFFECTIVE STIFFNESS MATRICES AND LOAD VECTORS FOR NONLINEARITIES	147.01
SOLUTION OF EQUATIONS	7565.63
EQUILIBRIUM ITERATIONS	0.0
CALCULATION AND PRINTING OF DISPLACEMENTS, VELOCITIES, AND ACCELERATIONS	1.63
CALCULATION AND PRINTING OF STRESSES	17.99
STEP-BY-STEP TOTAL	7790.57
TOTAL SOLUTION TIME (SEC)	8319.24

8. REFERENCES

- Bathe, K.J. (1976a), "ADINA-A Finite Element Program for Automatic Dynamic Incremental Nonlinear Analysis," Report 82448-1, Acoustics and Vibration Laboratory, Mechanical Engineering Department, M.I.T.
- Bathe, K.J. (1976b), "Static and Dynamic Geometric and Material Nonlinear Analysis Using ADINA," Report 82448-2, Acoustics and Vibration Laboratory, Mechanical Engineering Department, M.I.T.
- Bathe, K.J. and Wilson, E.L. (1976), "Numerical Methods in Finite Element Analysis," Prentice-Hall, Inc., Englewood Cliffs, New Jersey.
- Einstein, H.H., et al. (1977), "Improved Design for Tunnel Supports," Report Prepared for U.S. Department of Transportation, Contract No. DOT-OS-60136.
- Kulhawy, F.H. (1977), "Finite Element Analyses of Twin Running Tunnels and Research Chamber at Marta Cain Street Station, Atlanta, Georgia," Report Prepared for Parsons, Brinkerhoff, Quade & Douglas, Inc./Tudor Engineering Company.
- Law Engineering Testing Company (1977), "Report of Geology and Instrumentation--Peachtree Center Station Pilot Tunnel (Construction Unit CN-124)," 3 Volumes.
- Law Engineering Testing Company (1976), "Report of Subsurface Investigation--Final Design (Construction Unit DN-11/Tunneling Alternative)," 3 Volumes.
- Schwartz, C.W. and Einstein, H.H. (1978), "Improvement of Ground Support Performance by Full Consideration of Ground Displacements," Accepted for Publication, Transportation Research Record, No. 684.

APPENDIX A
DESCRIPTION OF COMPUTER PROGRAM - ADINA

ADINA (Automatic Dynamic Incremental Nonlinear Analysis) is a general purpose linear and nonlinear, static and dynamic three-dimensional finite element analysis program. It was developed by Professor K.J. Bathe of the M.I.T. Mechanical Engineering Department as a further development of the NONSAP and SAP IV programs. The following brief description summarizes the features of the program which are particularly useful in the analysis of underground structures.

In its present form, the program contains the following element types:

1. Three-dimensional truss elements
2. Two-dimensional plane stress or plane strain elements
3. Two-dimensional axisymmetric shell or solid elements
4. Three-dimensional solid elements
5. Three-dimensional thick shell elements
6. Three-dimensional beam elements

Depending upon the element type, several material behavior models are available. These include:

1. Isotropic linear elastic
2. Orthotropic linear elastic
3. Isotropic thermo-elastic
4. Curve description model (includes tension cracking)
5. Concrete model (includes tension cracking)
6. Elastic-plastic materials, Von Mises or Drucker-Prager yield criteria

7. Thermo-elastic-plastic-creep, Von Mises yield criterion

8. Mooney-Rivlin material

For a detailed description of these material models, the reader is referred to Bathe (1976a, b). In addition to material non-linearity, the effects of large displacements and strains (geometric nonlinearity) can also be included.

Excavation and support installation operations can be modeled using a "birth/death" option in which elements are activated or deactivated during the calculations. Simulation of the incremental advance of the face of a tunnel is thus possible by deactivating each "round" of elements sequentially.

Variable-number-of-nodes isoparametric finite elements (Bathe and Wilson, 1976) are available for both two and three-dimensional continuum analyses. These elements are efficient and accurate and allow much flexibility in mesh layout and boundary geometry. The variable-number-of-nodes option permits effective modeling from coarse to fine element meshes.

In ADINA, all system matrices and vectors are stored in a compact form and processed using an out-of-core equation solver. This results in maximum system capacity, virtually eliminating any high speed memory constraints for very large problems. Wilson and Newmark time integration methods are available for dynamic analyses.

Versions of ADINA are compatible with IBM, CDC, and UNIVAC computer systems.

APPENDIX B

REPORT OF NEW TECHNOLOGY

The work performed under this contract has led to the development of improved practical design tools to provide more accurate representations of the ground-structure interaction in tunneling. Sophisticated finite element techniques which utilize a three-dimensional finite element program, Automatic Dynamic Incremental Nonlinear Analysis (ADINA), are demonstrated by the specific analysis of the Peachtree Center Station in Atlanta. The practicality of the 3-D analysis is constrained but not excluded by time and cost requirements for such sophisticated analyses.

HE 18.5 : A37 no. 1
UMTA- 80-27.1
AZZOUZ, A. S.

Improved design
supports :

Form DOT F 1720.2 (8)
FORMERLY FORM DOT F 170

DOT LIBRARY



00009994

**U.S. DEPARTMENT OF TRANSPORTATION
RESEARCH AND SPECIAL PROGRAMS ADMINISTRATION**

**TRANSPORTATION SYSTEMS CENTER
KENDALL SQUARE, CAMBRIDGE, MA. 02142**

**OFFICIAL BUSINESS
PENALTY FOR PRIVATE USE, \$300**

**POSTAGE AND FEES PAID
U.S. DEPARTMENT OF TRANSPORTATION
\$13**

